

4

Quantum trajectories

4.1 Introduction

A very general concept of a quantum trajectory would be the path taken by the state of a quantum system over time. This state could be conditioned upon measurement results, as we considered in Chapter 1. This is the sort of quantum trajectory we are most interested in, and it is generally stochastic in nature. In ordinary use, the word trajectory usually implies a path that is also continuous in time. This idea is not always applicable to quantum systems, but we can maintain its essence by defining a quantum trajectory as the path taken by the conditional state of a quantum system for which the unconditioned system state evolves continuously. As explained in Chapter 1, the unconditioned state is that obtained by averaging over the random measurement results which condition the system.

With this motivation, we begin in Section 4.2 by deriving the simplest sort of quantum trajectory, which involves jumps (that is, *discontinuous* conditioned evolution). In the process we will reproduce Lindblad's general form for *continuous* Markovian quantum evolution as presented in Section 3.6. In Section 4.3 we relate these quantum jumps to photon-counting measurements on the bath for the model introduced in Section 3.11, and also derive correlation functions for these measurement records. In Section 4.4 we consider the addition of a coherent field (the 'local oscillator') to the output before detection. In the limit of a strong local oscillator this is called homodyne detection, and is described by a *continuous* (diffusive) quantum trajectory. In Section 4.5 we generalize this theory to describe heterodyne detection and even more general diffusive quantum trajectories. In Section 4.6 we illustrate the detection schemes discussed by examining the conditioned evolution of a simple system: a damped, driven two-level atom. In Section 4.7 we show that there is a complementary description of continuous measurement in the Heisenberg picture, and that this can also be used to derive correlation functions and other statistics of the measurement results. In Section 4.8 we show how quantum trajectory theory can be generalized to deal with imperfect detection, incorporating inefficiency, thermal and squeezed bath noise, dark noise and finite detector bandwidth. In Section 4.9 we turn from optical examples to mesoscopic electronics, including a discussion of imperfect detection. We conclude with further reading in Section 4.10.

4.2 Quantum jumps

4.2.1 Master equations and continuous measurements

The evolution of an isolated quantum system in the absence of measurement is Markovian:

$$|\psi(t+T)\rangle = \hat{U}(T)|\psi(t)\rangle = \exp(-i\hat{H}T)|\psi(t)\rangle, \quad (4.1)$$

where \hat{H} is the Hamiltonian. This equation leads to a finite differential

$$\lim_{\tau \rightarrow 0} \frac{|\psi(t+\tau)\rangle - |\psi(t)\rangle}{\tau} = |\dot{\psi}(t)\rangle = -i\hat{H}(t)|\psi(t)\rangle = \text{finite} \quad (4.2)$$

and hence to continuous evolution. We now seek to generalize this unitary evolution by incorporating measurements. To consider the unconditioned state, averaged over the possible measurement results, we have to represent the system by a state matrix rather than a state vector. Then continuous evolution of ρ implies

$$\lim_{\tau \rightarrow 0} \frac{\rho(t+\tau) - \rho(t)}{\tau} = \dot{\rho}(t) = \text{finite}. \quad (4.3)$$

In order to obtain a differential equation for $\rho(t)$, we require the measurement time T to be infinitesimal. In this limit, we say that we are *monitoring* the system. Then, from Eq. (1.86), the state matrix at time $t + dt$, averaging over all possible results, is

$$\rho(t+dt) = \sum_r \mathcal{J}[\hat{M}_r(dt)]\rho(t). \quad (4.4)$$

If $\rho(t+dt)$ is to be infinitesimally different from $\rho(t)$, then a first reasonable guess at how to generalize Eq. (4.1) would be to consider just one r , say $r = 0$, and set

$$\hat{M}_0(dt) = \hat{1} - (\hat{R}/2 + i\hat{H})dt, \quad (4.5)$$

where \hat{R} and \hat{H} are Hermitian operators. However, we find that this single measurement operator does not satisfy the completeness condition (1.78), since, to order dt ,

$$\hat{M}_0^\dagger(dt)\hat{M}_0(dt) = \hat{1} - \hat{R}dt \neq \hat{1}. \quad (4.6)$$

The above result reflects the fact that a measurement with only one possible result is not really a measurement at all and hence the ‘measurement operator’ (4.5) must be a unitary operator, as it is with $\hat{R} = 0$. If $\hat{R} \neq 0$ then we require at least one other possible result to enable $\sum_r \hat{M}_r^\dagger(dt)\hat{M}_r(dt) = \hat{1}$. The simplest suggestion is to consider two results 0 and 1. We let $\hat{M}_0(dt)$ be as above, and define

$$\hat{M}_1(dt) = \sqrt{dt} \hat{c}, \quad (4.7)$$

where \hat{c} is an arbitrary operator obeying

$$\hat{c}^\dagger \hat{c} = \hat{R}, \quad (4.8)$$

which implies that we must have $\hat{R} \geq 0$, so that

$$\hat{M}_0^\dagger(dt)\hat{M}_0(dt) + \hat{M}_1^\dagger(dt)\hat{M}_1(dt) = \hat{1}. \quad (4.9)$$

This gives the non-selective evolution

$$\rho(t + dt) = [\hat{1} - (\hat{c}^\dagger \hat{c}/2 + i\hat{H})dt]\rho(t)[\hat{1} - (\hat{c}^\dagger \hat{c}/2 - i\hat{H})dt] + dt \hat{c}\rho(t)\hat{c}^\dagger, \quad (4.10)$$

which has the differential form

$$\dot{\rho} = -i[\hat{H}, \rho] + \mathcal{D}[\hat{c}]\rho \equiv \mathcal{L}\rho. \quad (4.11)$$

Allowing for more than one irreversible term, we obtain exactly the master equation derived by Lindblad by more formal means [Lin76] (see Section 3.6).

4.2.2 Stochastic evolution

Let us consider the evolution implied by the two measurement operators above. The probability for the result $r = 1$ is

$$\wp_1(dt) = \text{Tr}[\mathcal{J}[\hat{M}_1(dt)]\rho] = dt \text{Tr}[\hat{c}^\dagger \hat{c}\rho], \quad (4.12)$$

which is infinitesimal (provided that $\hat{c}^\dagger \hat{c}$ is bounded as assumed by Lindblad [Lin76]). That is to say, for almost all infinitesimal time intervals, the measurement result is $r = 0$, because $\wp_0(dt) = 1 - O(dt)$. The result $r = 0$ is thus regarded as a null result. In the case of no result, the system state changes infinitesimally, but not unitarily, via the operator $\hat{M}_0(dt)$. At random times, occurring at rate $\wp_1(dt)/dt$, there is a result $r = 1$, which we will call a *detection*. When this occurs, the system undergoes a finite evolution induced by the operator $\hat{M}_1(dt)$. This change can validly be called a *quantum jump*. However, it must be remembered that it represents a sudden change in the observer's knowledge, not an objective physical event as in Bohr's original conception in the 1910s [Boh13].

Real measurements that correspond approximately to this ideal measurement model are made routinely in experimental quantum optics. If $\hat{c} = \sqrt{\gamma}\hat{a}$ then Eq. (4.11) is the damped-cavity master equation derived in Section 3.3.2, and this theory describes the system evolution in terms of photodetections of the cavity output. Note that we are ignoring the time delay between emission from the system and detection by the detector. Loosely, we can think of the conditioned state here as being the state the system *was* in at the time of emission. When it comes to considering feedback control of the system we will see that any time delay, whether between the emission and detection or between the detection and feedback action, must be taken into account.

Let us denote the number of photodetections up to time t by $N(t)$, and say for simplicity that the system state at time t is a pure state $|\psi(t)\rangle$. Then the stochastic increment $dN(t)$ obeys

$$dN(t)^2 = dN(t), \quad (4.13)$$

$$E[dN(t)] = \langle \hat{M}_1^\dagger(dt)\hat{M}_1(dt) \rangle = dt \langle \psi(t) | \hat{c}^\dagger \hat{c} | \psi(t) \rangle, \quad (4.14)$$

where a classical expectation value is denoted by E and the quantum expectation value by angle brackets. The first equation here simply says that dN is either zero or one, as it

must be since it is the increment in N in an infinitesimal time. The second equation gives the mean of dN , which is identical with the probability of detecting a photon. This is an example of a point process – see Section B.6.

From the measurement operators (4.5) and (4.7) we see that, when $dN(t) = 1$, the state vector changes to

$$|\psi_1(t + dt)\rangle = \frac{\hat{M}_1(dt)|\psi(t)\rangle}{\sqrt{\langle \hat{M}_1^\dagger(dt)\hat{M}_1(dt) \rangle(t)}} = \frac{\hat{c}|\psi(t)\rangle}{\sqrt{\langle \hat{c}^\dagger \hat{c} \rangle(t)}}, \quad (4.15)$$

where the denominator gives the normalization. If there is no detection, $dN(t) = 0$ and

$$\begin{aligned} |\psi_0(t + dt)\rangle &= \frac{\hat{M}_0(dt)|\psi(t)\rangle}{\sqrt{\langle \hat{M}_0^\dagger(dt)\hat{M}_0(dt) \rangle(t)}} \\ &= \left\{ \hat{1} - dt \left[i\hat{H} + \frac{1}{2}\hat{c}^\dagger \hat{c} - \frac{1}{2}\langle \hat{c}^\dagger \hat{c} \rangle(t) \right] \right\} |\psi(t)\rangle, \end{aligned} \quad (4.16)$$

where the denominator has been expanded to first order in dt to yield the nonlinear term.

This stochastic evolution can be written explicitly as a nonlinear stochastic Schrödinger equation (SSE):

$$d|\psi(t)\rangle = \left[dN(t) \left(\frac{\hat{c}}{\sqrt{\langle \hat{c}^\dagger \hat{c} \rangle(t)}} - 1 \right) + [1 - dN(t)] dt \left(\frac{\langle \hat{c}^\dagger \hat{c} \rangle(t)}{2} - \frac{\hat{c}^\dagger \hat{c}}{2} - i\hat{H} \right) \right] |\psi(t)\rangle. \quad (4.17)$$

It is called a Schrödinger equation only because it preserves the purity of the state, like Eq. (4.1). We will call a solution to this equation a *quantum trajectory* for the system.

We can simplify the stochastic Schrödinger equation by using the rule (see Section B.6)

$$dN(t)dt = o(dt). \quad (4.18)$$

This notation means that the order of $dN(t)dt$ is smaller than that of dt and so the former is negligible compared with the latter. Then Eq. (4.17) becomes

$$d|\psi(t)\rangle = \left[dN(t) \left(\frac{\hat{c}}{\sqrt{\langle \hat{c}^\dagger \hat{c} \rangle(t)}} - \hat{1} \right) + dt \left(\frac{\langle \hat{c}^\dagger \hat{c} \rangle(t)}{2} - \frac{\hat{c}^\dagger \hat{c}}{2} - i\hat{H} \right) \right] |\psi(t)\rangle. \quad (4.19)$$

Exercise 4.1 Verify that the only difference between the two equations is that the state vector after a jump is infinitesimally different. Since the total number of jumps in any finite time is finite, the difference between the two equations is negligible.

From Eq. (4.19) it is simple to reconstruct the master equation using the rules (4.13) and (4.14). First define a projector

$$\hat{\pi}(t) = |\psi(t)\rangle \langle \psi(t)|, \quad (4.20)$$

and find (using the notation $d|\psi\rangle = d|\psi\rangle$)

$$d\hat{\pi}(t) = |d\psi(t)\rangle\langle\psi(t)| + |\psi(t)\rangle\langle d\psi(t)| + |d\psi(t)\rangle\langle d\psi(t)| \quad (4.21)$$

$$= \{dN(t)\mathcal{G}[\hat{c}] - dt \mathcal{H}[\hat{H} + \frac{1}{2}\hat{c}^\dagger\hat{c}]\}\hat{\pi}(t). \quad (4.22)$$

Here, the nonlinear (in ρ) superoperators \mathcal{G} and \mathcal{H} are defined by

$$\mathcal{G}[\hat{r}]\rho = \frac{\hat{r}\rho\hat{r}^\dagger}{\text{Tr}[\hat{r}\rho\hat{r}^\dagger]} - \rho, \quad (4.23)$$

$$\mathcal{H}[\hat{r}]\rho = \hat{r}\rho + \rho\hat{r}^\dagger - \text{Tr}[\hat{r}\rho + \rho\hat{r}^\dagger]\rho. \quad (4.24)$$

Now define

$$\rho(t) = E[\hat{\pi}(t)], \quad (4.25)$$

that is, the state matrix is the expected value or ensemble average of the projector. From Eq. (B.54), the rule (4.14) generalizes to

$$E[dN(t)g(\hat{\pi}(t))] = dt E[\text{Tr}[\hat{\pi}(t)\hat{c}^\dagger\hat{c}]g(\hat{\pi}(t))], \quad (4.26)$$

for any function g . Using this yields finally

$$d\rho = -i dt [\hat{H}, \rho] + dt \mathcal{D}[\hat{c}]\rho, \quad (4.27)$$

as required.

Exercise 4.2 Verify Eqs. (4.22) and (4.27) following the above steps.

4.2.3 Quantum trajectories for simulations

For the most general master-equation evolution,

$$\dot{\rho} = -i[\hat{H}, \rho] + \sum_{\mu} \mathcal{D}[\hat{c}_{\mu}]\rho, \quad (4.28)$$

the above SSE can be generalized to

$$d|\psi(t)\rangle = \sum_{\mu} \left[dN_{\mu}(t) \left(\frac{\hat{c}_{\mu}}{\sqrt{\langle\hat{c}_{\mu}^\dagger\hat{c}_{\mu}\rangle(t)}} - \hat{1} \right) + dt \left(\frac{\langle\hat{c}_{\mu}^\dagger\hat{c}_{\mu}\rangle(t)}{2} - \frac{\hat{c}_{\mu}^\dagger\hat{c}_{\mu}}{2} - i\hat{H} \right) \right] |\psi(t)\rangle, \quad (4.29)$$

with

$$E[dN_{\mu}(t)] = \langle\psi(t)|\hat{c}_{\mu}^\dagger\hat{c}_{\mu}|\psi(t)\rangle dt, \quad (4.30)$$

$$dN_{\mu}(t)dN_{\nu}(t) = dN_{\mu}(t)\delta_{\mu\nu}. \quad (4.31)$$

Equations of this form have been used extensively since the mid 1990s in order to obtain numerical solutions of master equations [DZR92, MCD93]. The solution $\rho(t)$ is approximated by the ensemble average $E[|\psi(t)\rangle\langle\psi(t)|]$ over a finite number $M \gg 1$ of numerical realizations of the stochastic evolution (4.29).

The advantage of doing this rather than solving the master equation (4.28) is that, if the system requires a Hilbert space of dimension N in order to be represented accurately, then in general storing the state matrix ρ requires of order N^2 real numbers, whereas storing the state vector $|\psi\rangle$ requires only of order N . For large N , the time taken to compute the evolution of the state matrix via the master equation scales as N^4 , whereas the time taken to compute the ensemble of state vectors via the quantum trajectory scales as N^2M , or just N^2 if parallel processors are available. Even though one requires $M \gg 1$, reasonable results may be obtainable with $M \ll N^2$. For extremely large N it may be impossible even to store the state matrix on most computers. In this case the quantum trajectory method may still be useful, if one wishes to calculate only certain system averages, rather than the entire state matrix, via

$$E[\langle\psi(t)|\hat{A}|\psi(t)\rangle] = \text{Tr}[\rho(t)\hat{A}]. \quad (4.32)$$

One area where this technique has been applied to good effect is the quantized motion of atoms undergoing spontaneous emission [DZR92].

The simplest method of solution for Eq. (4.29) is to replace all differentials d by small but finite differences δ . That is, in a small interval of time δt , a random number $R(t)$ chosen uniformly from the unit interval is generated. If

$$R(t) < \wp_{\text{jump}} = \sum_{\mu} \langle\psi(t)|\hat{c}_{\mu}^{\dagger}\hat{c}_{\mu}|\psi(t)\rangle\delta t \quad (4.33)$$

then a jump happens. One of the possible jumps (μ) is chosen randomly using another (or the same) random number, with the weights $\langle\psi(t)|\hat{c}_{\mu}^{\dagger}\hat{c}_{\mu}|\psi(t)\rangle\delta t/\wp_{\text{jump}}$. The appropriate δN_{μ} is then set to 1, all others set to zero, and the increment (4.29) calculated.

In practice, this is not the most efficient method for simulation. Instead, the following method is generally used. Say the system starts at time 0. A random number R is generated as above. Then the unnormalized evolution

$$\frac{d}{dt}|\tilde{\psi}(t)\rangle = -\left(\sum_{\mu}\hat{c}_{\mu}^{\dagger}\hat{c}_{\mu}/2 + i\hat{H}\right)|\tilde{\psi}(t)\rangle \quad (4.34)$$

is solved for a time T such that $\langle\tilde{\psi}(T)|\tilde{\psi}(T)\rangle = R$. This time T will have to be found iteratively. However, since Eq. (4.34) is an ordinary linear differential equation, it can be solved efficiently using standard numerical techniques. The decay in the state-matrix norm $\langle\tilde{\psi}(t)|\tilde{\psi}(t)\rangle$ is because Eq. (4.34) keeps track only of the no-jump evolution, derived from the repeated action of $\hat{M}_0(dt)$. That is, the norm is equal to the probability of this series of results occurring (see Section 1.4). Thus this method generates T , the time at which the first jump occurs, with the correct statistics. Which jump (i.e. which μ) occurs at this time can be determined by the technique described above. The relevant collapse operator \hat{c}_{μ} is then

applied to the system $|\tilde{\psi}(T)\rangle$, and the state normalized again. The simulation then repeats as if time $t = T$ were the initial time $t = 0$.

4.3 Photodetection

4.3.1 Photon emission and detection

We claimed above that jumpy quantum trajectories are realized routinely in quantum-optics laboratories by counting photons in the output beam from a cavity. We now show this explicitly for this sort of measurement which we call *direct detection*. Recall from Eq. (3.158) in Section 3.11 that the interaction between the system and the bath in the infinitesimal interval $[t, t + dt]$ is described by the unitary operator

$$\hat{U}(t + dt, t) = \exp[\hat{c} d\hat{B}^\dagger - \hat{c}^\dagger d\hat{B} - i\hat{H} dt]. \quad (4.35)$$

Here, for convenience, we are using the short-hand $d\hat{B} = d\hat{B}_{z:=t}$, and we have included a system Hamiltonian \hat{H} , all in the interaction frame. If the system is in a pure state at time t (as it will be if the bath has been monitored up to that time), then we need consider only the bath mode on which $d\hat{B}$ acts, which is initially in the vacuum state. That is, the entangled system–bath state at the end of the interval is $\hat{U}(t + dt, t)|0\rangle|\psi(t)\rangle$.

Keeping only the non-normally ordered second-order terms $d\hat{B} d\hat{B}^\dagger = dt$ (see Section 3.11.1), and given the fact that $d\hat{B}|0\rangle = 0$, one finds

$$\hat{U}(t + dt, t)|0\rangle|\psi(t)\rangle = [\hat{1} - dt \hat{c}^\dagger \hat{c}/2 - i\hat{H} dt]|0\rangle|\psi(t)\rangle + d\hat{B}^\dagger|0\rangle\hat{c}|\psi(t)\rangle. \quad (4.36)$$

Clearly $d\hat{B}^\dagger|0\rangle$ is a bath state containing one photon. But it is not a normalized one-photon state; rather, it has a norm of

$$\langle 0|d\hat{B} d\hat{B}^\dagger|0\rangle = dt. \quad (4.37)$$

Thus, the probability of finding one photon in the bath is

$$\langle 0|d\hat{B} d\hat{B}^\dagger|0\rangle \langle \psi(t)|\hat{c}^\dagger \hat{c}|\psi(t)\rangle = \wp_1(dt), \quad (4.38)$$

where $\wp_1(dt)$ is defined in Eq. (4.12). Moreover, from Eq. (4.36) it is apparent that the system state conditioned on the bath containing a photon is exactly as given in Eq. (4.15). The probability of finding no photons in the bath is $\wp_0(dt) = 1 - \wp_1(dt)$, and the conditioned system state is again as given previously in Eq. (4.16).

In the above, we have not specified whether the measurement on the bath is projective (which would leave the number of photons unchanged) or non-projective. In reality, photon detection, at least at optical frequencies, is done by absorption, so the field state at the end of the measurement is the vacuum state. However, it should be emphasized that this is in no way essential to the theory. The field state at the beginning of the next interval $[t + dt, t + 2dt]$ is a vacuum state, but not because we have assumed the photons to have been absorbed. Rather, it is a vacuum state for a *new* field operator, which pertains to the part of the field which has ‘moved in’ to interact with the system while the previous part (which has now become the emitted field) ‘moves out’ to be detected – see Section 3.11.

4.3.2 Output correlation functions

In experimental quantum optics, it is more usual to consider a photocurrent than a photo-count. Any multiplier in the definition of a photocurrent is either purely conventional, or has meaning only for a particular detector, so we simply define the photocurrent to be

$$I(t) = dN(t)/dt. \quad (4.39)$$

Note that $dN(t)$, since its mean depends on the quantum state at time t , is conditioned on the record $dN(s)$ for $s < t$. That is, I is what is known as a self-exciting point process [Haw71]. We write the quantum state at time t (which in general may be mixed) as $\rho_I(t)$. Here the subscript I emphasizes that it is conditioned on the photocurrent. To consider mixed states, it is necessary to reformulate the stochastic Schrödinger equation (4.19) as a *stochastic master equation* (SME). This simply means replacing the projector $\hat{\pi}(t)$ in Eq. (4.22) by $\rho_I(t)$ to get

$$d\rho_I(t) = \{dN(t)\mathcal{G}[\hat{c}] - dt \mathcal{H}[i\hat{H} + \frac{1}{2}\hat{c}^\dagger\hat{c}]\}\rho_I(t), \quad (4.40)$$

where the jump probability is

$$E[dN(t)] = dt \operatorname{Tr}[\hat{c}^\dagger\hat{c}\rho_I(t)]. \quad (4.41)$$

The photocurrent (4.39) is a singular quantity, consisting of a series of Dirac δ -functions at the times of photodetections. The most common ways to investigate its statistical properties are to find its mean and its autocorrelation function. The first of these statistics is simply

$$E[I(t)] = \operatorname{Tr}[\rho(t)\hat{c}^\dagger\hat{c}]. \quad (4.42)$$

The second is defined as

$$F^{(2)}(t, t + \tau) = E[I(t + \tau)I(t)]. \quad (4.43)$$

We will now show how this can be evaluated using Eq. (4.40). We take the state at time t to be a given $\rho(t)$.

First consider τ finite. Now $dN(t)$ is either zero or one. If it is zero, then the function is automatically zero. Hence,

$$F^{(2)}(t, t + \tau)(dt)^2 = \operatorname{Pr}[dN(t) = 1] \times E[dN(t + \tau)|dN(t) = 1], \quad (4.44)$$

where $E[A|B]$ means the expectation value of the variable A given the event B . This is equal to

$$F^{(2)}(t, t + \tau)(dt)^2 = \operatorname{Tr}[\hat{c}^\dagger\hat{c}\rho(t)]dt \times \operatorname{Tr}[\hat{c}^\dagger\hat{c}dt E[\rho_I(t + \tau)|dN(t) = 1]]. \quad (4.45)$$

Note that the ensemble average of $\rho_I(t + \tau)$ conditioned on $dN(t) = 1$ appears because we have no knowledge about photodetector clicks in the interval $[t + dt, t + \tau)$, and hence we must average over any such jumps. Now, if $dN(t) = 1$, then from Eq. (4.40) we obtain (to leading order in dt)

$$\rho_I(t + dt) = \rho(t) + \mathcal{G}[\hat{c}]\rho(t) = \hat{c}\rho(t)\hat{c}^\dagger/\operatorname{Tr}[\hat{c}\rho(t)\hat{c}^\dagger]. \quad (4.46)$$

By virtue of the linearity of the ensemble-average evolution (4.27),

$$E[\rho_I(t + \tau) | dN(t) = 1] = \exp(\mathcal{L}\tau) \hat{c} \rho(t) \hat{c}^\dagger / \text{Tr}[\hat{c} \rho(t) \hat{c}^\dagger]. \quad (4.47)$$

Here the superoperator $e^{\mathcal{L}\tau}$ acts on the product of all operators to its right. Thus, the final expression for τ finite is

$$F^{(2)}(t, t + \tau) = \text{Tr}[\hat{c}^\dagger \hat{c} e^{\mathcal{L}\tau} \hat{c} \rho(t) \hat{c}^\dagger]. \quad (4.48)$$

For \hat{c} an annihilation operator for a cavity mode, this is equal to Glauber's second-order coherence function, $G^{(2)}(t, t + \tau)$ [Gla63].

If $\tau = 0$, then the expression (4.43) diverges, because $dN(t)^2 = dN(t)$. Naively,

$$F^{(2)}(t, t) = \text{Tr}[\hat{c}^\dagger \hat{c} \rho(t)] / dt. \quad (4.49)$$

However, since we are effectively discretizing time in bins of size dt , the expression $1/dt$ at $\tau = 0$ is properly interpreted as the Dirac $\delta(\tau)$ – see the discussion following Eq. (3.160). Since this is infinitely larger than any finite term at $\tau = 0$, we can write the total expression as

$$F^{(2)}(t, t + \tau) = \text{Tr}[\hat{c}^\dagger \hat{c} e^{\mathcal{L}\tau} \hat{c} \rho(t) \hat{c}^\dagger] + \text{Tr}[\hat{c}^\dagger \hat{c} \rho(t)] \delta(\tau). \quad (4.50)$$

Often we are interested in the *stationary* or *steady-state* statistics of the current, in which case the time argument t disappears and $\rho(t)$ is replaced by ρ_{ss} , the (assumed unique) stationary solution of the master equation:

$$\mathcal{L}\rho_{ss} = 0. \quad (4.51)$$

4.3.3 Coherent field input

In the preceding section we have assumed a bath in the vacuum state. In Section 3.11.2 we showed how to derive the quantum Langevin equations and master equations for the case of a white-noise (thermal or squeezed) bath. If one tried to consider photodetection in such a case, one would run into the problem that a white-noise bath has a theoretically infinite photon flux. It is not possible to count the photons in such a beam; no matter how small the time interval, one would still expect a finite number of counts. In practice, such noise is not strictly white, and in any case the bandwidth of the detector will keep the count rate finite.¹ Nevertheless, in the limit where the white-noise approximation is a good one, the photon flux due to the bath will be much greater than that due to the system. Hence, direct detection will yield negligible information about the system state, so the quantum trajectory will simply be the unconditioned master equation (4.27).

However, the vacuum input considered so far can still be generalized by adding a coherent field, as explained in Section 3.11.2. Given that $d\hat{B} d\hat{B}^\dagger = dt$, to obtain a state with $\langle d\hat{B} \rangle = \beta dt$ as in Eq. (3.179), we can assume an initial state of the form $[\hat{1} + \beta d\hat{B}^\dagger]|0\rangle$,

¹ Or the detector may burn out!

which is normalized to leading order. Now recall from Section 4.3.1 that a normalized one-photon state is $d\hat{B}^\dagger|0\rangle/\sqrt{dt}$. Therefore, the jump measurement operator is

$$\hat{M}_1(dt) = (dt)^{-1/2} \langle 0 | d\hat{B} \hat{U}(t + dt, t) [\hat{1} + \beta d\hat{B}^\dagger] | 0 \rangle, \quad (4.52)$$

which to leading order evaluates to

$$\hat{M}_1(dt) = (dt)^{1/2} (\hat{c} + \beta). \quad (4.53)$$

Similarly, the no-jump measurement operator

$$\hat{M}_0(dt) = \langle 0 | \hat{U}(t + dt, t) [\hat{1} + \beta d\hat{B}^\dagger] | 0 \rangle \quad (4.54)$$

evaluates to

$$\hat{M}_0(dt) = \hat{1} - [i\hat{H} + \frac{1}{2}\hat{c}^\dagger\hat{c} + \hat{c}^\dagger\beta]dt. \quad (4.55)$$

Exercise 4.3 *Show these.*

These measurement operators define the following SSE:

$$\begin{aligned} d|\psi_I(t)\rangle = & \left[dN(t) \left(\frac{\hat{c} + \beta}{\sqrt{\langle (\hat{c}^\dagger + \beta^*)(\hat{c} + \beta) \rangle_I(t)}} - 1 \right) + dt \right. \\ & \left. \times \left(\frac{\langle \hat{c}^\dagger \hat{c} \rangle_I(t)}{2} - \frac{c^\dagger \hat{c}}{2} + \frac{\langle \hat{c}^\dagger \beta + \beta^* \hat{c} \rangle_I(t)}{2} - \hat{c}^\dagger \beta - i\hat{H} \right) \right] |\psi_I(t)\rangle. \end{aligned} \quad (4.56)$$

The ensemble-average evolution is the master equation

$$\dot{\rho} = \mathcal{D}[\hat{c}]\rho - i[\hat{H} + i\beta^*\hat{c} - i\hat{c}^\dagger\beta, \rho], \quad (4.57)$$

which is as expected from Eq. (3.182) with $N = M = 0$. To ‘unravel’ this master equation for purposes of numerical calculation, one could choose the SSE as for the vacuum input (4.19), merely changing the Hamiltonian as indicated in the master equation (4.57). However, this would be a mistake if the trajectories were meant to represent the actual conditional evolution of the system, which is given by Eq. (4.56).

4.4 Homodyne detection

4.4.1 Adding a local oscillator

As noted in Section 3.6, the master equation

$$d\rho = -i dt [\hat{H}, \rho] + dt \mathcal{D}[\hat{c}]\rho \quad (4.58)$$

is invariant under the transformation

$$\hat{c} \rightarrow \hat{c} + \gamma; \quad \hat{H} \rightarrow \hat{H} - i\frac{1}{2}(\gamma^*\hat{c} - \gamma\hat{c}^\dagger), \quad (4.59)$$

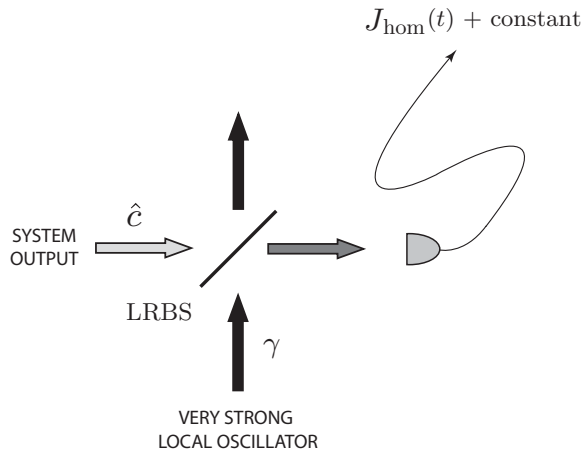


Fig. 4.1 A scheme for simple homodyne detection. A low-reflectivity beam-splitter (LRBS) transmits almost all of the system output, and adds only a small amount of the local oscillator through reflection. Nevertheless, the local oscillator is so strong that this reflected field dominates the intensity at the single photoreceiver. This is a detector that does not resolve single photons but rather produces a photocurrent proportional to $J_{\text{hom}}(t)$ plus a constant.

where γ is an arbitrary complex number (in particular, it is not related to the system damping rate for which we sometimes use γ). Under this transformation, the measurement operators transform to

$$\hat{M}_1(dt) = \sqrt{dt}(\hat{c} + \gamma), \quad (4.60)$$

$$\hat{M}_0(dt) = \hat{1} - dt \left[i\hat{H} + \frac{1}{2}(\hat{c}\gamma^* - \hat{c}^\dagger\gamma) + \frac{1}{2}(\hat{c}^\dagger + \gamma^*)(\hat{c} + \gamma) \right]. \quad (4.61)$$

This shows that the *unravelling* of the deterministic master-equation evolution into a set of stochastic quantum trajectories is not unique.

Physically, the above transformation can be achieved by homodyne detection. In the simplest configuration (see Fig. 4.1), the output field of the cavity is sent through a beam-splitter of transmittance η . The transformation of a field operator \hat{b} entering one port of a beam-splitter can be taken to be

$$\hat{b} \rightarrow \sqrt{\eta}\hat{b} + \sqrt{1-\eta}\hat{o}, \quad (4.62)$$

where \hat{o} is the operator for the field incident on the other port of the beam-splitter, which is reflected into the path of the transmitted beam. This other field transforms on transmission as $\hat{o} \rightarrow \sqrt{\eta}\hat{o} - \sqrt{1-\eta}\hat{b}$. (Note the minus sign.) In the case of homodyne detection, this other field is a very strong coherent field. It has the same frequency as the system dipole, and is known as the local oscillator. It can be modelled as $\hat{o} = \gamma/\sqrt{1-\eta} + \hat{v}$. The first part represents the coherent amplitude of the local oscillator, with $|\gamma|^2/(1-\eta)$ being its photon flux. The second part represents the ‘vacuum fluctuations’; \hat{v} is a continuum field

that satisfies $[\hat{v}(t), \hat{v}^\dagger(t')] = \delta(t - t')$ and can be assumed to act on the vacuum state. For η very close to unity, as is desired here, the transformation (4.62) reduces to

$$\hat{b} \rightarrow \hat{b} + \gamma, \quad (4.63)$$

which is called a displacement of the field (see Section A.4). A perfect measurement of the photon number of the displaced field leads to the above measurement operators.

Exercise 4.4 *Convince yourself of this.*

Let the coherent field γ be real, so that the homodyne detection leads to a measurement of the x quadrature of the system dipole. This can be seen from the rate of photodetections at the detector:

$$E[dN(t)/dt] = \text{Tr}[(\gamma^2 + \gamma \hat{x} + \hat{c}^\dagger \hat{c})\rho_I(t)]. \quad (4.64)$$

Here we are defining the two system quadratures by²

$$\hat{x} = \hat{c} + \hat{c}^\dagger; \quad \hat{y} = -i(\hat{c} - \hat{c}^\dagger). \quad (4.65)$$

In the limit that γ is much larger than $\langle \hat{c}^\dagger \hat{c} \rangle$, the rate (4.64) consists of a large constant term plus a term proportional to \hat{x} , plus a small term. From the measurement operators (4.60) and (4.61), the stochastic master equation for the conditioned state matrix is

$$d\rho_I(t) = \{dN(t)\mathcal{G}[\hat{c} + \gamma] + dt \mathcal{H}[-i\hat{H} - \gamma\hat{c} - \tfrac{1}{2}\hat{c}^\dagger \hat{c}]\}\rho_I(t). \quad (4.66)$$

This SME can be equivalently written as the SSE

$$\begin{aligned} d|\psi_I(t)\rangle = & \left[dN(t) \left(\frac{\hat{c} + \gamma}{\sqrt{\langle (\hat{c}^\dagger + \gamma)(\hat{c} + \gamma) \rangle_I(t)}} - 1 \right) + dt \right. \\ & \times \left(\frac{\langle \hat{c}^\dagger \hat{c} \rangle_I(t)}{2} - \frac{\hat{c}^\dagger \hat{c}}{2} + \frac{\langle \hat{c}^\dagger \gamma + \gamma \hat{c} \rangle_I(t)}{2} - \gamma \hat{c} - i\hat{H} \right) \Big] |\psi_I(t)\rangle. \end{aligned} \quad (4.67)$$

This shows how the master equation (4.58) can be unravelled in a completely different manner from the usual quantum trajectory (4.19). Note the minor difference from the coherently driven SSE (4.56), which makes the latter simulate a different master equation (4.57).

4.4.2 The continuum limit

The ideal limit of homodyne detection is when the local oscillator amplitude goes to infinity. In this limit, the rate of photodetections goes to infinity, but the effect of each detection on the system goes to zero, because the field being detected is almost entirely due to the local

² Be aware of the following possibility for confusion: for a two-level atom we typically have $\hat{c} = \hat{\sigma}_-$, in which case $\hat{x} = \hat{\sigma}_x$ but $\hat{y} = -\hat{\sigma}_y$!

oscillator. Thus, it should be possible to approximate the photocurrent by a continuous function of time, and also to derive a smooth evolution equation for the system. This was done first by Carmichael [Car93]; the following is a somewhat more rigorous working of the derivation he sketched.

Let the system operators be of order unity, and let the local oscillator amplitude γ be an arbitrarily large real parameter. Consider a time interval $[t, t + \delta t)$, where $\delta t = O(\gamma^{-3/2})$. This scaling is chosen so that, within this time interval, the number of detections $\delta N \sim \gamma^2 \delta t = O(\gamma^{1/2})$ is very large, but the systematic change in the system, of $O(\delta t) = O(\gamma^{-3/2})$, is very small. Taking the latter change into account, the mean number of detections in this time will be

$$\begin{aligned}\mu &= \text{Tr}[(\gamma^2 + \gamma \hat{x} + \hat{c}^\dagger \hat{c})\{\rho_I(t) + O(\gamma^{-3/2})\}]\delta t \\ &= [\gamma^2 + \gamma \langle \hat{x} \rangle_I(t) + O(\gamma^{1/2})]\delta t.\end{aligned}\quad (4.68)$$

The error in μ (due to the change in the system over the interval) is larger than the contribution from $\hat{c}^\dagger \hat{c}$. The variance in δN will be dominated by the Poissonian number statistics of the coherent local oscillator (see Section A.4.2). Because the number of counts is very large, these Poissonian statistics will be approximately Gaussian. Specifically, it can be shown [WM93b] that the statistics of δN are consistent with those of a Gaussian random variable of mean (4.68) and variance

$$\sigma^2 = [\gamma^2 + O(\gamma^{3/2})]\delta t. \quad (4.69)$$

The error in σ^2 is necessarily as large as expressed here in order for the statistics of δN to be consistent with Gaussian statistics. Thus, δN can be written as

$$\delta N = \gamma^2 \delta t [1 + \langle \hat{x} \rangle_I(t)/\gamma] + \gamma \delta W, \quad (4.70)$$

where the accuracy in both terms is only as great as the highest order expression in $\gamma^{-1/2}$. Here δW is a Wiener increment satisfying $E[\delta W] = 0$ and $E[(\delta W)^2] = \delta t$ (see Appendix B).

Now, insofar as the system is concerned, the time δt is still very small. Expanding Eq. (4.66) in powers of γ^{-1} gives

$$\begin{aligned}\delta \rho_I(t) &= \delta N(t) \left(\frac{\mathcal{H}[\hat{c}]}{\gamma} + \frac{\langle \hat{c}^\dagger \hat{c} \rangle_I(t) \mathcal{G}[\hat{c}] - \langle \hat{x} \rangle_I(t) \mathcal{H}[\hat{c}]}{\gamma^2} + O(\gamma^{-3}) \right) \rho_I(t) \\ &\quad + \delta t \mathcal{H}[-i\hat{H} - \gamma \hat{c} - \tfrac{1}{2} \hat{c}^\dagger \hat{c}] \rho_I(t),\end{aligned}\quad (4.71)$$

where \mathcal{G} and \mathcal{H} are as defined previously in Eqs. (4.23) and (4.24).

Exercise 4.5 Show this.

Although Eq. (4.66) requires that $dN(t)$ be a point process, it is possible simply to substitute the expression obtained above for δN as a Gaussian random variable into Eq. (4.71). This is because each jump is infinitesimal, so the effect of many jumps is approximately equal to

the effect of one jump scaled by the number of jumps. This can be justified by considering an expression for the system state given precisely δN detections, and then taking the large- δN limit [WM93b]. The simple procedure adopted here gives the correct answer more rapidly.

Keeping only the lowest-order terms in $\gamma^{-1/2}$ and letting $\delta t \rightarrow dt$ yields the SME

$$d\rho_J(t) = -i[\hat{H}, \rho_J(t)]dt + dt \mathcal{D}[\hat{c}]\rho_J(t) + dW(t)\mathcal{H}[\hat{c}]\rho_J(t), \quad (4.72)$$

where the subscript J is explained below, under Eq. (4.75). Here $dW(t)$ is an infinitesimal Wiener increment satisfying

$$dW(t)^2 = dt, \quad (4.73)$$

$$E[dW(t)] = 0. \quad (4.74)$$

That is, the jump evolution of Eq. (4.66) has been replaced by diffusive evolution.

Exercise 4.6 Derive Eq. (4.72).

By its derivation, Eq. (4.72) is an Itô stochastic differential equation, which we indicate by our use of the explicit increment (rather than the time derivative). It is trivial to see that the ensemble-average evolution reproduces the non-selective master equation by using Eq. (4.74) to eliminate the noise term. Readers unfamiliar with stochastic calculus, or unfamiliar with our conventions regarding the Itô and Stratonovich versions, are referred to Appendix B.

Just as $\gamma \rightarrow \infty$ leads to continuous evolution for the state, so does it change the point-process photocount into a continuous photocurrent with white noise. Removing the constant local oscillator contribution gives

$$J_{\text{hom}}(t) \equiv \lim_{\gamma \rightarrow \infty} \frac{\delta N(t) - \gamma^2 \delta t}{\gamma \delta t} = \langle \hat{x} \rangle_J(t) + \xi(t), \quad (4.75)$$

where $\xi(t) = dW(t)/dt$. This is why the subscript I has been replaced by J in Eq. (4.72).

Finally, it is worth noting that these equations can all be derived from balanced homodyne detection, in which the beam-splitter transmittance is one half, rather than close to unity (see Fig. 4.2). In that case, one photodetector is used for each output beam, and the signal photocurrent is the difference between the two currents. This configuration has the advantage of needing smaller local oscillator powers to achieve the same ratio of system amplitude to local oscillator amplitude, because all of the local oscillator beam is detected. Also, if the local oscillator has classical intensity fluctuations then these cancel out when the photocurrent difference is taken; with simple homodyne detection, these fluctuations are indistinguishable from (and may even swamp) the signal. Thus, in practice, balanced homodyne detection has many advantages over simple homodyne detection. But, in theory, the ideal limit is the same for both, which is why we have considered only simple homodyne detection. An analysis for balanced homodyne detection can be found in Ref. [WM93b].

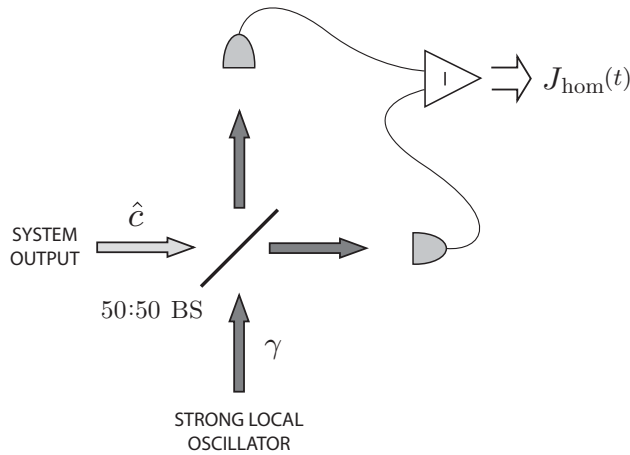


Fig. 4.2 A scheme for balanced homodyne detection. A 50 : 50 beam-splitter equally mixes the system output field and the local oscillator in both output ports. The local oscillator here can be weaker, but still dominates the intensity at the two photoreceivers. The difference between the two photocurrents is proportional to $J_{\text{hom}}(t)$.

4.4.3 Linear quantum trajectories

For pure initial states the homodyne SME (4.72) is equivalent to the SSE

$$\begin{aligned} d|\psi_J(t)\rangle = & \left\{ -i\hat{H} dt - \frac{1}{2}[\hat{c}^\dagger \hat{c} - 2\langle \hat{x}/2 \rangle_J(t)\hat{c} + \langle \hat{x}/2 \rangle_J^2(t)] dt \right. \\ & \left. + [\hat{c} - \langle \hat{x}/2 \rangle_J(t)] dW(t) \right\} |\psi_J(t)\rangle. \end{aligned} \quad (4.76)$$

If one ignores the normalization of the state vector, then one gets the simpler equation

$$d|\bar{\psi}_J(t)\rangle = dt \left[-i\hat{H} - \frac{1}{2}\hat{c}^\dagger \hat{c} + J_{\text{hom}}(t)\hat{c} \right] |\bar{\psi}_J(t)\rangle. \quad (4.77)$$

This SSE (which is the form Carmichael originally derived [Car93]) very elegantly shows how the state is conditioned on the measured photocurrent. We have used a bar rather than a tilde to denote the unnormalized state because its norm alone does not tell us the probability for a measurement result, unlike in the case of the unnormalized states introduced in Section 1.4. Nevertheless, the linearity of this equation suggests that it should be possible to derive it simply using quantum measurement theory, rather than in the complicated way we derived it above. This is indeed the case, as we will show below. In fact, a derivation for quantum diffusion equations like Eq. (4.76) was first given by Belavkin [Bel88] along the same lines as below, but more rigorously.

Consider the infinitesimally entangled bath–system state introduced in Eq. (4.36):

$$|\Psi(t + dt)\rangle = [\hat{1} - i\hat{H} dt - \frac{1}{2}\hat{c}^\dagger \hat{c} dt + d\hat{B}^\dagger \hat{c}] |0\rangle |\psi(t)\rangle. \quad (4.78)$$

Now because $d\hat{B}|0\rangle = 0$, it is possible to replace $d\hat{B}^\dagger$ in Eq. (4.78) by $d\hat{B}^\dagger + d\hat{B}$, giving

$$|\Psi(t + dt)\rangle = \left\{ \hat{1} - i\hat{H} dt - \frac{1}{2}\hat{c}^\dagger \hat{c} dt + \hat{c}[d\hat{B}^\dagger + d\hat{B}] \right\} |\psi(t)\rangle |0\rangle. \quad (4.79)$$

This is useful since we wish to consider measuring the x quadrature of the bath after it has interacted with the system. This measurement is modelled by projecting the field onto the eigenstates $|J\rangle$, where

$$[\hat{b} + \hat{b}^\dagger]|J\rangle = J|J\rangle. \quad (4.80)$$

The unnormalized system state conditioned on the measurement is thus

$$\begin{aligned} |\tilde{\psi}_J(t + dt)\rangle &= \langle J|\Psi(t + dt)\rangle \\ &= \left[\hat{1} - i\hat{H} dt - \frac{1}{2}\hat{c}^\dagger \hat{c} dt + \hat{c}J dt \right] |\psi(t)\rangle \sqrt{\wp_{\text{ost}}(J)}, \end{aligned} \quad (4.81)$$

where $\wp_{\text{ost}}(J)$ is the vacuum probability distribution for J ,

$$\wp_{\text{ost}}(J) = |\langle J|0\rangle|^2 = \sqrt{\frac{dt}{2\pi}} \exp\left[-\frac{1}{2} dt J^2\right]. \quad (4.82)$$

Exercise 4.7 Derive Eq. (4.82) from the wavefunction for the vacuum state (see Section A.4), remembering that $\sqrt{dt} \hat{b}$, not \hat{b} , acts like an annihilation operator.

We will call $\wp_{\text{ost}}(J)$ the *ostensible probability distribution* for J for reasons that will become obvious. The state-matrix norm of the state $|\tilde{\psi}_J(t + dt)\rangle$ gives the probability for the result J .

Taking the trace over the bath is the same as averaging over the measurement result, yielding

$$\rho(t + dt) = \int_{-\infty}^{\infty} dJ |\tilde{\psi}_J(t + dt)\rangle \langle \tilde{\psi}_J(t + dt)|. \quad (4.83)$$

Exercise 4.8 Show that this gives $d\rho(t) = dt \mathcal{L}\rho$, as in Eq. (4.11).

Note, however, that, since J is a continuous variable, the choice of integration measure in this integral is not unique. That is, we can remove the factor $\sqrt{\wp_{\text{ost}}(J)}$ in the state vector by changing the integration measure for the measurement result:

$$\rho(t + dt) = \int d\mu(J) |\tilde{\psi}_J(t + dt)\rangle \langle \tilde{\psi}_J(t + dt)|, \quad (4.84)$$

where

$$|\tilde{\psi}_J(t + dt)\rangle = \left[\hat{1} - i\hat{H} dt - \frac{1}{2}\hat{c}^\dagger \hat{c} dt + \hat{c}J dt \right] |\psi(t)\rangle \quad (4.85)$$

and $d\mu(J) = \wp_{\text{ost}}(J)dJ$. That is, we have a linear differential equation for a non-normalized state that nevertheless averages to the correct ρ , if $J(t)$ is chosen not according to its actual distribution, but according to its ostensible distribution, $\wp_{\text{ost}}(J)$. This equation (4.85) is known as a *linear quantum trajectory*.

Now Eq. (4.85) is the same as Eq. (4.77), where here we see that the homodyne photocurrent J_{hom} as we have defined it in Eq. (4.75) is simply a measurement of $\hat{b}^\dagger + \hat{b}$. All that remains is to show that the above theory correctly predicts the statistics for J . The true probability distribution for J is

$$\wp(J)dJ = \langle \tilde{\psi}_J(t+dt) | \tilde{\psi}_J(t+dt) \rangle dJ = \langle \bar{\psi}_J(t+dt) | \bar{\psi}_J(t+dt) \rangle d\mu(J). \quad (4.86)$$

That is, the *actual* probability for the result J equals the *ostensible* probability multiplied by the state-matrix norm of $|\bar{\psi}_J(t+dt)\rangle$. From Eq. (4.85), this evaluates to

$$\wp(J)dJ = \wp_{\text{ost}}(J)\{1 + J\langle\hat{x}\rangle dt - \langle\hat{c}^\dagger\hat{c}\rangle[dt - (J dt)^2]\}dJ. \quad (4.87)$$

We can clarify the orders of the terms here by defining a new variable $S = J\sqrt{dt}$ which is of order unity. Then

$$\wp(S)dS = (2\pi)^{-1/2} \exp(-S^2/2)[1 + S\langle\hat{x}\rangle\sqrt{dt} + O(dt)]dS, \quad (4.88)$$

or, to the same order in dt ,

$$\wp(S)dS = (2\pi)^{-1/2} \exp[-(S - \langle\hat{x}\rangle\sqrt{dt})^2/2]dS. \quad (4.89)$$

That is, the true distribution for the measured current J is

$$\wp(J)dJ = \wp_{\text{ost}}(J - \langle\hat{x}\rangle)dJ, \quad (4.90)$$

which is precisely the statistics generated by Eq. (4.75).

Exercise 4.9 *Convince yourself of this.*

It is also useful to consider the state-matrix version of Eq. (4.85):

$$d\bar{\rho}_J = dt \mathcal{L}\bar{\rho}_J + J dt (\hat{c}\bar{\rho}_J + \bar{\rho}_J\hat{c}^\dagger), \quad (4.91)$$

where we have used $(J dt)^2 = dt$, which is true in the statistical sense under the ostensible distribution – see Section B.2 (the same holds for the actual distribution to leading order). From this form it is easy to see that the ensemble-average evolution (with J chosen according to its ostensible distribution) is the master equation $\dot{\rho} = \mathcal{L}\rho$, because the ostensible mean of J is zero. The actual distribution of J is again the ostensible distribution multiplied by the norm of $\bar{\rho}_J$.

It is not a peculiarity of homodyne detection that we can reformulate a *nonlinear* equation for a *normalized* state in which $dW(t) = J(t)dt - \langle J(t) \rangle dt$ is white noise as a *linear* equation for a *non-normalized* state in which $J(t)$ has some other (ostensible) statistics. Rather, it is a completely general aspect of quantum or classical measurement theory. It is useful primarily in those cases in which the ostensible distribution for the measurement result $J(t)$ can be chosen so as to yield a particularly simple linear equation. That was the case above, where we chose $J(t)$ to have the ostensible statistics of white noise. Another convenient choice might be for the ostensible statistics of $J(t)$ to be Gaussian with a variance of $1/dt$ (as in white noise) but a mean of μ . In that case Eq. (4.91) becomes

$$d\bar{\rho}_J = dt \mathcal{L}\bar{\rho}_J + (J - \mu)dt (\hat{c}\bar{\rho}_J + \bar{\rho}_J\hat{c}^\dagger - \mu\bar{\rho}_J). \quad (4.92)$$

Exercise 4.10 Show that this does give the correct average ρ , and the correct actual distribution for $J(t)$.

From this, we see that the *nonlinear* quantum trajectory (4.72) is just a special case in which μ is chosen to be equal to the *actual* mean of $J(t)$, since then

$$J(t) - \mu = J(t) - \langle J(t) \rangle_J = J(t) - \text{Tr}[(\hat{c} + \hat{c}^\dagger)\rho_J(t)] = dW(t)/dt. \quad (4.93)$$

4.4.4 Output field correlation functions

As for direct detection, the dynamics of the system can be conveniently quantified by calculating the mean and autocorrelation function of the homodyne photocurrent. The mean is simply

$$E[J_{\text{hom}}(t)] = \text{Tr}[\rho(t)\hat{x}], \quad (4.94)$$

where $\hat{x} = \hat{c} + \hat{c}^\dagger$, as usual, and $\rho(t)$ is assumed given (it could be ρ_{ss}). The autocorrelation function is defined as

$$F_{\text{hom}}^{(1)}(t, t + \tau) = E[J_{\text{hom}}(t + \tau)J_{\text{hom}}(t)]. \quad (4.95)$$

We use a superscript (1), rather than (2), because this function is related to Glauber's *first-order* coherence function [Gla63], as will be shown in Section 4.5.1.

From Eq. (4.75) and the fact that $\xi(t + \tau)$ is independent of the system at the past times t , this expression can be split into three terms,

$$F_{\text{hom}}^{(1)}(t, t + \tau) = E[\langle \hat{x} \rangle_J(t + \tau)\xi(t)] + E[\xi(t + \tau)\xi(t)] + E[\langle \hat{x} \rangle_J(t + \tau)]\langle \hat{x} \rangle(t), \quad (4.96)$$

where the factorization of the third term is due to the fact that $\rho(t)$ is given. The second term here is equal to $\delta(\tau)$. The first term is non-zero because the conditioned state of the system at time $t + \tau$ depends on the noise in the photocurrent at time t . That noise enters by the conditioning equation (4.72), so

$$\rho_J(t + dt) = \rho(t) + O(dt) + dW(t)\mathcal{H}[\hat{c}]\rho(t). \quad (4.97)$$

The subsequent stochastic evolution of the system will be independent of the noise $\xi(t) = dW(t)/dt$ and hence may be averaged, giving

$$E[\langle \hat{x} \rangle_J(t + \tau)\xi(t)] = \text{Tr}\left[\hat{x}e^{\mathcal{L}\tau}E\{[1 + dW(t)\mathcal{H}[\hat{c}]]\rho_J(t)dW(t)/dt\}\right]. \quad (4.98)$$

Using the Itô rules for $dW(t)$ and expanding the superoperator \mathcal{H} yields

$$E[\langle \hat{x} \rangle_J(t + \tau)\xi(t)] = \text{Tr}[\hat{x}e^{\mathcal{L}\tau}(\hat{c}\rho(t) + \rho(t)\hat{c}^\dagger)] - \text{Tr}[\hat{x}e^{\mathcal{L}\tau}\rho(t)]\text{Tr}[\hat{x}\rho(t)]. \quad (4.99)$$

The second term here cancels out the third term in Eq. (4.96), to give the final expression

$$F_{\text{hom}}^{(1)}(t, t + \tau) = \text{Tr}[\hat{x}e^{\mathcal{L}\tau}(\hat{c}\rho(t) + \rho(t)\hat{c}^\dagger)] + \delta(\tau). \quad (4.100)$$

Experimentally, it is more common to represent the information in the correlation function by its Fourier transform. At steady state, this is known as the *spectrum* of the homodyne

photocurrent,

$$S(\omega) = \lim_{t \rightarrow \infty} \int_{-\infty}^{\infty} d\tau F_{\text{hom}}^{(1)}(t, t + \tau) e^{-i\omega\tau} \quad (4.101)$$

$$= 1 + \int_{-\infty}^{\infty} d\tau e^{-i\omega\tau} \text{Tr}[\hat{x} e^{\mathcal{L}\tau} (\hat{c}\rho_{\text{ss}} + \rho_{\text{ss}}\hat{c}^\dagger)]. \quad (4.102)$$

The unit contribution is known as the local oscillator shot noise or vacuum noise because it is present even when there is no light from the system.

4.5 Heterodyne detection and beyond

4.5.1 Heterodyne detection

Homodyne detection has the advantage over direct detection that it can detect phase-dependent properties of the system. By choosing the phase of the local oscillator, any given quadrature of the system can be measured. However, only one quadrature can be measured at a time. It would be possible to obtain information about two orthogonal quadratures simultaneously by splitting the system output beam into two by use of a beam-splitter, and then homodyning each beam with the same local oscillator apart from a $\pi/2$ phase shift. An alternative way to achieve this double measurement is to detune the local oscillator from the system dipole frequency by an amount Δ much larger than any other system frequency. The photocurrent will then oscillate rapidly at frequency Δ , and the two Fourier components (cos and sin) of this oscillation will correspond to two orthogonal quadratures of the output field. This is known as heterodyne detection, which is the subject of this section

Begin with the homodyne SME (4.72), which assumed a constant local oscillator amplitude and phase. Detuning the local oscillator to a frequency Δ above that of the system will affect only the final (stochastic) term in Eq. (4.72). Its effect will be simply to replace \hat{c} by $\hat{c} \exp(i\Delta t)$, giving

$$\begin{aligned} d\rho_J(t) = & -i[\hat{H}, \rho_J(t)]dt + \mathcal{D}[\hat{c}]\rho_J(t)dt \\ & + dW(t)\{e^{i\Delta t} [\hat{c}\rho_J(t) - \langle\hat{c}\rangle_J(t)\rho_J(t)] + \text{H.c.}\}. \end{aligned} \quad (4.103)$$

Consider a time δt , small on a characteristic time-scale of the system, but large compared with Δ^{-1} so that there are many cycles due to the detuning. One might think that averaging the rotating exponentials over this time would eliminate the terms in which they appear. However, this is not the case because these terms are stochastic, and, since the noise is white by assumption, it will vary even faster than the rotation at frequency Δ . Define two new Gaussian random variables

$$\delta W_x(t) = \int_t^{t+\delta t} \sqrt{2} \cos(\Delta s) dW(s), \quad (4.104)$$

$$\delta W_y(t) = - \int_t^{t+\delta t} \sqrt{2} \sin(\Delta s) dW(s). \quad (4.105)$$

It is easy to show that, to zeroth order in Δ^{-1} , these obey

$$E[\delta W_q(t)\delta W_{q'}(t')] = \delta_{q,q'}(\delta t - |t - t'|)\Theta(\delta t - |t - t'|), \quad (4.106)$$

where q and q' stand for x or y , and Θ is the Heaviside function, which is zero when its argument is negative and one when its argument is positive.

On the system's time-scale δt is infinitesimal. Thus the $\delta W_q(t)$ can be replaced by infinitesimal Wiener increments $dW_q(t)$ obeying

$$\langle \xi_q(t)\xi_{q'}(t') \rangle = \delta_{q,q'}\delta(t - t'), \quad (4.107)$$

where $\xi_q(t) = dW_q(t)/dt$. Taking the average over many detuning cycles therefore transforms Eq. (4.103) into

$$\begin{aligned} d\rho_J(t) = & -i[\hat{H}, \rho_J(t)]dt + \mathcal{D}[\hat{c}]\rho_J(t)dt \\ & + \sqrt{1/2}(dW_x(t)\mathcal{H}[\hat{c}] + dW_y(t)\mathcal{H}[-i\hat{c}])\rho_J(t). \end{aligned} \quad (4.108)$$

Exercise 4.11 Verify Eq. (4.106) and hence convince yourself of Eqs. (4.107) and (4.108).

Hint: Show that the right-hand side of Eq. (4.106) is zero when $|t - t'| > \delta t$, and that integrating over t or t' yields $(\delta t)^2$.

This is equivalent to homodyne detection of the two quadratures simultaneously, each with efficiency $1/2$. (Non-unit efficiency will be discussed in Section 4.8.1). On defining a normalized complex Wiener process by

$$dZ = (dW_x + i dW_y)/\sqrt{2}, \quad (4.109)$$

which satisfies $dZ^* dZ = dt$ but $dZ^2 = 0$, we can write Eq. (4.108) more elegantly as

$$d\rho_J(t) = -i[\hat{H}, \rho_J(t)]dt + \mathcal{D}[\hat{c}]\rho_J(t)dt + \mathcal{H}[dZ^*(t)\hat{c}]\rho_J(t). \quad (4.110)$$

In order to record the measurements of the two quadratures, it is necessary to find the Fourier components of the photocurrent. These are defined by

$$J_x(t) = (\delta t)^{-1} \int_t^{t+\delta t} 2 \cos(\Delta s) J_{\text{hom}}(s) ds, \quad (4.111)$$

$$J_y(t) = -(\delta t)^{-1} \int_t^{t+\delta t} 2 \sin(\Delta s) J_{\text{hom}}(s) ds. \quad (4.112)$$

To zeroth order in Δ^{-1} , these are

$$J_x(t) = \langle \hat{x} \rangle_J(t) + \sqrt{2}\xi_x(t), \quad (4.113)$$

$$J_y(t) = \langle \hat{y} \rangle_J(t) + \sqrt{2}\xi_y(t). \quad (4.114)$$

(Recall that \hat{x} and \hat{y} are the quadratures defined in Eq. (4.65).) Again, these are proportional to the homodyne photocurrents that are expected for an efficiency of $1/2$ (see Section 4.8.1).

We can combine these photocurrents to make a complex heterodyne photocurrent

$$J_{\text{het}}(t) = (\delta t)^{-1} \int_t^{t+\delta t} \exp(-i\Delta s) J_{\text{hom}}(s) ds \quad (4.115)$$

$$= \frac{1}{2} [J_x(t) + iJ_y(t)] \quad (4.116)$$

$$= \langle \hat{c} \rangle_J(t) + dZ(t)/dt, \quad (4.117)$$

where dZ is as defined in Eq. (4.109). In terms of this current, one can derive an unnormalized SSE analogous to Eq. (4.77):

$$d|\bar{\psi}_J(t)\rangle = dt \left[-i\hat{H} - \frac{1}{2}\hat{c}^\dagger \hat{c} + J_{\text{het}}(t)^* \hat{c} \right] |\bar{\psi}_J(t)\rangle. \quad (4.118)$$

Equation (4.118), with the expression (4.117) in place of J_{het} , was introduced by Gisin and Percival in 1992 [GP92b] as ‘quantum state diffusion’. However, they considered it to describe the objective evolution of a single open quantum system, rather than the conditional evolution under a particular detection scheme as we are interpreting it.

Using the same techniques as in Section 4.4.4, it is simple to show that the average complex heterodyne photocurrent is

$$E[J_{\text{het}}(t)] = \text{Tr}[\rho(t)\hat{c}], \quad (4.119)$$

and the autocorrelation function (note the use of the complex conjugate) is

$$E[J_{\text{het}}(t+\tau)^* J_{\text{het}}(t)] = \text{Tr}[\hat{c}^\dagger e^{\mathcal{L}\tau} \hat{c} \rho(t)] + \delta(\tau). \quad (4.120)$$

Ignoring the second (δ -function) term in this autocorrelation function, the remainder is simply Glauber’s first-order coherence function $G^{(1)}(t, t+\tau)$ [Gla63]. In steady state this is related to the so-called *power spectrum* of the system by

$$P(\omega) = \frac{1}{2\pi} \int_{-\infty}^{\infty} d\tau e^{-i\omega\tau} \text{Tr}[\hat{c}^\dagger e^{\mathcal{L}\tau} \hat{c} \rho_{\text{ss}}]. \quad (4.121)$$

This can be interpreted as the photon flux in the system output per unit frequency (a dimensionless quantity).

Exercise 4.12 Show that $\int_{-\infty}^{\infty} d\omega P(\omega) = \text{Tr}[\hat{c}^\dagger \hat{c} \rho_{\text{ss}}]$ and that this is consistent with the above interpretation.

In practice it is this second interpretation that is usually used to measure $P(\omega)$. That is, the power spectrum is usually measured by using a spectrometer to determine the output intensity as a function of frequency, rather than by autocorrelating the heterodyne photocurrent.

4.5.2 Completely general dyne detection

Heterodyne detection, like homodyne detection, leads to an unravelling that is continuous in time. For convenience, we will call unravellings with this property *dyne* unravellings.

In this section, we give a complete classification of all such unravellings, for the general Lindblad master equation

$$\dot{\rho} = \mathcal{L}\rho \equiv -i[\hat{H}, \rho] + \hat{c}_k \rho \hat{c}_k^\dagger - \frac{1}{2} \left\{ \hat{c}_k^\dagger \hat{c}_k, \rho \right\}. \quad (4.122)$$

Here, and in related sections, we are using the Einstein summation convention because this simplifies many of the formulae. That is, there is an implicit sum for repeated indices, which for k is from 1 to K . Using this convention, the most general SME was shown in Ref. [WD01] to be

$$d\rho_{\bar{j}} = dt \mathcal{L}\rho_{\bar{j}} + [\hat{c}_k - \langle \hat{c}_k \rangle] \rho_{\bar{j}} dZ_k^* + \text{H.c.}] \quad (4.123)$$

Here the dZ_k are complex Wiener increments satisfying

$$dZ_j(t) dZ_k^*(t) = dt \delta_{jk}, \quad (4.124)$$

$$dZ_j(t) dZ_k(t) = dt \Upsilon_{jk}. \quad (4.125)$$

The $\Upsilon_{jk} = \Upsilon_{kj}$ are arbitrary complex numbers subject only to the condition that the cross-correlations for Z are consistent with the self-correlations. This is the case iff (if and only if) the $2K \times 2K$ correlation matrix of the vector $(\text{Re}[d\vec{Z}], \text{Im}[d\vec{Z}])$ is positive semi-definite.³ That is,

$$\frac{dt}{2} \begin{pmatrix} I + \text{Re}[\Upsilon] & \text{Im}[\Upsilon] \\ \text{Im}[\Upsilon] & I - \text{Re}[\Upsilon] \end{pmatrix} \geq 0. \quad (4.126)$$

Here the real part of a matrix A is defined as $\text{Re}[A] = (A + A^*)/2$, and similarly $\text{Im}[A] = -i(A - A^*)/2$. Equation (4.126) is satisfied in turn iff the spectral norm of Υ is bounded from above by unity. That is,

$$\|\Upsilon\|^2 \equiv \lambda_{\max}(\Upsilon^\dagger \Upsilon) \leq 1, \quad (4.127)$$

where $\lambda_{\max}(A)$ denotes the maximum of the real parts of the eigenvalues of A . In the present context, the eigenvalues of A are real, of course, since $\Upsilon^\dagger \Upsilon$ is Hermitian.

Exercise 4.13 Show that Eq. (4.126) is satisfied iff Eq. (4.127) is satisfied.

Hint: Consider the real symmetric matrix

$$X = \begin{pmatrix} \text{Re}[\Upsilon] & \text{Im}[\Upsilon] \\ \text{Im}[\Upsilon] & -\text{Re}[\Upsilon] \end{pmatrix}. \quad (4.128)$$

Show that the eigenvalues of X are symmetrically placed around the origin. Thus we will have $I + X \geq 0$ iff $\|X\| \leq 1$. This in turn will be the case iff X^{2n} converges as $n \rightarrow \infty$. Show that

$$X^{2n} = \begin{pmatrix} \text{Re}[A^n] & \text{Im}[A^n] \\ -\text{Im}[A^n] & \text{Re}[A^n] \end{pmatrix}, \quad (4.129)$$

where $A = \Upsilon^\dagger \Upsilon$, and hence show the desired result.

³ A positive semi-definite matrix A is an Hermitian matrix with no negative eigenvalues, indicated by $A \geq 0$.

Box 4.1 Gauge-invariance of SMEs

Consider the following transformation of a state vector:

$$|\psi(t)\rangle \rightarrow |\phi\rangle = \exp[i\chi(t)]|\psi(t)\rangle, \quad (4.130)$$

where $\chi(t)$ is an arbitrary real function of time. This is known as a *gauge transformation*. It has no effect on any physical properties of the system. However, it can radically change the appearance of a stochastic Schrödinger equation, since $\chi(t)$ may be stochastic. Consider for example the simple SSE

$$d|\psi\rangle = [-i\hat{H} - \frac{1}{2}(\hat{x} - \langle\hat{x}\rangle)^2]dt|\psi\rangle + (\hat{x} - \langle\hat{x}\rangle)dZ^*|\psi\rangle, \quad (4.131)$$

where $dZ dZ^* = dt$ and $dZ^2 = \nu dt$. Let the global phase χ obey the equation

$$d\chi = f dZ^* + f^* dZ, \quad (4.132)$$

where $f(t)$ is an arbitrary smooth function of time that may even be a function of $|\psi\rangle$ itself. Then

$$|\phi\rangle + d|\phi\rangle = (1 + i d\chi - \frac{1}{2} d\chi d\chi) e^{i\chi(t)} (|\psi\rangle + d|\psi\rangle). \quad (4.133)$$

The resultant equation for $|\phi\rangle$ is

$$\begin{aligned} d|\phi\rangle = & [-i\hat{H} - \text{Re}(f^2\nu^* + |f|^2)]dt|\phi\rangle \\ & - \frac{1}{2}(\hat{x} - \langle\hat{x}\rangle)(\hat{x} - \langle\hat{x}\rangle + if\nu^* + if^*)dt|\phi\rangle \\ & + [(\hat{x} - \langle\hat{x}\rangle + if)dZ^* + if^*dZ]|\phi\rangle, \end{aligned} \quad (4.134)$$

which appears quite different from Eq. (4.131) (think of the case $f = -i\langle\hat{x}\rangle$, for example). By contrast, the SME is invariant under global phase changes:

$$d\rho = -i dt [\hat{H}, \rho] + dt \mathcal{D}[\hat{x}]\rho + \mathcal{H}[dZ^* \hat{x}]\rho. \quad (4.135)$$

The above formulae apply for *efficient detection* (see Section 4.8 for a discussion of inefficient detection and Section 6.5.2 for the required generalization). Thus we could write the unravelling as a SSE rather than the SME (4.123). However, there are good reasons to prefer the SME form, even for efficient detection. First, it is more general in that it can describe the purification of an initially mixed state. Second, it is easier to see the relation between the quantum trajectories and the master equation which the system still obeys on average. Third, it is invariant under gauge transformations (see Box 4.1).

As expected from Section 4.4.3, the SME (4.123) can be derived directly from quantum measurement theory. We describe the measurement result in the infinitesimal time interval $[t, t + dt]$ by a vector of complex numbers $\vec{J}(t) = \{J_k(t)\}_{k=1}^K$. As functions of time, these are continuous but not differentiable, and, following the examples of homodyne and heterodyne

detection, we will call them currents. Explicitly, they are given by

$$J_k dt = d\left\langle \Upsilon_{kj} \hat{c}_j^\dagger + \hat{c}_k \right\rangle + dZ_k. \quad (4.136)$$

We can prove this relation between the noise in the quantum trajectory and the noise in the measurement record by using the measurement operators

$$\hat{M}_{\vec{J}} = \hat{1} - i\hat{H} dt - \frac{1}{2} \hat{c}_k^\dagger \hat{c}_k dt + J_k^* \hat{c}_k dt. \quad (4.137)$$

These obey the completeness relation

$$\int d\mu(\vec{J}) \hat{M}_{\vec{J}}^\dagger \hat{M}_{\vec{J}} = \hat{1} \quad (4.138)$$

if we choose $d\mu(\vec{J})$ to be the measure yielding the ostensible moments

$$\int d\mu(\vec{J}) (J_k dt) = 0, \quad (4.139)$$

$$\int d\mu(\vec{J}) (J_j^* dt)(J_k dt) = \delta_{jk} dt, \quad (4.140)$$

$$\int d\mu(\vec{J}) (J_j dt)(J_k dt) = \Upsilon_{jk} dt. \quad (4.141)$$

Exercise 4.14 Show this.

These moments are the same as those of the Wiener increment $d\vec{Z}$ as defined above.

With this assignment of measurement operators $\hat{M}_{\vec{J}}$ and measure $d\mu(\vec{J})$ we can easily show that the expected value of the result \vec{J} is

$$E[J_k] = \int d\mu(\vec{J}) \text{Tr}[\hat{M}_{\vec{J}} \rho \hat{M}_{\vec{J}}^\dagger] J_k = \left\langle \Upsilon_{kj} \hat{c}_j^\dagger + \hat{c}_k \right\rangle. \quad (4.142)$$

This is consistent with the previous definition in Eq. (4.136). Furthermore, as in Section 4.4.3, we can show that the second moments of $\vec{J} dt$ are (to leading order in dt) independent of the system state and can be calculated using $d\mu$. In other words, they are identical to the statistics of $d\vec{Z}$ as defined above. This completes the proof that Eq. (4.136) gives the correct probability for the result \vec{J} .

The next step is to derive the conditioned state of the system after the measurement. This is given by

$$\rho + d\rho_{\vec{J}} = \frac{\hat{M}_{\vec{J}} \rho \hat{M}_{\vec{J}}^\dagger}{\text{Tr}[\hat{M}_{\vec{J}} \rho \hat{M}_{\vec{J}}^\dagger]}. \quad (4.143)$$

Expanding to order dt gives

$$\begin{aligned} d\rho_{\vec{J}} = & -\frac{1}{2} \left\{ \hat{c}_k^\dagger \hat{c}_k, \rho_{\vec{J}} \right\} dt + J_k^* dt \hat{c}_k \rho_{\vec{J}} \hat{c}_l^\dagger J_l dt + (J_k^* dt J_k - 1) \left\langle \hat{c}_j^\dagger \hat{c}_j \right\rangle \rho_{\vec{J}} dt \\ & - i[\hat{H}, \rho_{\vec{J}}] dt + \left[J_k^* (\hat{c}_k - \langle \hat{c}_k \rangle) \rho_{\vec{J}} dt + \rho_{\vec{J}} \left(\hat{c}_k^\dagger - \langle \hat{c}_k^\dagger \rangle \right) J_k dt \right] \\ & \times \left(1 - J_l^* \langle \hat{c}_l \rangle dt - J_l \langle \hat{c}_l^\dagger \rangle dt \right). \end{aligned} \quad (4.144)$$

Exercise 4.15 Verify Eqs. (4.142) and (4.144).

Substituting into the above result (4.136) for \vec{J} yields the required equation (4.123). From this it is again obvious that on average the system obeys the master equation (4.11).

Exercise 4.16 Verify that Eq. (4.144) gives Eq. (4.123). Also find the linear version of Eq. (4.144) for the ostensible distribution used above.

4.6 Illustration on the Bloch sphere

Before proceeding further with the theory, we will pause to illustrate the different sorts of quantum trajectories introduced above using a simple example. Perhaps the simplest nontrivial open quantum system is the driven and damped two-level atom as introduced in Section 3.3.1. Taking the bath temperature to be zero ($\bar{n} = 0$), the resonance fluorescence master equation (3.36) is

$$\dot{\rho} = -i \left[\frac{\Omega}{2} \hat{\sigma}_x + \frac{\Delta}{2} \hat{\sigma}_z, \rho \right] + \gamma \mathcal{D}[\hat{\sigma}_-] \rho. \quad (4.145)$$

The solutions to this equation were the subject of Exercise 3.26. We now consider five different unravellings of this master equation.

4.6.1 Direct photodetection

The state of a classically driven two-level atom conditioned on direct photodetection of its resonance fluorescence was one of the inspirations for the development of the quantum trajectory theory in optics [CSVR89, DCM92, DZR92]. The treatment here is restricted to formulating the stochastic evolution in the manner of Section 4.2.2 and giving a closed-form expression for the stationary probability distribution of states on the Bloch sphere [WM93a].

Consider a two-level atom situated in an experimental apparatus such that the light it emits is all collected and enters a detector. (In principle this could be achieved by placing the atom at the focus of a large parabolic mirror, as shown in Fig. 4.3.) Then the direct detection theory of Section 4.3.1 can be applied, with $\hat{c} = \sqrt{\gamma} \hat{\sigma}_-$. The state vector of the atom conditioned on the photodetector count obeys the following SSE:

$$\begin{aligned} d|\psi_I(t)\rangle = & \left[dN(t) \left(\frac{\hat{\sigma}_-}{\sqrt{\langle \hat{\sigma}_-^\dagger \hat{\sigma}_- \rangle_I(t)}} - 1 \right) \right. \\ & \left. - dt \left(\frac{\gamma}{2} [\hat{\sigma}_-^\dagger \hat{\sigma}_- - \langle \hat{\sigma}_-^\dagger \hat{\sigma}_- \rangle_I(t)] + i\hat{H} \right) \right] |\psi_I(t)\rangle, \end{aligned} \quad (4.146)$$

where $\hat{H} = \frac{1}{2}(\Omega \hat{\sigma}_x + \Delta \hat{\sigma}_z)$ and the photocount increment $dN(t)$ satisfies $E[dN(t)] = \gamma \langle \hat{\sigma}_-^\dagger \hat{\sigma}_- \rangle_I(t) dt$.

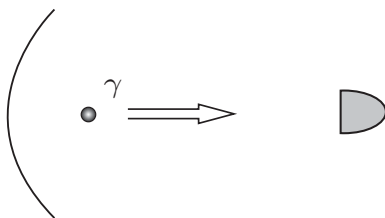


Fig. 4.3 A scheme for direct detection of an atom. The atom is placed at the focus of a parabolic mirror so that all the fluorescence emitted by the atom is detected by the photodetector. Figure 1 adapted with permission from J. Gambetta *et al.*, *Phys. Rev. A* **64**, 042105, (2001). Copyrighted by the American Physical Society.

With the conditioned subscript understood, one can write the conditioned state in terms of the Euler angles (ϕ, θ) parameterizing the surface of the Bloch sphere. Since we are assuming a pure state (see Box. 3.1),

$$|\psi(t)\rangle = c_g|g\rangle + c_e|e\rangle, \quad (4.147)$$

these angles are given by

$$\phi(t) = \arg[c_g(t)c_e^*(t)], \quad (4.148)$$

$$\theta(t) = 2 \arctan[|c_g(t)/c_e(t)|]. \quad (4.149)$$

Exercise 4.17 Show this, using the usual relation between $(\phi, \theta, r := 1)$ and (x, y, z) , with $|0\rangle = |g\rangle$ and $|1\rangle = |e\rangle$.

A typical stochastic trajectory is shown in Fig. 4.4. From an ensemble of these one could obtain the stationary distribution $\wp_{ss}(\phi, \theta)$ for the states on the Bloch sphere under direct detection.

In practice, it is easier to find the steady-state solution by returning to the SSE (4.146) and ignoring normalization terms. Consider the evolution of the system following a photodetection at time $t = 0$ so that $|\psi(0)\rangle = |g\rangle$. Assuming that no further photodetections take place, and omitting the normalization terms in Eq. (4.146), the state evolves via

$$\frac{d}{dt}|\tilde{\psi}_0(t)\rangle = -\left(\frac{\gamma}{2}\hat{\sigma}_-^\dagger\hat{\sigma}_- + i\hat{H}\right)|\tilde{\psi}_0(t)\rangle. \quad (4.150)$$

Here, the state vector has a state-matrix norm equal to the probability of it remaining in this no-jump state, as discussed in Section 4.2.3.

On writing the unnormalized conditioned state vector as

$$|\tilde{\psi}_0(t)\rangle = \tilde{c}_g(t)|g\rangle + \tilde{c}_e(t)|e\rangle, \quad (4.151)$$

the solution satisfying $\tilde{c}_j(0) = \delta_{j,g}$ is easily found to be

$$\tilde{c}_g(t) = \cos(\alpha t) + \frac{\gamma/2 + i\Delta}{2\alpha} \sin(\alpha t), \quad (4.152)$$

$$\tilde{c}_e(t) = -i\frac{\Omega}{2\alpha} \sin(\alpha t), \quad (4.153)$$

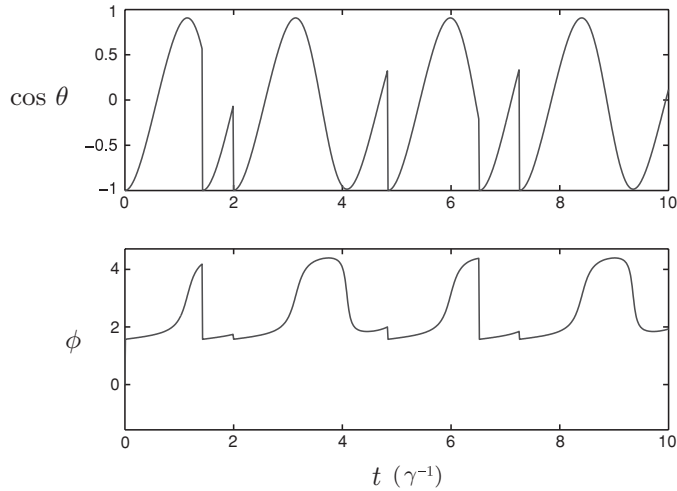


Fig. 4.4 A typical trajectory for the conditioned state of an atom under direct detection in terms of the Bloch angles ϕ and $\cos \theta$. The driving and detuning are $\Omega = 3$ and $\Delta = 0.5$, in units of the decay rate γ .

where

$$2\alpha = [(\Delta - i\gamma/2)^2 + \Omega^2]^{1/2} \quad (4.154)$$

is a complex number that reduces to the detuned Rabi frequency as $\gamma \rightarrow 0$. One can still use the definitions (4.148) and (4.149) with c_j replaced by \tilde{c}_j , since they are insensitive to normalization. The significance of the normalization is that

$$S(t) = \langle \tilde{\psi}_0(t) | \tilde{\psi}_0(t) \rangle = |\tilde{c}_g(t)|^2 + |\tilde{c}_e(t)|^2 \quad (4.155)$$

is the probability of there being no detections from time 0 up to time t .

Exercise 4.18 Show that for the case $\Delta = 0$, $\Omega > \gamma/2$, the no-jump quantum trajectory traverses the $x = 0$ great circle of the Bloch sphere.

Whenever a photodetection does occur, the system returns to its state at $t = 0$. It then takes a finite time until the excited-state population becomes finite and the atom can re-emit. This gives the obvious interpretation for the photon *antibunching* predicted [CW76] and observed [KDM77] in the resonance fluorescence of a two-level atom. This is the phenomenon that, for some time following one detection, another detection is *less likely*. The term was defined to contrast with photon *bunching* (where following one detection another detection is *more likely*), which was the only correlation that had hitherto been observed. The re-excitation of the atom is always identical, so the stationary probability distribution on the Bloch sphere $\wp_{ss}(\phi, \theta)$ is confined to the curve parameterized by $(\phi(t), \theta(t))$, with each point weighted by the survival probability $S(t)$. (For $\Delta = 0$ this curve wraps around on itself, so that each point obtains multiple contributions to its weight.)

4.6.2 Adaptive detection with a local oscillator

Recall that in Section 3.8.2 we discussed the conditions under which a probability distribution of pure states $\{(\hat{\pi}_k, \wp_k)\}_k$ could be *physically realizable* (PR). An ensemble is PR if there is a continuous measurement scheme such that an experimenter implementing it would be able to know, at some time far in the future from the initial preparation, that the system is in one of the states $\hat{\pi}_k$, and the probability for each state would be \wp_k .

From the preceding section it is evident that the stationary distribution $\wp_{ss}(\phi, \theta)$ on the surface of the Bloch sphere introduced in the preceding subsection is just such a PR ensemble. The continuous measurement scheme which realizes the ensemble is, of course, direct detection. As discussed above, in the case $\Delta = 0$, $\wp_{ss}(\phi, \theta)$ is confined to the $x = 0$ great circle of the Bloch sphere.

In Section 3.8.3 we presented an example of a PR ensemble for the resonance fluorescence master equation (4.145) (for $\Delta = 0$) that was quite different from that in the preceding section. Specifically, the ensemble contained just two pure states $\hat{\pi}_{\pm}$, equally weighted, defined by the Bloch vectors

$$\begin{pmatrix} u \\ v \\ w \end{pmatrix}_{\pm} = \begin{pmatrix} \pm\sqrt{1 - y_{ss}^2 - z_{ss}^2} \\ y_{ss} \\ z_{ss} \end{pmatrix}. \quad (4.156)$$

It turns out that this can be generalized for $\Delta \neq 0$, but it is a lot more complicated, so in this section we retain $\Delta = 0$. For large Ω , these points on the Bloch sphere approach the antipodal pair at $x = \pm 1$.

Exercise 4.19 Show this, and show that in the same limit the direct detection ensemble becomes equally spread over the $x = 0$ great circle.

Thus, these two PR ensembles are as different as they possibly can be.

In Section 3.8.3 we did not identify the measurement scheme that realizes this ensemble. Since the elements of the ensemble are discrete, the unravelling must involve jumps. Since it is not the direct detection unravelling of the preceding section, it must involve a local oscillator, as introduced in Section 4.4.1. Since here we are using γ for the atomic decay rate, in this section we use $\sqrt{\gamma}\mu$ for the local oscillator amplitude. The no-jump and jump measurement operators are then

$$\hat{M}_0(dt) = \hat{1} - \left(i\frac{\Omega}{2}\hat{\sigma}_x + \frac{\gamma}{2}\hat{\sigma}_-^{\dagger}\hat{\sigma}_- + \mu^*\gamma\hat{\sigma}_- + \frac{\gamma|\mu|^2}{2} \right) dt, \quad (4.157)$$

$$\hat{M}_1(dt) = \sqrt{\gamma dt} (\hat{\sigma}_- + \mu). \quad (4.158)$$

Direct detection is recovered by setting $\mu = 0$.

If the atom radiates into a beam as considered previously, the above measurement can be achieved by mixing it with a resonant local oscillator at a beam-splitter, as shown in Fig. 4.5. The transmittance of the beam-splitter must be close to unity. The phase of μ is of course defined relative to the field driving the atom, parameterized by Ω .

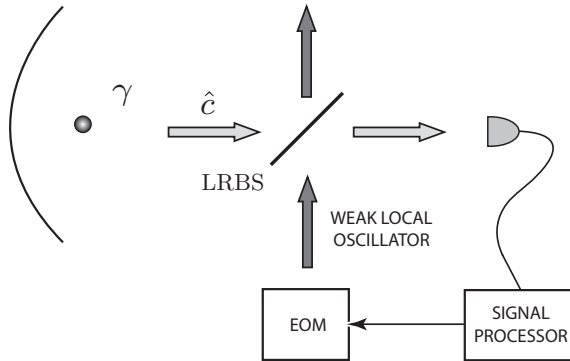


Fig. 4.5 A scheme for adaptive detection. The fluorescence emitted by the atom is coherently mixed with a weak local oscillator (LO) via a low-reflectivity beam-splitter (LRBS). The electro-optic modulator (EOM) reverses the amplitude of the LO every time the photodetector fires. Figure 5 adapted with permission from J. Gambetta *et al.*, *Phys. Rev. A* **64**, 042105, (2001). Copyrighted by the American Physical Society.

Since our aim is for the atom to remain in one of two fixed pure states, except when it jumps, we must examine the fixed points (i.e. eigenstates) of the operator $\hat{M}_0(dt)$. It turns out that it has two fixed states, such that, if $\text{Re}[\mu] \neq 0$, one is stable and one unstable. For $\text{Re}[\mu] > 0$, the stable fixed state is

$$|\tilde{\psi}_s^\mu\rangle = \left(\sqrt{\Omega^2 - 2i\Omega\gamma\mu^* - \frac{\gamma^2}{4}} + \frac{i\gamma}{2} \right) |g\rangle + \Omega |e\rangle. \quad (4.159)$$

Here the tilde denotes an unnormalized state. The corresponding eigenvalue is

$$\lambda_s^\mu = -\gamma \frac{1 + 2|\mu|^2}{4} - \frac{i}{2} \sqrt{\Omega^2 - 2i\Omega\gamma\mu^* - \frac{\gamma^2}{4}}. \quad (4.160)$$

The unstable state and eigenvalue are found by replacing the square root by its negative. It is unstable in the sense that its eigenvalue is *more* negative, indicating that its norm will decay faster than that of the stable eigenstate. Thus, an initial superposition of these two (linearly independent) states will, when normalized, evolve towards the stable eigenstate.

Let us say $\mu = \mu_+$, with $\text{Re}[\mu_+] > 0$, and assume the system is in the appropriate stable state $|\psi_s^+\rangle$. When a jump occurs the new state of the system is proportional to

$$\hat{M}_1^+ |\psi_s^+\rangle \propto (\hat{\sigma}_- + \mu_+) |\psi_s^+\rangle. \quad (4.161)$$

The new state will obviously be different from $|\psi_s^+\rangle$ and so will not remain fixed. This is in contrast to what we are seeking, namely a system that will remain fixed between jumps. However, let us imagine that, immediately following the detection, the value of the local oscillator amplitude μ is changed to some new value, μ_- . This is an example of an *adaptive* measurement scheme as discussed in Section 2.5, in that the parameters defining the measurement depend upon the past measurement record. We want this new μ_- to be

chosen such that the state $(\hat{\sigma}_- + \mu_+)|\psi_s^+\rangle$ is a stable fixed point of the new $\hat{M}_0^-(dt)$. The conditions for this to be so will be examined below. If they are satisfied then the state will remain fixed until another jump occurs. This time the new state will be proportional to

$$(\hat{\sigma}_- + \mu_-)(\hat{\sigma}_- + \mu_+)|\psi_s^+\rangle = [\mu_- \mu_+ + (\mu_- + \mu_+)\hat{\sigma}_-]|\psi_s^+\rangle. \quad (4.162)$$

If we want jumps between just two states then we require this to be proportional to $|\psi_s^+\rangle$. Clearly this will be so if and only if

$$\mu_- = -\mu_+. \quad (4.163)$$

Writing $\mu_+ = \mu$, we now return to the condition that $(\hat{\sigma}_- + \mu_+)|\psi_s^+\rangle$ be the stable fixed state of $\hat{M}_0^-(dt)$. From Eq. (4.159), and using Eq. (4.163), this gives the relation

$$\sqrt{\Omega^2 + 2i\Omega\gamma\mu^* - \frac{\gamma^2}{4}} = \sqrt{\Omega^2 - 2i\Omega\gamma\mu^* - \frac{\gamma^2}{4}} - \frac{\Omega}{\mu}. \quad (4.164)$$

This has just two solutions,

$$\mu_{\pm} = \pm \frac{1}{2}, \quad (4.165)$$

which, remarkably, are independent of the ratio γ/Ω . The stable and unstable fixed states for this choice are

$$|\psi_s^{\pm}\rangle = \frac{\pm\Omega - i\gamma}{\sqrt{2\Omega^2 + \gamma^2}}|g\rangle - \frac{\Omega}{\sqrt{2\Omega^2 + \gamma^2}}|e\rangle, \quad (4.166)$$

$$|\psi_u^{\pm}\rangle = \frac{1}{\sqrt{2}}|g\rangle \pm \frac{1}{\sqrt{2}}|e\rangle, \quad (4.167)$$

and the corresponding eigenvalues are

$$\lambda_s^{\pm} = -\frac{\gamma}{8} \pm \frac{i\Omega}{2}, \quad (4.168)$$

$$\lambda_u^{\pm} = -\frac{5\gamma}{8} \mp \frac{i\Omega}{2}. \quad (4.169)$$

Exercise 4.20 Show that the stable eigenstates correspond to the two states $\hat{\pi}_{\pm}$ defined by the Bloch vectors in Eq. (4.156).

We have thus constructed the measurement scheme that realizes the two-state PR ensemble for the two-level atom. Ignoring problems of collection and detector efficiency, it may seem that this adaptive measurement scheme would not be much harder to implement experimentally than homodyne detection; it requires simply an amplitude inversion of the local oscillator after each detection. In fact, this is very challenging, since the feedback delay must be very small compared with the characteristic time-scale of the system. For a typical atom the decay time ($\gamma^{-1} \sim 10^{-8}$ s) is shorter than currently feasible times for electronic feedback. Any experimental realization would have to use an atom with a very

long lifetime, or some other equivalent effective two-level system with radiative transitions in the optical frequency range.

Another difference from homodyne detection is that the adaptive detection has a very small local oscillator intensity at the detector: it corresponds to half the photon flux of the atom's fluorescence if the atom were saturated. In either stable fixed state, the actual photon flux entering the detector in this scheme is

$$\langle \psi_s^\pm | (\mu_\pm + \hat{\sigma}_-^\dagger)(\mu_\pm + \hat{\sigma}_-) | \psi_s^\pm \rangle = \frac{\gamma}{4}, \quad (4.170)$$

which is again independent of Ω/γ . This rate is also, of course, the rate for the system to jump to the other stable fixed state, so that the two are equally occupied in steady state.

There are many similarities between the stochastic evolution under this adaptive unravelling and the conditioned evolution of the atom under spectral detection, as investigated in Ref. [WT99]. Spectral detection uses optical filters to resolve the different frequencies of the photons emitted by the atom. As a consequence it is not possible to formulate a trajectory for the quantum state of the atom alone. For details, see Ref. [WT99]. In the case of a strongly driven atom ($\Omega \gg \gamma$), photons are emitted with frequencies approximately equal to the atomic resonance frequency, ω_a , and to the 'sideband' frequencies $\omega_a \pm \Omega$. (This is the characteristic Mollow power spectrum of resonance fluorescence [Mol69].) In the interaction frame these frequencies are 0 and $\pm\Omega$, and can be seen in the imaginary parts of (respectively) the eigenvalues $-\gamma/2$ and λ_\pm appearing in the solution to the resonance fluorescence master equation in Section 3.8.3. In this high-driving limit, the conditioned atomic state can be made approximately pure, and it jumps between states close to the $\hat{\sigma}_x$ eigenstates, just as in the adaptive detection discussed above. In this case the total detection rate is approximately $\gamma/2$, as expected for a strongly driven (saturated) atom. Of these detections, half are in the peak of the power spectrum near resonance (which do not give rise to state-changing jumps), while half are detections in the sidebands (which do). Thus the rate of state-changing jumps is approximately $\gamma/4$, just as in the case of adaptive detection.

4.6.3 Homodyne detection

We now turn to homodyne detection of the light emitted from the atom. Say the local oscillator has phase Φ . Then, from Eq. (4.77), the system obeys the following SSE:

$$\begin{aligned} d|\bar{\psi}_J(t)\rangle = & \left\{ -\left(\frac{\gamma}{2}\hat{\sigma}_-^\dagger\hat{\sigma}_- + i\hat{H}\right)dt \right. \\ & \left. + \left[\gamma dt \langle e^{-i\Phi}\hat{\sigma}_- + e^{i\Phi}\hat{\sigma}_-^\dagger \rangle_J(t) + \sqrt{\gamma} dW(t)\right] e^{-i\Phi}\hat{\sigma}_- \right\} |\bar{\psi}_J(t)\rangle, \end{aligned} \quad (4.171)$$

where $dW(t)$ is a real infinitesimal Wiener increment.

In Fig. 4.6, we plot a typical trajectory on the Bloch sphere for two values of Φ , namely 0 and $\pi/2$, corresponding to measuring the quadrature of the spontaneously emitted light in phase and in quadrature with the driving field, respectively. In both plots $\Omega = 3\gamma$ and

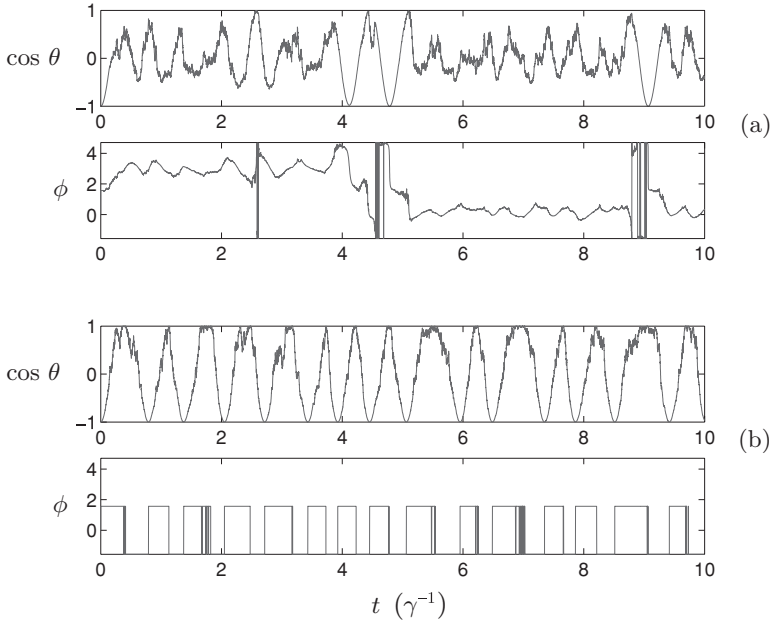


Fig. 4.6 A segment of a trajectory of duration $10\gamma^{-1}$ of an atomic state on the Bloch sphere under homodyne detection. The phase Φ of the local oscillator relative to the driving field is 0 in (a) and $\pi/2$ in (b). The driving and detuning are $\Omega = 3$ and $\Delta = 0$.

$\Delta = 0$, so the true distributions on the Bloch sphere are symmetric under reflection in the y - z plane. The effect of the choice of measurement is dramatic and readily understandable. The homodyne photocurrent from Eq. (4.75) is

$$J_{\text{hom}}(t) = \gamma \langle \hat{\sigma}_x \rangle \cos \Phi - \langle \hat{\sigma}_y \rangle \sin \Phi + \sqrt{\gamma} \xi(t). \quad (4.172)$$

When the local oscillator is in phase ($\Phi = 0$), the deterministic part of the photocurrent is proportional to $x(t)$. Under this measurement, the atom tends towards states with well-defined $\hat{\sigma}_x$. The eigenstates of $\hat{\sigma}_x$ are stationary states of the driving Hamiltonian, so this leads to trajectories that stay near these eigenstates for a relatively long time. This is seen in Fig. 4.6(a), where ϕ tends to stay around 0 or π . In contrast, measuring the $\Phi = \pi/2$ quadrature tries to force the system into an eigenstate of $\hat{\sigma}_y$. However, such an eigenstate will be rapidly spun around the Bloch sphere by the driving Hamiltonian. This effect is clearly seen in Fig. 4.6(b), where the trajectory is confined to the $\phi = \pm\pi/2$ great circle (like that for direct detection).

The above explanation for the nature of the quantum trajectories is also useful for understanding the noise spectra of the quadrature photocurrents in Eq. (4.172). The power spectrum (see Section 4.5.1) of resonance fluorescence of a strongly driven two-level atom has three peaks, as discussed in the preceding section. The central one is peaked at the atomic frequency, and the two sidebands (each of half the area) are displaced by the Rabi

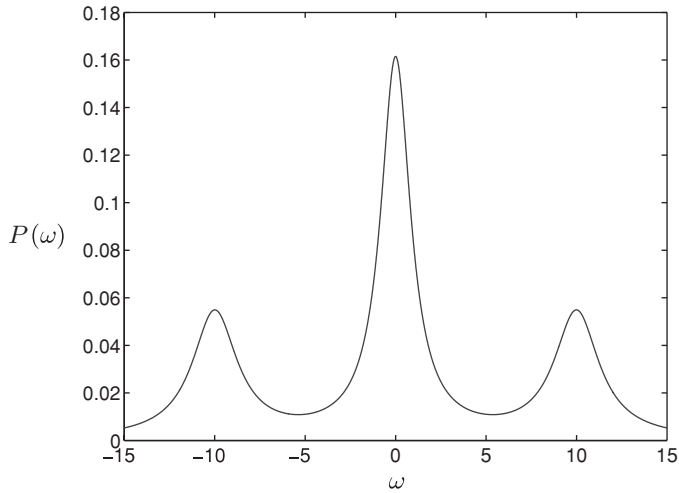


Fig. 4.7 A power spectrum for resonance fluorescence with $\gamma = 1$, $\Delta = 0$ and $\Omega = 10$. Note that this Rabi frequency is larger than that in Fig. 4.6, in order to show clearly the Mollow triplet.

frequency [Mol69], as shown in Fig. 4.7. It turns out that the spectrum of the in-phase homodyne photocurrent (see Section 4.4.4) gives the central peak, while the quadrature photocurrent gives the two sidebands [CWZ84]. This is readily explained qualitatively from the evolution of the atomic state under homodyne measurements. When $\hat{\sigma}_x$ is being measured, it varies slowly, remaining near one eigenvalue on a time-scale like γ^{-1} . This gives rise to an exponentially decaying autocorrelation function for the photocurrent (4.172), or a Lorentzian with width scaling as γ in the frequency domain. When $\hat{\sigma}_y$ is measured, it undergoes rapid sinusoidal variation at frequency Ω , with noise added at a rate γ . This explains the side peaks.

4.6.4 Heterodyne detection

If the atomic fluorescence enters a perfect heterodyne detection device, then, from Eq. (4.118), the system evolves via the SSE

$$\begin{aligned} |\bar{\psi}_J(t + dt)\rangle = & \left\{ \hat{1} - \left(\frac{\gamma}{2} \hat{\sigma}_-^\dagger \hat{\sigma}_- + i\hat{H} \right) dt \right. \\ & \left. + \left[\gamma dt \langle \hat{\sigma}_-^\dagger \rangle_J(t) + \sqrt{\gamma} dZ(t) \right] \hat{\sigma}_- \right\} |\bar{\psi}_J(t)\rangle, \end{aligned} \quad (4.173)$$

where here $dZ(t)$ is the complex infinitesimal Wiener increment introduced in Eq. (4.109).

As for the previous case, the steady-state probability distribution can be represented by an ensemble of points on the Bloch sphere drawn (at many different times) from a single long-time solution of the SSE. In this case, the stationary probability distribution is spread fairly well over the entire Bloch sphere. This can be understood as the result of the two competing measurements ($\hat{\sigma}_x$ and $\hat{\sigma}_y$) combined with the driving Hamiltonian causing

rotation around the x axis. The complex photocurrent as defined in Eq. (4.117) is

$$J_{\text{het}}(t) = \gamma \langle \hat{\sigma}_- \rangle + \sqrt{\gamma} \zeta(t), \quad (4.174)$$

where $\zeta(t) = dZ(t)/dt$. The spectrum of this photocurrent (the Fourier transform of the two-time correlation function (4.206)) gives the complete Mollow triplet, since y is rotated at frequency Ω with noise, while the dynamics of x is only noise.

4.7 Monitoring in the Heisenberg picture

4.7.1 Inputs and outputs

In this chapter so far we have described the monitoring of a quantum system in the Schrödinger picture, treating the measurement results as a classical record. However, we showed in Section 1.3.2 of Chapter 1 that it is possible to treat measurement results as operators, enabling a description in the Heisenberg picture. Moreover, we showed in Section 3.11 of Chapter 3 that the dynamics of open quantum systems can also be treated in this picture. Thus it is not surprising that we can describe monitoring in the Heisenberg picture. The crucial change from the earlier parts of this chapter is that now the measurement results are represented by bath operators.

Recall from Eq. (3.172) that, in the Heisenberg picture, the increment in an arbitrary system operator \hat{s} is

$$d\hat{s} = dt(\hat{c}^\dagger \hat{s} \hat{c} - \frac{1}{2} \{ \hat{c}^\dagger \hat{c}, \hat{s} \} + i[\hat{H}, \hat{s}]) - [d\hat{B}_{\text{in}}^\dagger(t) \hat{c} - \hat{c}^\dagger d\hat{B}_{\text{in}}(t), \hat{s}]. \quad (4.175)$$

Now there was nothing in the derivation of this equation that required \hat{s} to be specifically a system operator rather than a bath operator. Thus we could choose instead $\hat{s} = \hat{b}_{\text{in}}(t)$, the bath field operator interacting with the system at time t (see Section 3.11). Then, using Eq. (4.175) and Eq. (3.160), we find

$$d\hat{b}_{\text{in}}(t) = O(dt) + \hat{c}. \quad (4.176)$$

That is, the singularity of the bath commutation relations leads to a finite change in the bath field operator \hat{b}_{in} in an infinitesimal time.

Because of this finite change, it is necessary to distinguish between the bath operator \hat{b}_{in} interacting with the system at the beginning of the time interval $[t, t + dt)$ and that at the end, which we will denote $\hat{b}_{\text{out}}(t)$. Ignoring infinitesimal terms, Eq. (4.176) implies that

$$\hat{b}_{\text{out}} = \hat{b}_{\text{in}} + \hat{c}. \quad (4.177)$$

This is sometimes called the input–output relation [GC85]. To those unfamiliar with the Heisenberg picture, it may appear odd that a system operator appears in the expression for a bath operator, but this is just what one would expect with classical equations for dynamical variables. As explained in Section 1.3.2, Heisenberg equations such as this are the necessary counterpart to entanglement in the Schrödinger picture. If the system is an

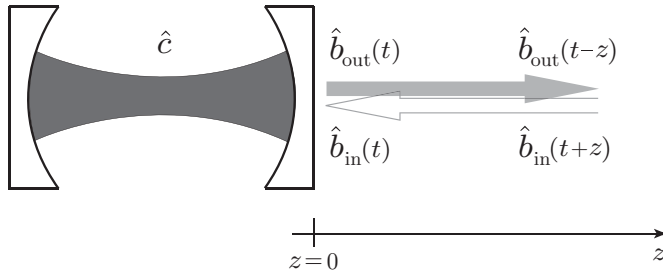


Fig. 4.8 A schematic diagram showing the relation between the input and output fields for a one-sided cavity with one relevant mode described by the annihilation operator \hat{c} . The distance from the cavity, z , appears as a time difference in the free field operators because we are using units such that the speed of light is unity. The commutation relations say that (for $z > 0$) $\hat{b}_{in}(t+z)$ and $\hat{b}_{out}(t-z)$ commute with any system operator at time t . This is readily understood from the figure, since these field operators apply to parts of the field that also exist (at a point in space removed from the system) at time t .

optical cavity, then this operator represents the field immediately after it has bounced off the cavity mirror. This is shown in Fig. 4.8.

Just as $\hat{b}_{in}(t)$ commutes with an arbitrary system operator $\hat{s}(t')$ at an earlier time $t' < t$, it can simply be shown that $\hat{b}_{out}(t)$ commutes with the system operators at a later time $t' > t$. As a consequence of this, the output field obeys the same commutation relations as the input field,

$$[\hat{b}_{out}(t), \hat{b}_{out}^\dagger(t')] = \delta(t - t'), \quad (4.178)$$

as required because it is a free field also.

Unlike $\hat{b}_{in}(t)$ for earlier times, $\hat{b}_{out}(t)$ for later times does depend on the state of the system. In fact, a measurement of the output field will yield information about the system. Monitoring of the system (as discussed above in the Schrödinger picture) corresponds to measuring, in every interval $[t, t + dt]$, a bath observable that is a function of $\hat{b}_{out}(t)$. Because $\hat{b}_{out}(t)$ commutes with $\hat{s}(t')$ for $t' > t$, the operator for the measurement record (which relates to the system in the past) will commute with all system operators in the present. That is, it is a c-number record insofar as the system is concerned. This fact is crucial to the Heisenberg-picture approach to feedback to be developed in Chapter 5. We will now examine how various monitoring schemes correspond to different operators for the measurement record.

4.7.2 Direct photodetection

From Section 4.3.1, it is apparent that the observable for photon flux is

$$\hat{I}_{out}(t) = \hat{b}_{out}^\dagger(t) \hat{b}_{out}(t). \quad (4.179)$$

It is easy to show that this is statistically identical to the classical photocurrent $I(t)$ used in Section 4.3.2. To see this, consider the Heisenberg operator $d\hat{N}_{\text{out}}(t) = \hat{b}_{\text{out}}^\dagger(t)\hat{b}_{\text{out}}(t)dt$ for the output field. This is found from Eq. (4.177) to be

$$d\hat{N}_{\text{out}}(t) = [\hat{c}^\dagger(t) + \hat{v}^\dagger(t)][\hat{c}(t) + \hat{v}(t)]dt. \quad (4.180)$$

Here we are using $\hat{v}(t)$ for $\hat{b}_{\text{in}}(t)$ to emphasize that the input field is in the vacuum state and so satisfies $\langle \hat{v}(t)\hat{v}^\dagger(t') \rangle = \delta(t - t')$, with all other second-order moments vanishing. It is then easy to show that

$$\langle d\hat{N}_{\text{out}}(t) \rangle = \text{Tr}[\hat{c}^\dagger(t)\hat{c}(t)\rho], \quad (4.181)$$

$$d\hat{N}_{\text{out}}(t)^2 = d\hat{N}_{\text{out}}(t). \quad (4.182)$$

These moments are identical to those of the photocount increment, Eqs. (4.41) and (4.13), with a change from Schrödinger to Heisenberg picture.

The identity between the statistics of the output photon-flux operator $\hat{I}_{\text{out}}(t)$ and the photocurrent $I(t)$ does not stop at the single-time moments (4.181) and (4.182). As discussed in Section 4.3.2, the most commonly calculated higher-order moment is the autocorrelation function. In the Heisenberg picture this is defined as

$$F^{(2)}(t, t + \tau) = \langle \hat{I}_{\text{out}}(t + \tau)\hat{I}_{\text{out}}(t) \rangle. \quad (4.183)$$

From the expression (4.180), this is found to be

$$F^{(2)}(t, t + \tau) = \langle \hat{c}^\dagger(t)\hat{c}^\dagger(t + \tau)\hat{c}(t + \tau)\hat{c}(t) \rangle + \delta(\tau)\langle \hat{c}^\dagger(t)\hat{c}(t) \rangle. \quad (4.184)$$

Exercise 4.21 Show this using the commutation relations (4.178) to put the field operators in normal order. (Doing this eliminates the input field operators, because they act directly on the vacuum, giving a null result.)

The autocorrelation function can be rewritten in the Schrödinger picture as follows. First, recall that the average of a system operator at time t is

$$\langle \hat{s}(t) \rangle = \text{Tr}_S[\rho(t)\hat{s}] = \text{Tr}_S[\text{Tr}_B[W(t)]\hat{s}] = \text{Tr}[W(t)\hat{s}], \quad (4.185)$$

where $\rho(t)$ is the system (S) state matrix and $W(t)$ is the state matrix for the system plus bath (B). Now $W(t) = \hat{U}(t)W(0)\hat{U}^\dagger(t)$, where in the Markovian approximation the unitary evolution is such that

$$\text{Tr}_B[\hat{U}(t)\tilde{W}(0)\hat{U}^\dagger(t)] = \exp(\mathcal{L}t)\tilde{\rho}(0), \quad (4.186)$$

where $\tilde{W}(0) = \tilde{\rho}(0) \otimes \rho_B(0)$ and $\tilde{\rho}(0)$ is arbitrary. This result can be generalized to a two-time correlation function for system operators \hat{s} and \hat{z} :

$$\langle \hat{s}(t)\hat{z}(0) \rangle = \text{Tr}[W(0)\hat{s}(t)\hat{z}(0)] \quad (4.187)$$

$$= \text{Tr}[W(0)\hat{U}^\dagger(t)\hat{s}\hat{U}(t)\hat{z}(0)] \quad (4.188)$$

$$= \text{Tr}[\hat{U}(t)\hat{z}(0)W(0)\hat{U}^\dagger(t)\hat{s}] \quad (4.189)$$

$$= \text{Tr}_S[\text{Tr}_B[\hat{U}(t)\hat{z}(0)W(0)\hat{U}^\dagger(t)]\hat{s}]. \quad (4.190)$$

Using the Markov assumption with $\tilde{\rho}(0) = \hat{z}(0)\rho(0)$,

$$\langle \hat{s}(t)\hat{z}(0) \rangle = \text{Tr}_S[\hat{s} \exp(\mathcal{L}t)\hat{z}\rho(0)] = \text{Tr}_S[\hat{s}\tilde{\rho}(t)], \quad (4.191)$$

where $\tilde{\rho}(t)$ is the solution of the master equation with the given initial conditions. This is sometimes known as the *quantum regression theorem*.

Exercise 4.22 Generalize the above result to two-time correlation functions of the form $\langle \hat{x}(0)\hat{s}(t)\hat{z}(0) \rangle$.

Applying the result of this exercise to the above autocorrelation function (4.184) gives

$$F^{(2)}(t, t + \tau) = \text{Tr}[\hat{c}^\dagger \hat{c} e^{\mathcal{L}\tau} \hat{c} \rho(t) \hat{c}^\dagger] + \text{Tr}[\hat{c}^\dagger \hat{c} \rho(t)] \delta(\tau). \quad (4.192)$$

This is identical to Eq. (4.50) obtained using the conditional evolution in Section 4.3.2. In fact, any statistical comparison between the two will agree because $\hat{I}_{\text{out}}(t)$ and $I(t)$ are merely different representations of the same physical quantity. Conceptually, the two representations are quite different. In the Heisenberg-operator derivation, the shot-noise term (the delta function) in the autocorrelation function arises from the commutation relations of the electromagnetic field. By contrast, the quantum trajectory model produces shot noise because photodetections are discrete events, which is a far more intuitive explanation. As we will see, some results may be more obvious using one method, others more obvious with the other, so it is good to be familiar with both.

4.7.3 Homodyne detection

Adding a local oscillator to the output field transforms it to

$$\hat{b}'_{\text{out}}(t) = \hat{b}_{\text{out}}(t) + \gamma = \hat{c}(t) + \hat{v}(t) + \gamma. \quad (4.193)$$

On dropping the time arguments, the photon-flux operator for this field is

$$\hat{I}'_{\text{out}} = \gamma^2 + \gamma(\hat{c} + \hat{c}^\dagger + \hat{v} + \hat{v}^\dagger) + (\hat{c}^\dagger + \hat{v}^\dagger)(\hat{c} + \hat{v}). \quad (4.194)$$

In the limit that $\gamma \rightarrow \infty$, the last term can be ignored for the homodyne photocurrent operator,

$$\hat{J}_{\text{out}}^{\text{hom}}(t) \equiv \lim_{\gamma \rightarrow \infty} \frac{\hat{I}'_{\text{out}}(t) - \gamma^2}{\gamma} = \hat{x}(t) + \hat{\xi}(t). \quad (4.195)$$

Here, \hat{x} is the quadrature operator defined in Eq. (4.65) and $\hat{\xi}(t)$ is the vacuum input operator

$$\hat{\xi}(t) = \hat{v}(t) + \hat{v}^\dagger(t), \quad (4.196)$$

which has statistics identical to those of the normalized Gaussian white noise for which the same symbol is used.

Exercise 4.23 Convince yourself of this.

The operator nature of $\hat{\xi}(t)$ is evident only from its commutation relations with its conjugate variable $\hat{v}(t) = -i\hat{p}(t) + i\hat{p}^\dagger(t)$:

$$[\hat{\xi}(t), \hat{v}(t')] = 2i\delta(t - t'). \quad (4.197)$$

The output quadrature operator (4.195) evidently has the same single-time statistics as the homodyne photocurrent operator (4.75), with a mean equal to the mean of \hat{x} , and a white-noise term. The two-time correlation function of the operator $\hat{J}_{\text{out}}^{\text{hom}}(t)$ is defined by

$$F_{\text{hom}}^{(1)}(t, t + \tau) = \langle \hat{J}_{\text{out}}^{\text{hom}}(t + \tau) \hat{J}_{\text{out}}^{\text{hom}}(t) \rangle. \quad (4.198)$$

Using the commutation relations for the output field (4.178), this can be written as

$$F_{\text{hom}}^{(1)}(t, t + \tau) = \langle : \hat{x}(t + \tau) \hat{x}(t) : \rangle + \delta(\tau), \quad (4.199)$$

where the annihilation of the vacuum has been used as before. Here the colons denote time and normal ordering of the operators \hat{c} and \hat{c}^\dagger . The meaning of this can be seen in the Schrödinger picture:

$$F_{\text{hom}}^{(1)}(t, t + \tau) = \text{Tr}[\hat{x} e^{\mathcal{L}\tau} (\hat{c}\rho(t) + \rho(t)\hat{c}^\dagger)] + \delta(\tau), \quad (4.200)$$

where \mathcal{L} is as before and $\rho(t)$ is the state of the system at time t , which is assumed known.

Again, this is in exact agreement with that calculated from the quantum trajectory method in Section 4.4.4. The operator quantity $\hat{J}_{\text{out}}^{\text{hom}}(t)$ has the same statistics as those of the classical photocurrent $J_{\text{hom}}(t)$. Again the different conceptual basis is reflected in the origin of the delta function in the autocorrelation function: operator commutation relations in the Heisenberg picture versus local oscillator shot noise from the quantum trajectories.

4.7.4 Heterodyne detection

The equivalence between the Heisenberg picture and quantum trajectory calculations of the output field correlation functions applies for heterodyne detection in much the same way as for homodyne detection. For variation, we construct the Heisenberg operator for the ‘heterodyne photocurrent’ from two homodyne measurements, rather than from the Fourier components of the heterodyne signal. To make two homodyne measurements, it is necessary to use a 50 : 50 beam-splitter to divide the cavity output before the local oscillator is added. This gives two output beams,

$$\hat{b}_{\text{out}}^\pm = \sqrt{1/2}(\hat{v} + \hat{c} \pm \hat{\mu}). \quad (4.201)$$

Here we have introduced an ancilla vacuum annihilation operator $\hat{\mu}$ that enters at the free port of the beam-splitter.

Exercise 4.24 Show that

$$\hat{b}_{\text{out}}^{\dagger+} \hat{b}_{\text{out}} = \hat{b}_{\text{out}}^{\dagger+} \hat{b}_{\text{out}}^+ + \hat{b}_{\text{out}}^{-\dagger} \hat{b}_{\text{out}}^-, \quad (4.202)$$

so that photon flux is preserved.

Let the \hat{b}_{out}^+ beam enter a homodyne apparatus to measure the x quadrature, and the \hat{b}_{out}^- beam one to measure the y quadrature. Then the operators for the two photocurrents, normalized with respect to the system signal, are

$$\hat{J}_{\text{out}}^x = \hat{x} + [\hat{v} + \hat{v}^\dagger + \hat{\mu} + \hat{\mu}^\dagger], \quad (4.203)$$

$$\hat{J}_{\text{out}}^y = \hat{y} - i[\hat{v} - \hat{v}^\dagger - \hat{\mu} + \hat{\mu}^\dagger], \quad (4.204)$$

where \hat{y} is defined in Eq. (4.65). Defining the complex heterodyne photocurrent as in Eq. (4.116) gives

$$\hat{J}_{\text{out}}^{\text{het}} = \hat{c} + \hat{v} + \hat{\mu}^\dagger. \quad (4.205)$$

Exercise 4.25 Convince yourself that $\hat{\zeta}(t) = \hat{v}(t) + \hat{\mu}^\dagger(t)$ has the same statistics as the complex Gaussian noise $\zeta(t)$ defined in Section 4.6.4.

Thus, the operator (4.205) has the same statistics as the photocurrent (4.117). The autocorrelation function

$$F_{\text{het}}^{(1)}(t, t + \tau) = \langle \hat{J}_{\text{out}}^{\text{het}\dagger}(t + \tau) \hat{J}_{\text{out}}^{\text{het}}(t) \rangle, \quad (4.206)$$

evaluates to

$$F_{\text{het}}^{(1)}(t, t + \tau) = \langle \hat{c}^\dagger(t + \tau) \hat{c}(t) \rangle + \delta(\tau). \quad (4.207)$$

Again, this is equal to the Schrödinger-picture expression (4.120).

4.7.5 Completely general dyne detection

In the Heisenberg picture, the completely general Lindblad evolution (4.122) becomes

$$\begin{aligned} d\hat{s} = dt & \left(\hat{c}_k^\dagger \hat{s} \hat{c}_k - \frac{1}{2} \left\{ \hat{c}_k^\dagger \hat{c}_k, \hat{s} \right\} + i[\hat{H}, \hat{s}] \right) \\ & - [d\hat{B}_{k;\text{in}}^\dagger(t) \hat{c}_k - \hat{c}_k^\dagger d\hat{B}_{k;\text{in}}(t), \hat{s}], \end{aligned} \quad (4.208)$$

where we are using the Einstein summation convention as before and $d\hat{B}_{k;\text{in}} = \hat{b}_{k;\text{in}} dt$ where the $\hat{b}_{k;\text{in}}$ are independent vacuum field operators. The output field operators are

$$\hat{b}_{k;\text{out}} = \hat{b}_{k;\text{in}} + \hat{c}_k. \quad (4.209)$$

Recall that for a completely general dyne unravelling the measurement result was a vector of complex currents $J_k(t)$ given by (4.136), where the noise correlations are defined by a complex symmetric matrix Υ . In the Heisenberg picture the operators for these currents are

$$\hat{J}_k = \hat{b}_{k;\text{out}} + \Upsilon_{kj} \hat{b}_{j;\text{out}}^\dagger + \text{T}_{kj} \hat{a}_j^\dagger. \quad (4.210)$$

Here \hat{a}_k are ancillary annihilation operators, which are also assumed to act on a vacuum state, and obey the usual continuum-field commutation relations,

$$[\hat{a}_j(t), \hat{a}_k^\dagger(t')] dt = \delta_{jk} \delta(t - t'). \quad (4.211)$$

These ancillary operators ensure that all of the components \hat{J}_k commute with one another. This is necessary since this vector operator represents an observable quantity. Assuming \mathbf{T} (a capital τ) to be a symmetric matrix like Υ , we find

$$[\hat{J}_j, \hat{J}_k]dt = \Upsilon_{jk} - \Upsilon_{kj} = 0, \quad (4.212)$$

$$[\hat{J}_j, \hat{J}_k^\dagger]dt = \delta_{jk} - \Upsilon_{jl}\Upsilon_{lk}^* - \mathbf{T}_{jl}\mathbf{T}_{lk}^*. \quad (4.213)$$

Thus we require the matrix \mathbf{T} to satisfy

$$\mathbf{T}^*\mathbf{T} = \mathbf{I} - \Upsilon^*\Upsilon. \quad (4.214)$$

The right-hand side of this equation is always positive (see Section 4.5.2), so it is always possible to find a suitable \mathbf{T} .

From these definitions one can show that

$$\hat{J}_k = \hat{c}_k + \Upsilon_{kj}\hat{c}_j^\dagger + \delta\hat{J}_k, \quad (4.215)$$

where

$$\delta\hat{J}_k = \hat{b}_{k;\text{in}} + \Upsilon_{kj}\hat{b}_{j;\text{in}}^\dagger + \mathbf{T}_{kj}\hat{a}_j^\dagger \quad (4.216)$$

has a zero mean. Thus the mean of \hat{J}_k is the same as that of the classical current in Section 4.5.2. Also, one finds that

$$(\delta\hat{J}_j dt)(\delta\hat{J}_k dt)^\dagger = \delta_{jk} dt, \quad (4.217)$$

$$(\delta\hat{J}_j dt)(\delta\hat{J}_k dt) = \Upsilon_{jk} dt, \quad (4.218)$$

the same correlations as for the noise in Section 4.5.2.

4.7.6 Relation to distribution functions

Obviously direct, homodyne and heterodyne detection are related to measurements of, respectively, the intensity, one quadrature and the complex amplitude of the radiating dipole of the system. Equally obviously, the measurements described are far removed from simple measurements of these quantities, such as by the projective measurements. Nevertheless, there must be some elementary relation between the two types of measurements for at least some cases. For example, counting the number of photons in a cavity should give the same results (statistically) irrespective of whether this is done by allowing the photons to escape gradually through an end mirror into a photodetector or whether the measurement is a projection of the cavity mode into photon-number eigenstates, provided that the system Hamiltonian commutes with photon number. The purpose of this section is to establish a relationship between quantum monitoring and simpler descriptions of measurements, for the three schemes discussed. In all cases we must wait until $t = \infty$ for the measurement to be complete.

For simplicity, we consider the case of a freely decaying optical cavity with unit linewidth, so that $\hat{c} = \hat{a}$ with $[\hat{a}, \hat{a}^\dagger] = 1$. We will see that the Heisenberg-picture formalism is a

powerful framework for establishing the relations we seek. In this picture, the dynamics of the system is given by the quantum Langevin equation

$$d\hat{a}(t) = -\frac{1}{2}\hat{a}(t)dt + \hat{v}(t)dt, \quad (4.219)$$

which has the solution

$$\hat{a}(t) = \hat{a}(0)e^{-t/2} - \int_0^t e^{(s-t)/2} \hat{v}(s)ds. \quad (4.220)$$

Exercise 4.26 Verify these equations.

The output field is of course

$$\hat{b}_{\text{out}}(t) = \hat{a}(t) + \hat{v}(t). \quad (4.221)$$

Photon-number distribution. We begin with photon counting. The most obvious difference between a projective measurement of photon number and an external counting of escaped photons from a freely decaying cavity is that the final state of the cavity mode is the appropriate photon-number eigenstate in the first case and the vacuum in the second. The latter result comes about because the counting time must be infinite to allow all photons to escape. Although extra-cavity detection is not equivalent to projective detection, it should give the same statistics in the infinite time limit.

The output photon flux is

$$\hat{I}(t) = [\hat{a}^\dagger(t) + \hat{v}^\dagger(t)][\hat{a}(t) + \hat{v}(t)], \quad (4.222)$$

which using Eq. (4.220) evaluates to

$$\begin{aligned} \hat{I}(t) = & \left[\hat{a}^\dagger(0)e^{-t/2} - \int_0^t e^{(s-t)/2} \hat{v}^\dagger(s)ds + \hat{v}^\dagger(t) \right] \\ & \times \left[\hat{a}(0)e^{-t/2} - \int_0^t e^{(s-t)/2} \hat{v}(s)ds + \hat{v}(t) \right]. \end{aligned} \quad (4.223)$$

The operator for the total photocount is then

$$\hat{N} \equiv \int_0^\infty \hat{I}(t)dt. \quad (4.224)$$

On using integration by parts (we show this explicitly for the simpler cases of homodyne detection below), it is possible to evaluate this as

$$\hat{N} = \hat{a}^\dagger(0)\hat{a}(0) + \hat{n}. \quad (4.225)$$

Here \hat{n} contains only bath operators, and annihilates on the vacuum. Hence it commutes with the first term and contributes nothing to the expectation value of any function of \hat{N} , provided that the bath is in a vacuum state. This confirms that the integral of the photocurrent does indeed measure the operator $\hat{a}^\dagger\hat{a}$ for the initial cavity state.

Quadrature distribution. Now consider homodyne detection. Unlike direct detection, one should not simply integrate the photocurrent from zero to infinity because even when all light has escaped the cavity the homodyne measurement continues to give a non-zero

current (vacuum noise). Thus, for long times the additional current is merely adding noise to the record. This can be circumvented by properly mode-matching the local oscillator to the system. That is to say, by matching the decay rate, as well as the frequency, of the local oscillator amplitude to that of the signal. Equivalently, the current could be electronically multiplied by the appropriate factor and then integrated.

For the cavity decay in Eq. (4.220) the appropriately scaled homodyne current operator is

$$\hat{J}_{\text{out}}^{\text{hom}}(t) = e^{-t/2}[\hat{x}(t) + \hat{\xi}(t)]. \quad (4.226)$$

From Eq. (4.220), this is equal to

$$\hat{J}_{\text{out}}^{\text{hom}}(t) = e^{-t/2} \left[\hat{x}(0)e^{-t/2} - \int_0^t e^{(s-t)/2} \hat{\xi}(s) ds + \hat{\xi}(t) \right], \quad (4.227)$$

and so

$$\hat{X} \equiv \int_0^\infty \hat{J}_{\text{out}}^{\text{hom}}(t) dt \quad (4.228)$$

$$= \hat{x}(0) + \int_0^\infty e^{-t/2} \hat{\xi}(t) dt - \int_0^\infty dt e^{-t} \int_0^t e^{s/2} \hat{\xi}(s) ds. \quad (4.229)$$

Using integration by parts on the last term, it is easy to show that it cancels out the penultimate term, so the operator of the integrated photocurrent is simply

$$\hat{X} = \hat{x}(0). \quad (4.230)$$

Thus it is possible to measure a quadrature of the field by homodyne detection. Unlike the case of direct detection, this derivation requires no assumptions about the statistics of the bath field.

Husimi distribution. Heterodyne detection is different from direct and homodyne detection in that it does not measure an Hermitian system operator. That is because it measures both quadratures simultaneously. However, it does measure a *normal operator* (see Box 1.1). The (normal) operator for the heterodyne photocurrent (4.205) is, with appropriate photocurrent scaling factor,

$$\hat{J}_{\text{out}}^{\text{het}}(t) = e^{-t/2}[\hat{a}(t) + \hat{\zeta}(t)], \quad (4.231)$$

where $\hat{\zeta} = \hat{v} + \hat{\mu}^\dagger$. Proceeding as above, the operator for the measurement result is

$$\hat{A} \equiv \int_0^\infty \hat{J}_{\text{out}}^{\text{het}}(t) dt = \hat{a}(0) + \hat{e}^\dagger, \quad (4.232)$$

where $\hat{e}^\dagger = \int_0^\infty e^{-t/2} \hat{\mu}^\dagger(t) dt$.

Exercise 4.27 Show that $[\hat{e}^\dagger, \hat{e}] = -1$ and hence show that \hat{A} commutes with its Hermitian conjugate.

From this exercise it follows that \hat{A} is a normal operator, and hence there is no ambiguity in the calculation of its moments. That is, all orderings are equivalent. The most convenient operator ordering is one of normal ordering with respect to \hat{e} . (Recall that normal ordering,

defined in Section A.5, has nothing to do with normal operators.) For a vacuum-state bath, the expectation value of any expression normally ordered in \hat{e} will have zero contribution from all terms involving \hat{e} . Now normal ordering with respect to \hat{e} is *antinormal* ordering with respect to \hat{a} . Thus the statistics of \hat{A} are the antinormally ordered statistics of \hat{a} . As shown in Section A.5, these statistics are those found from the so-called Husimi or Q function,

$$Q(\alpha)d^2\alpha = \frac{d^2\alpha}{\pi} \langle \alpha | \rho | \alpha \rangle, \quad (4.233)$$

where $|\alpha\rangle$ is a coherent state as usual.

Adaptive measurements. One should not conclude from the above analyses that the Heisenberg picture is necessarily always more powerful than the Schrödinger picture. Take, for example, adaptive measurements, as considered in Sections 2.5 and 4.6.2. In these cases, the measured currents are fed back to alter the future conditions of the measurement. This leads to intractable nonlinear Heisenberg equations, even for a system as simple as a decaying cavity [Wis95]. However, the problem can be tackled using *linear* quantum trajectory theory as introduced in Section 4.4.3. By this method it is possible to obtain an exact analytical treatment of the adaptive phase-estimation algorithm [Wis95, WK97, WK98] implemented in the experiment [AAS⁺02] described in Section 2.6. This will be discussed in detail in Section 7.9.

4.8 Imperfect detection

In all of the above we have considered detection under perfect conditions. That is, the detectors were *efficient*, detecting all of the output field; the input field was in a pure state; the detectors added no electronic noise to the measured signal; and the detectors did not filter the measured signal. In reality some or all of these assumptions will be invalid, and this means that an observer will not have access to perfect information about the system. Since the quantum state of the system *is* the observer's knowledge about the system, imperfect knowledge means a different (more mixed) quantum state. In this section we consider each of these imperfections in turn and derive the appropriate quantum trajectory to describe it.

4.8.1 Inefficient detection

The simplest sort of imperfection to describe is inefficiency. A photodetector of efficiency η (with $0 \leq \eta \leq 1$) can be modelled as a perfect detector detecting only a proportion η of the output beam. Thus, we can split the general master equation Eq. (4.11) into

$$\dot{\rho} = -i[\hat{H}, \rho] + (1 - \eta)\mathcal{D}[\hat{c}]\rho + \mathcal{D}[\sqrt{\eta}\hat{c}]\rho \quad (4.234)$$

and unravel only the last term.

For direct detection, Eq. (4.40) is replaced by

$$d\rho_I(t) = \{dN(t)\mathcal{G}[\sqrt{\eta}\hat{c}] + dt\mathcal{H}[-i\hat{H} - \eta\frac{1}{2}\hat{c}^\dagger\hat{c}] + dt(1 - \eta)\mathcal{D}[\hat{c}]\}\rho_I(t), \quad (4.235)$$

where now Eq. (4.41) becomes

$$E[dN(t)] = \eta \text{Tr}[\hat{c}\rho(t)\hat{c}^\dagger]dt. \quad (4.236)$$

In this case a SSE does not exist because the conditioned state will not remain pure even if it begins pure. Note that in the limit $\eta \rightarrow 0$ one obtains the unconditioned master equation.

For homodyne detection, the homodyne photocurrent is obtained simply by replacing \hat{c} by $\sqrt{\eta} \hat{c}$ to give

$$J_{\text{hom}}(t) = \sqrt{\eta} \langle \hat{x} \rangle_J(t) + \xi(t). \quad (4.237)$$

Note that here the shot noise (the final term) remains normalized so as to give a unit spectrum; other choices of normalization are also used. The SME (4.72) is modified to

$$d\rho_J = -i[\hat{H}, \rho_J(t)]dt + \mathcal{D}[\hat{c}]\rho_J(t)dt + \sqrt{\eta} dW(t)\mathcal{H}[\hat{c}]\rho_J(t). \quad (4.238)$$

Again, there is no SSE. The generalization of the heterodyne SME (4.110) is left as an exercise for the reader.

4.8.2 Detection with a white-noise input field

So far, we have considered optical measurements with the input in a vacuum, or coherent, state. As explained in Section 4.3.3, the photon flux is infinite for an input bath in a more general state, such as with thermal or squeezed white noise. This indicates that direct detection is impossible (or at least useless, as explained in Section 4.3.3). However, the output field quadrature operators are well defined even with white noise, because they are only linear in the noise. Thus, field operators for homodyne- and heterodyne-detection photocurrents can be defined without difficulty, simply by replacing the vacuum operator \hat{v} by the more general input bath operator \hat{b}_0 . This indicates that it should be possible to treat homodyne and heterodyne detection in such situations. In this section, we develop the quantum trajectory theory for detection in the presence of white noise.

The homodyne-detection theory of Section 4.4 began with a finite local oscillator amplitude γ , so that the quantum trajectories were jump-like. Diffusive trajectories were obtained when the $\gamma \rightarrow \infty$ limit was taken. This approach would fail if the input field were contaminated by white noise, for the same reason as that rendering direct detection impossible with white noise: the infinite photon flux due to the noise would swamp the signal. However, as noted in Section 4.3.3, a physical noise source would not be truly white, and in any case the response of the detector would give a cut-off to the flux. If the local oscillator were made sufficiently intense, then the signal due to this would overcome that due to the noise. Thus, in order to treat detection with white noise, it is necessary to begin with an infinitely large local oscillator. Then one can assume that the homodyne detection effects an ideal measurement of the instantaneous quadrature of the output field, without worrying about individual jumps.

Rather than doing a completely general derivation, we consider first the case of a white-noise bath in a pure, but non-vacuum, state. That is, as in Section 3.11.2,

$$d\hat{B}^\dagger(t)d\hat{B}(t) = N dt, \quad (4.239)$$

$$d\hat{B}(t)d\hat{B}(t) = M dt, \quad (4.240)$$

$$[d\hat{B}(t), d\hat{B}^\dagger(t)] = dt, \quad (4.241)$$

but the inequality (3.180) is replaced by the equality

$$|M|^2 = N(N+1). \quad (4.242)$$

In this case the pure state of the bath, which we denote $|M\rangle$, obeys

$$[(N+M^*+1)\hat{b}(t) - (N+M)\hat{b}^\dagger(t)]|M\rangle = 0. \quad (4.243)$$

Exercise 4.28 From Eqs. (4.241)–(4.243), derive Eqs. (4.239) and (4.240).

Now replacing the vacuum bath state $|0\rangle$ by $|M\rangle$ in Eq. (4.36) and expanding the unitary operator $\hat{U}(dt)$ to second order yields

$$\begin{aligned} |\Psi(t+dt)\rangle = & \left\{ 1 - \frac{1}{2}dt[(N+1)\hat{c}^\dagger\hat{c} + N\hat{c}\hat{c}^\dagger - M\hat{c}^{\dagger 2} - M^*\hat{c}^2] \right. \\ & \left. + \hat{c} d\hat{B}^\dagger(t) - \hat{c}^\dagger d\hat{B}(t) \right\} |\psi(t)\rangle |M\rangle. \end{aligned} \quad (4.244)$$

Consider homodyne detection on the output. Any multiple of the operator in Eq. (4.243) can be added to Eq. (4.244) without affecting it. Thus it is possible to replace $d\hat{B}^\dagger$ by

$$d\hat{B}^\dagger + \frac{N+M^*+1}{L} d\hat{B} - \frac{N+M}{L} d\hat{B}^\dagger = \frac{N+M^*+1}{L} [d\hat{B}^\dagger + d\hat{B}] \quad (4.245)$$

and $d\hat{B}$ by

$$d\hat{B} - \frac{N+M^*+1}{L} d\hat{B} + \frac{N+M}{L} d\hat{B}^\dagger = \frac{N+M}{L} [d\hat{B}^\dagger + d\hat{B}], \quad (4.246)$$

where

$$L = 2N + M^* + M + 1. \quad (4.247)$$

This yields

$$\begin{aligned} |\Psi(t+dt)\rangle = & \left\{ 1 - \frac{1}{2}dt[(N+1)\hat{c}^\dagger\hat{c} + N\hat{c}\hat{c}^\dagger - M\hat{c}^{\dagger 2} - M^*\hat{c}^2] \right. \\ & \left. + [\hat{c}(N+M^*+1)/L - \hat{c}^\dagger(N+M)/L] \right\} \\ & \times [d\hat{B}^\dagger(t) + d\hat{B}(t)] |\psi(t)\rangle |M\rangle. \end{aligned} \quad (4.248)$$

Projecting onto eigenstates $|J\rangle$ of the output quadrature $\hat{b} + \hat{b}^\dagger$ then gives the unnormalized conditioned state

$$\begin{aligned} |\tilde{\psi}_J(t+dt)\rangle = & \left\{ 1 - \frac{1}{2}dt[(N+1)\hat{c}^\dagger\hat{c} + N\hat{c}\hat{c}^\dagger - M\hat{c}^{\dagger 2} - M^*\hat{c}^2] \right. \\ & \left. + J dt [\hat{c}(N+M^*+1)/L - \hat{c}^\dagger(N+M)/L] \right\} \\ & \times |\psi(t)\rangle \sqrt{\wp_{\text{ost}}^M(J)}, \end{aligned} \quad (4.249)$$

where the state-matrix norm $\wp_{\text{ost}}^M(J)$ gives the probability of obtaining the result J and the ostensible probability distribution for J is

$$\wp_{\text{ost}}^M(J) = |\langle J|M \rangle|^2 = \sqrt{\frac{dt}{2\pi L}} \exp(-\frac{1}{2} J^2 dt/L). \quad (4.250)$$

Note that from this ostensible distribution the variance of J^2 is L/dt , which, depending on the modulus and argument of M , may be larger or smaller than its vacuum value of $1/dt$.

Now, by following the method in Section 4.4.3, one obtains the following SSE for the unnormalized state vector:

$$d|\bar{\psi}_J(t)\rangle = \left\{ -\frac{dt}{2} [(N+1)\hat{c}^\dagger \hat{c} + N\hat{c}\hat{c}^\dagger - M\hat{c}^{\dagger 2} - M^*\hat{c}^2] + J(t)dt \left(\hat{c} \frac{N+M^*+1}{L} - \hat{c}^\dagger \frac{N+M}{L} \right) \right\} |\bar{\psi}_J(t)\rangle, \quad (4.251)$$

where the *actual* statistics of the homodyne photocurrent J are given by

$$J_{\text{hom}}(t) = \langle \hat{x}(t) \rangle + \sqrt{L}\xi(t), \quad (4.252)$$

where $\xi(t) = dW(t)/dt$ is white noise as usual. Note that the high-frequency spectrum of the photocurrent is no longer unity, but L .

Turning Eq. (4.251) into an equation for $\bar{\rho}_J = |\bar{\psi}_J\rangle\langle\bar{\psi}_J|$ and then normalizing it yields

$$d\rho_J(t) = \left(dt \mathcal{L} + \frac{1}{\sqrt{L}} dW(t) \mathcal{H}[(N+M^*+1)\hat{c} - (N+M)\hat{c}^\dagger] \right) \rho_J(t), \quad (4.253)$$

where the unconditional evolution is

$$\mathcal{L}\rho = (N+1)\mathcal{D}[\hat{c}]\rho + N\mathcal{D}[\hat{c}^\dagger]\rho + \frac{M}{2}[\hat{c}^\dagger, [\hat{c}^\dagger, \rho]] + \frac{M^*}{2}[\hat{c}, [\hat{c}, \rho]] - i[\hat{H}, \rho]. \quad (4.254)$$

Exercise 4.29 *Verify this.*

The general case of an impure bath is now obtained simply by relaxing the equality in Eq. (4.242) back to the inequality in Eq. (3.180).

Note that, even for $M = 0$, the quantum trajectory described by Eq. (4.253) is not simply the homodyne quantum trajectory for a vacuum bath (4.72) with the addition of the thermal terms

$$N(\mathcal{D}[\hat{c}] + \mathcal{D}[\hat{c}^\dagger])\rho \quad (4.255)$$

in the non-selective evolution. Rather, the conditioning term depends upon N and involves both \hat{c} and \hat{c}^\dagger . In quantum optics, N is typically negligible, but for quantum-electromechanical systems (see Section 3.10.1), N is not negligible. Thus, for continuous measurement of such devices by electro-mechanical means, it may be necessary to apply a SME of form similar to Eq. (4.253).

From this conditioning equation and the expressions for the photocurrent, it is easy to find the two-time correlation function for the output field using the method of Section 4.4.4.

The result is

$$F_{\text{hom}}^{(1)}(t, t + \tau) = E[J_{\text{hom}}(t + \tau)J_{\text{hom}}(t)] \quad (4.256)$$

$$= \text{Tr}[(\hat{c} + \hat{c}^\dagger)e^{\mathcal{L}\tau}\{(N + M^* + 1)\hat{c}\rho(t) - (N + M)\hat{c}^\dagger\rho(t) + (N + M + 1)\rho(t)\hat{c}^\dagger - (N + M^*)\rho(t)\hat{c}\}] + L\delta(\tau). \quad (4.257)$$

Note that, unlike in the case of a vacuum input, there is no simple relationship between this formula and the Glauber coherence functions.

This correlation function could be derived from the Heisenberg field operators. The relevant expression is

$$\langle[\hat{x}(t + \tau) + \hat{b}_{\text{in}}(t + \tau) + \hat{b}_{\text{in}}^\dagger(t + \tau)][\hat{x}(t) + \hat{b}_{\text{in}}(t) + \hat{b}_{\text{in}}^\dagger(t)]\rangle. \quad (4.258)$$

We will not attempt to prove that this evaluates to Eq. (4.257), because it is considerably more difficult than with a vacuum input $\hat{b}_{\text{in}} = \hat{v}$. The reason for this is that it is impossible to choose an operator ordering such that the contributions due to the bath input vanish. The necessary method would have to be more akin to that used in obtaining Eq. (4.257), where the stochastic equation analogous to the SME is the quantum Langevin equation (3.181).

4.8.3 Detection with dark noise

The next sort of imperfection we consider is that of dark noise in the detector. This terminology is used for electronic noise generated within the detector because it is present even when no field illuminates the detector (i.e. in the dark). For simplicity we will treat only the case of detection of the homodyne type. Once again, it is convenient to use the approach of Section 4.4.3. We use the linear SME (4.91)

$$d\bar{\rho} = dt\{\mathcal{L}\bar{\rho} + J_0(t)[\hat{c}\bar{\rho} + \text{H.c.}]\}, \quad (4.259)$$

where $\mathcal{L} = \mathcal{H}[-i\hat{H}] + \mathcal{D}[\hat{c}]$. This corresponds to detection by an ideal detector with current J_0 having an ostensible distribution corresponding to Gaussian white noise. We model the addition of dark noise by setting the output of the realistic detector to be the current

$$J(t)dt = [J_0(t)dt + \sqrt{N}dW_1]/\sqrt{1 + N}, \quad (4.260)$$

where dW_1 is an independent Wiener increment and N is the dark-noise power relative to the shot noise. Note that we have included the normalization factor so that the ostensible distribution for $J(t)$ is also that of normalized Gaussian white noise.

The problem is to determine the quantum trajectory for the system state ρ_J conditioned on Eq. (4.260), rather than that conditioned on the ideal current J_0 . To proceed, we rewrite J_0 as

$$J_0(t)dt = [J(t)dt + \sqrt{N}dW'(t)]/\sqrt{1 + N}, \quad (4.261)$$

where

$$dW' = (\sqrt{N}J_0 dt - dW_1)/\sqrt{1+N} \quad (4.262)$$

is ostensibly a Wiener increment and is independent of $J(t)$.

Exercise 4.30 Verify that $(J dt)^2 = (dW')^2 = dt$ and that $(J dt)dW' = 0$.

Substituting this into Eq. (4.259) yields

$$d\bar{\rho} = \mathcal{L}\bar{\rho} dt + (1+N)^{-1/2}[J(t)dt + \sqrt{N}dW'][\hat{c}\bar{\rho} + \text{H.c.}]. \quad (4.263)$$

Now we can average over the unobserved noise to get

$$d\bar{\rho} = \mathcal{L}\bar{\rho} dt + (1+N)^{-1/2}J(t)dt[\hat{c}\bar{\rho} + \text{H.c.}]. \quad (4.264)$$

Converting this into a nonlinear SME for the normalized state matrix gives

$$d\rho = \mathcal{L}\rho dt + \sqrt{\eta}dW(t)\mathcal{H}[\hat{c}]\rho, \quad (4.265)$$

where $\eta \equiv 1/(1+N)$ and $dW(t)$ is the Gaussian white noise which appears in the actual photocurrent:

$$J(t) = \sqrt{\eta}\langle\hat{c} + \hat{c}^\dagger\rangle + dW(t)/dt. \quad (4.266)$$

In comparison with Section 4.8.1 we see that the addition of Gaussian white noise to the photocurrent before the experimenter has access to it is exactly equivalent to an inefficient homodyne detector.

For direct detection, dark noise is *not* the same as an inefficiency. Modelling it is actually more akin to the methods of the following subsection, explicitly involving the detector. The interested reader is referred to Refs. [WW03a, WW03b].

4.8.4 Detectors with a finite bandwidth

The final sort of detector imperfection we consider is a finite detector bandwidth. By contrast with dark noise, this produces something quite different from what we have seen before. Specifically, it leads to a non-Markovian quantum trajectory. The system still obeys a Markovian master equation on average, but, because the observer has access only to a filtered output from the system, the information the observer needs to update their system state $\rho(t)$ is not contained solely in $\rho(t)$ and the measurement result in the infinitesimal interval $[t, t + dt)$. We will see instead that the observer must keep track of a joint state of the quantum system and the classical detector, in which there are correlations between these two systems.

Actually, all of these remarks apply only if the realistic detector adds noise to the output of an ideal homodyne detector (as in the preceding section) as well as filtering it. For example, say the output of the ideal detector was $J(t)$, and the output of the realistic detector was put through a low-pass filter of bandwidth B :

$$Q(t) = \int_{-\infty}^t B e^{-B(t-s)} J(s) ds. \quad (4.267)$$

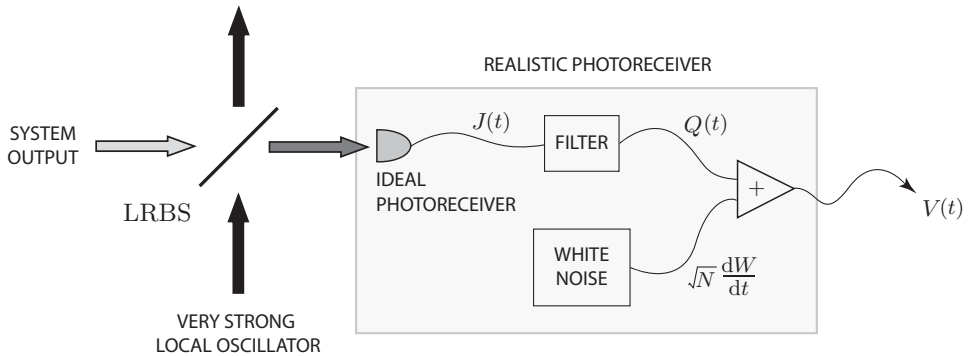


Fig. 4.9 A schematic diagram of the model for simple homodyne detection by a realistic photoreceiver. The realistic photoreceiver is modelled by a hypothetical ideal photoreceiver, the output $J(t)$ of which is passed through a low-pass filter to give $Q(t)$. White noise $\sqrt{N} dW/dt$ is added to this to yield the observable output $V(t)$ of the realistic photoreceiver.

Then an observer could obtain J from Q simply as

$$J(t) = Q(t) + \dot{Q}(t)/B. \quad (4.268)$$

Thus, the quantum state conditioned on $Q(t)$ is the same as that conditioned on $J(t)$. However a nontrivial result is obtained if we say that the output is

$$V(t) = Q(t) + \sqrt{N} dW_1(t)/dt, \quad (4.269)$$

where dW_1 is an independent Wiener increment. This is shown in Fig. 4.9

An equation of the form of Eq. (4.269) can be derived by considering the output of a realistic homodyne detector, called a photoreceiver. This consists of a p–i–n photodiode (which acts as an ideal detector, apart from a small inefficiency), which produces a current $\propto J$ that is fed into an operational amplifier set up as a transimpedance amplifier. This has a low effective input impedance, so the diode acts as a current source, and J is converted into a charge $\propto Q$ on a capacitor of capacitance C in parallel with the feedback resistor of resistance R . The bandwidth B in Eq. (4.267) is equal to $1/(RC)$. The resistor, being at a finite temperature, introduces Johnson noise with power $\propto N$ into the amplifier output V , which is what the observer can see. For details, see Ref. [WW03a].

The general method we adopt is the following. First, we determine the SME for the state of the quantum system conditioned on J . Then we determine a stochastic Fokker–Planck equation (FPE) (see Section B.5) for the state of the detector. This is represented by $\wp(q)$, the probability distribution for $Q(t)$, and also depends upon J . Next we consider $\wp_V(q)$, the conditioned classical state based on our observation of V , which involves another stochastic process. Finally, we combine all of these equations together to derive an equation for the state of a *supersystem*

$$\rho_V(q) = E_J[\rho^J \wp_V^J(q)]. \quad (4.270)$$

Here the J superscript represents dependence upon the unobservable microscopic current J . This is the variable which is averaged over to find the expectation value. From this equation we can obtain our state of knowledge of the system, conditioned on V , as

$$\rho_V = \int dq \rho_V(q). \quad (4.271)$$

Similarly, our state of knowledge of the detector is

$$\wp_V(q) = \text{Tr}[\rho_V(q)]. \quad (4.272)$$

Note, however, that $\rho(q)$ contains more information than do ρ and $\wp(q)$ combined, because of correlations between the quantum system and the classical detector.

The ideal stochastic master equation. As in the previous cases of imperfect detection, it is convenient to use the linear form of the SME as in Section 4.4.3. For a detector that is ideal apart from an efficiency η , this is

$$d\bar{\rho}^J = \mathcal{L}\bar{\rho}^J dt + \sqrt{\eta}[J(t)dt](\hat{c}\bar{\rho}^J + \bar{\rho}^J\hat{c}^\dagger), \quad (4.273)$$

where the ostensible distribution for the current $J(t)$ is that of Gaussian white noise.

The stochastic FPE for the detector. The detector state is given by $\wp(q)$, the probability distribution for Q . From Eq. (4.267), Q obeys the SDE

$$dQ = -B[Q - J(t)]dt, \quad (4.274)$$

where J as given above satisfies $(J dt)^2 = dt$. From Section B.5, the probability distribution $\wp(q)$ obeys the stochastic Fokker–Planck equation (FPE)

$$d\wp^J(q) = \left\{ B \frac{\partial}{\partial q} [q - J(t)]dt + \frac{1}{2} B^2 \frac{\partial^2}{(\partial q)^2} dt \right\} \wp^J(q). \quad (4.275)$$

This assumes knowledge of J , as shown explicitly by the superscript. Note that this equation has the solution

$$\wp^J(q) = \delta(q - Q^J), \quad (4.276)$$

where Q^J is the solution of Eq. (4.274). It is only later, when we average over J , that we will obtain an equation with diffusion leading to a non-singular distribution. If we were to do this at this stage we would derive a FPE of the usual (deterministic) type, without the J -dependent term in Eq. (4.275).

The Zakai equation for the detector. Now we consider how $\wp(q)$ changes when the observer obtains the information in V . That is, we determine the conditioned state by Bayesian inference:

$$\wp_V(q) \equiv \wp(q|V) = \frac{\wp(V|q)\wp(q)}{\wp(V)}. \quad (4.277)$$

From Eq. (4.269), in any infinitesimal time interval, the noise in V is infinitely greater than the signal. Specifically, the root-mean-square noise in an interval of duration dt is

\sqrt{N}/dt , while the signal is Q . Thus, the amount of information about Q contained in $V(t)$ is infinitesimal, and hence the change from $\wp(q)$ to $\wp_V(q)$ is infinitesimal, of order \sqrt{dt} . This means that it is possible to derive a stochastic differential equation for $\wp_V(q)$. This is called a *Kushner–Stratonovich* equation (KSE). Such a KSE is exactly analogous to the stochastic master equation describing the update of an observer's knowledge of a quantum system.

Just as in the quantum case one can derive a linear version of the SME for an unnormalized state $\bar{\rho}$, one can derive a linear version of the KSE for an unnormalized probability distribution $\bar{\wp}_V(q)$. This involves choosing an ostensible distribution $\wp_{\text{ost}}(V)$, such as $\wp_{\text{ost}}(V) = \wp(V|q := 0)$. Then

$$\bar{\wp}_V(q) = \frac{\wp(V|q)\bar{\wp}(q)}{\wp_{\text{ost}}(V)} \quad (4.278)$$

has the interpretation that $\wp_{\text{ost}}(V) \int dq \bar{\wp}_V(q)$ is the actual probability distribution for V . Note the analogy with the quantum case in Section 4.4.3, where a trace rather than an integral is used (see also Table 1.1). The linear version of the KSE is called the *Zakai* equation and it will be convenient to use it in our derivation.

From Eq. (4.269), the distribution of V given that $Q = q$ is

$$\wp(V|q) = [dt/(2\pi N)]^{1/2} \exp[-(V - q)^2 dt/(2N)]. \quad (4.279)$$

Hence, with the above choice,

$$\wp_{\text{ost}}(V) = [dt/(2\pi N)]^{1/2} \exp[-V^2 dt/(2N)], \quad (4.280)$$

and the ratio multiplying $\bar{\wp}(q)$ in Eq. (4.278) is

$$\exp[(2Vq - q^2)dt/(2N)]. \quad (4.281)$$

Now the width of $\wp(q)$ will not depend upon dt (as we will see), so we can assume that $\wp(q)$ has support that is finite. Hence the q in Eq. (4.281) can be assumed finite. By contrast, V is of order $1/\sqrt{dt}$, as explained above. Thus, the leading term in the exponent of Eq. (4.281) is $Vq/(dt N)$, and this is of order \sqrt{dt} . Expanding the exponent to leading order gives

$$\bar{\wp}_V(q) = [1 + qV(t)dt/N]\bar{\wp}(q). \quad (4.282)$$

Expressing this in terms of differentials, we have the Zakai equation

$$d\bar{\wp}_V(q) = (1/\sqrt{N})[V(t)dt/\sqrt{N}]q\bar{\wp}(q), \quad (4.283)$$

where $V(t)dt/\sqrt{N}$ has the ostensible distribution of a Wiener process.

The joint stochastic equation. We now combine the three stochastic equations we have derived above (the SME for the system, the stochastic FPE for the detector and the Zakai equation for the detector) to obtain a joint stochastic equation. We define

$$\bar{\rho}_V^J(q) = \bar{\rho}^J \bar{\wp}_V^J(q). \quad (4.284)$$

On introducing a time-argument for ease of presentation, we have

$$\bar{\rho}_V^J(q; t + dt) = [1 + qV(t)dt/N][\wp^J(q; t) + d\wp^J(q; t)][\bar{\rho}^J(t) + d\bar{\rho}^J(t)], \quad (4.285)$$

where we have used Eq. (4.282), and $d\wp^J(q; t)$ is given by Eq. (4.275) and $d\bar{\rho}^J(t)$ by Eq. (4.273). By expanding these out we find

$$\begin{aligned} d\bar{\rho}_V^J(q) = dt & \left\{ B \frac{\partial}{\partial q} [q - J(t)] + \frac{1}{2} B^2 \frac{\partial^2}{(\partial q)^2} + \mathcal{L} \right\} \bar{\rho}^J(q) \\ & + \sqrt{\eta} [J(t)dt] \left\{ 1 - [J(t)dt] B \frac{\partial}{\partial q} \right\} [\hat{c} \bar{\rho}^J(q) + \bar{\rho}^J(q) \hat{c}^\dagger] \\ & + (1/\sqrt{N}) [V(t)dt/\sqrt{N}] q \bar{\rho}^J(q). \end{aligned} \quad (4.286)$$

Averaging over unobserved processes. By construction, the joint stochastic equation in Eq. (4.286) will preserve the factorization of $\bar{\rho}^J(q)$ in the definition Eq. (4.284). This is because this equation assumes that J , the output of the ideal (apart from its inefficiency) detector, is known. In practice, the experimenter knows only V , the output of the realistic detector. Therefore we should average over J . Since we are using a linear SME, this means using the ostensible distribution for Jdt in which it has a mean of zero and a variance of dt . Thus we obtain

$$\begin{aligned} d\bar{\rho}_V(q) = dt & \left\{ B \frac{\partial}{\partial q} q + \frac{1}{2} B^2 \frac{\partial^2}{(\partial q)^2} + \mathcal{L} \right\} \bar{\rho}(q) \\ & - dt \sqrt{\eta} B \frac{\partial}{\partial q} [\hat{c} \bar{\rho}(q) + \bar{\rho}(q) \hat{c}^\dagger] \\ & + (1/\sqrt{N}) [V(t)dt/\sqrt{N}] q \bar{\rho}(q). \end{aligned} \quad (4.287)$$

We call this the superoperator Zakai equation.

The superoperator Kushner–Stratonovich equation. Let $\bar{\rho}(q)$ at the start of the interval be normalized. That is, let it equal $\rho(q)$, where

$$\int_{-\infty}^{\infty} dq \operatorname{Tr}[\rho(q)] = 1. \quad (4.288)$$

Then the infinitesimally evolved unnormalized state determines the actual distribution for V according to

$$\wp(V) = \wp_{\text{ost}}(V) \int_{-\infty}^{\infty} dq \operatorname{Tr}[\rho(q) + d\bar{\rho}_V(q)]. \quad (4.289)$$

Using the same arguments as in Section 4.4.3, we see that the actual statistics for V are

$$V dt = \langle Q \rangle dt + \sqrt{N} dW(t), \quad (4.290)$$

where

$$\langle Q \rangle = \int_{-\infty}^{\infty} dq \operatorname{Tr}[\rho(q)] q. \quad (4.291)$$

Note that $dW(t)$ is *not* the same as $dW_1(t)$ in Eq. (4.269). Specifically,

$$\sqrt{N} dW = \sqrt{N} dW_1 + (Q - \langle Q \rangle). \quad (4.292)$$

The realistic observer cannot find dW_1 from dW , since that observer does not know Q .

The final step is to obtain an equation for the normalized state, using the actual distribution for V . If we again assume that the state is normalized at the start of the interval, we find

$$d\rho_V(q) = \frac{\rho(q) + d\bar{\rho}_V(q)}{\int dq \text{Tr}[\rho(q) + d\bar{\rho}_V(q)]} - \rho(q). \quad (4.293)$$

Now taking the trace and integral of Eq. (4.287) gives zero for every term except for the last, so the denominator evaluates to

$$1 + (1/\sqrt{N})[V(t)dt/\sqrt{N}]\langle Q \rangle. \quad (4.294)$$

By expanding the reciprocal of this to *second* order and using Eq. (4.290) to replace $[V(t)dt/\sqrt{N}]^2$ by dt , we find

$$\begin{aligned} d\rho_V(q) = dt & \left\{ B \frac{\partial}{\partial q} q + \frac{1}{2} B^2 \frac{\partial^2}{(\partial q)^2} + \mathcal{L} \right\} \rho_V(q) \\ & - dt \sqrt{\eta} B \frac{\partial}{\partial q} [\hat{c} \rho_V(q) + \rho_V(q) \hat{c}^\dagger] \\ & + (1/\sqrt{N}) dW(t)(q - \langle Q \rangle) \rho_V(q). \end{aligned} \quad (4.295)$$

Exercise 4.31 *Work this all through explicitly.*

We call Eq. (4.295) a superoperator Kushner–Stratonovich equation. Note that we have placed the V subscript on the state on the right hand side, because typically this will be conditioned on earlier measurements of the output V . The first line describes the evolution of the detector and quantum system separately. The second line describes the coupling of the system to the detector. The third line describes the acquisition of knowledge about the detector from its output Eq. (4.290). This term has the typical form of the information-gathering part of the classical Kushner–Stratonovich equation. Here this information also tells us about the quantum system $\rho_V = \int_{-\infty}^{\infty} dq \rho_V(q)$, because of the correlations between the system and the detector caused by their coupling.

If one ignores the output of the detector, then one obtains the unconditioned evolution equation

$$\begin{aligned} d\rho(q) = dt & \left\{ B \frac{\partial}{\partial q} q + \frac{1}{2} B^2 \frac{\partial^2}{(\partial q)^2} + \mathcal{L} \right\} \rho(q) \\ & - dt \sqrt{\eta} B \frac{\partial}{\partial q} [\hat{c} \rho(q) + \rho(q) \hat{c}^\dagger]. \end{aligned} \quad (4.296)$$

The coupling term here will still generate correlations between the system and the detector. Note, however, that this coupling does not cause any back-action on the system, only

forward-action on the detector. This can be verified by showing that the *unconditioned* system state $\rho = \int_{-\infty}^{\infty} dq \rho(q)$ obeys the original master equation

$$\dot{\rho} = \mathcal{L}\rho = -i[\hat{H}, \rho] + \mathcal{D}[\hat{c}]\rho. \quad (4.297)$$

Exercise 4.32 Verify this, using the fact that $\wp(q)$, and hence $\rho(q)$, can be assumed to go smoothly to zero as $q \rightarrow \pm\infty$.

The superoperator Kushner–Stratonovich equation is clearly considerably more complicated than the stochastic master equations used to describe other imperfections in detection. In general it is possible only to simulate it numerically. (One technique is given in Ref. [WW03b], where it is applied to the homodyne detection of a two-level atom.) Nevertheless, it is possible to study some of its properties analytically [WW03a, WW03b]. From these, some general features of the quantum trajectories this equation generates can be identified. First, in the limit $B \rightarrow \infty$, the detector simply adds dark noise and the appropriate SME (4.265) with effective efficiency $\eta/(1 + N)$ can be rederived. Second, for B finite and $N \ll 1$, the detector has an *effective bandwidth* of

$$B_{\text{eff}} = B/\sqrt{N}, \quad (4.298)$$

which is much greater than B . That is, the detector is insensitive to changes in the system on a time-scale less than \sqrt{N}/B . In the limit $N \rightarrow 0$ the effective bandwidth becomes infinite and the noise becomes zero, so the detector is perfect (apart from η). That is, the quantum trajectories reduce to those of the SME (4.238), as expected from the arguments at the beginning of this subsection.

4.9 Continuous measurement in mesoscopic electronics

4.9.1 Monitoring a single quantum dot

In Section 3.5 we discussed the irreversible dynamics of a single-electron quantum dot coupled to two fermionic reservoirs. Experiments using a two-dimensional electron gas, confined to the interface between GaAs and AlGaAs and further confined using surface gates, can be configured to enable real-time monitoring of tunnelling electrons [LJP⁺03, BDD05, VES⁺04, SJG⁺07]. In this section we will consider a model of such an experiment.

Physical model. A quantum point contact or QPC is the simplest mesoscopic tunnelling device and consists of two fermionic reservoirs connected by a single electrostatically defined tunnelling barrier [BB00]. A QPC can be used as a sensitive electrometer if the tunnelling barrier is modulated by the charge on a nearby quantum dot.

We will consider the device shown in Fig. 4.10. A quantum dot is connected to two Fermi reservoirs biased so that electrons can tunnel onto the dot from the left reservoir and off the dot onto the right reservoir. Close to the quantum dot is the QPC. As the electron moves into the quantum dot it increases the height of the tunnel barrier for the nearby QPC. In

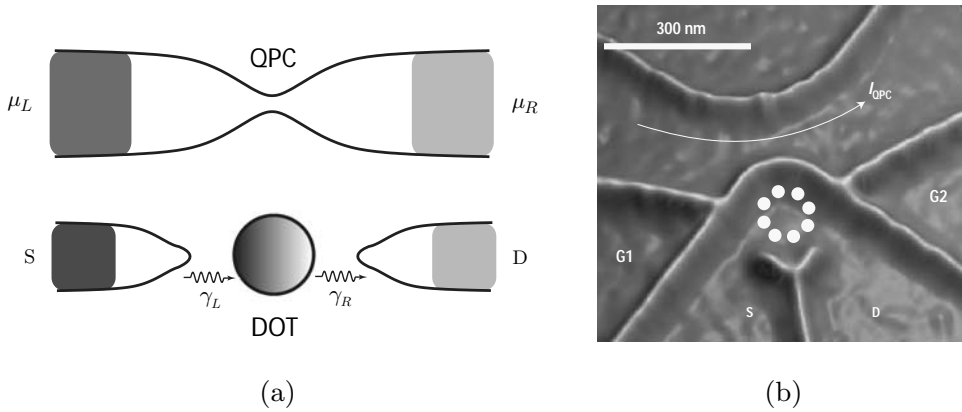


Fig. 4.10 (a) A quantum dot with a single-electron quasibound state is connected to two Fermi reservoirs, a source (S) and drain (D) by tunnel junctions. Tunnelling through the quantum dot modulates the tunnelling current through a quantum point contact. (b) An experimental realization using potentials (defined by surface gates) in a GaAs/AlGaAs two-dimensional electron-gas system. Part (b) is reprinted by permission from Macmillan Publishers Ltd, *Nature Physics*, E. V. Sukhorukov *et al.*, **3**, 243, Fig. 1(a), copyright 2007.

this way the modulated current through the QPC can be used continuously to monitor the occupation of the dot. We will follow the treatment given in Ref. [GM01].

The irreversible dynamics of the tunnelling through a single quasibound state on a quantum dot from source to drain is treated in Section 3.5. We assume here that the interaction of the dot with the QPC is weak, and hence does not significantly change the master equation derived there. Here we need a model to describe the tunnelling current through the QPC and its interaction with the quantum dot. We use the following Hamiltonian (with $\hbar = 1$):

$$\hat{H} = \hat{H}_{\text{QD+leads}} + \hat{H}_{\text{QPC}} + \hat{H}_{\text{coup}}. \quad (4.299)$$

Here $\hat{H}_{\text{QD+leads}}$ is as in Eq. (3.64), and describes the tunnelling of electrons from the source to the dot and from the dot to the drain. This leads to the master equation (3.73) in which the tunnelling rate from source to dot is γ_L and that from dot to drain is γ_R . The new Hamiltonian terms in this chapter are

$$\hat{H}_{\text{QPC}} = \sum_k \left(\omega_k^L \hat{a}_{Lk}^\dagger \hat{a}_{Lk} + \omega_k^R \hat{a}_{Rk}^\dagger \hat{a}_{Rk} \right) + \sum_{k,q} \left(\tau_{kq} \hat{a}_{Lk}^\dagger \hat{a}_{Rq} + \tau_{qk}^* \hat{a}_{Rq}^\dagger \hat{a}_{Lk} \right), \quad (4.300)$$

$$\hat{H}_{\text{coup}} = \sum_{k,q} \hat{c}^\dagger \hat{c} \left(\chi_{kq} \hat{a}_{Lk}^\dagger \hat{a}_{Rq} + \chi_{qk}^* \hat{a}_{Rq}^\dagger \hat{a}_{Lk} \right). \quad (4.301)$$

Here, as in Section 3.5, \hat{c} is the electron annihilation operator for the quantum dot. The Hamiltonian for the QPC detector is represented by \hat{H}_{QPC} , in which \hat{a}_{Lk} , \hat{a}_{Rk} and ω_k^L , ω_k^R are, respectively, the electron (fermionic) annihilation operators and energies for the left and right reservoir modes for the QPC at wave number k . Also, there is tunnelling between

these modes with amplitudes τ_{kq} . Finally, Eq. (4.301) describes the interaction between the detector and the dot: when the dot contains an electron, the effective tunnelling amplitudes of the QPC detector change from τ_{kq} to $\tau_{kq} + \chi_{kq}$.

In the interaction frame and Markovian approximation, the (unconditional) zero-temperature master equation of the reduced state matrix for the quantum-dot system is [Gur97, GMWS01]

$$\dot{\rho}(t) = \gamma_L \mathcal{D}[\hat{c}^\dagger]\rho + \gamma_R \mathcal{D}[\hat{c}]\rho + \mathcal{D}[\tilde{\tau} + \tilde{\chi}\hat{n}]\rho(t) \quad (4.302)$$

$$\equiv \mathcal{L}\rho(t), \quad (4.303)$$

where $\hat{n} = \hat{c}^\dagger \hat{c}$ is the occupation-number operator for the dot, $\tilde{\tau} = \alpha\tau_{00}$ and $\tilde{\chi} = \alpha\chi_{00}$. Here τ_{00} and χ_{00} are the tunnelling amplitudes for energies near the chemical potentials (μ_L and $\mu_R = \mu_L - eV$ in the left and right reservoirs, respectively), while $\alpha^2 = 2\pi(\mu_L - \mu_R)g_L g_R$, where g_L and g_R are the appropriate densities of states for the reservoirs.

Physically, the presence of the electron in the dot raises the effective tunnelling barrier of the QPC due to electrostatic repulsion. As a consequence, the effective tunnelling amplitude through the QPC becomes lower, i.e. $D' = |\tilde{\tau} + \tilde{\chi}|^2 < D = |\tilde{\tau}|^2$. This sets a condition on the relative phase θ between $\tilde{\chi}$ and $\tilde{\tau}$: $\cos\theta < -|\tilde{\chi}|/(2|\tilde{\tau}|)$.

The unconditional dynamics of the number of electrons on the dot is unchanged by the presence of the QPC, and so is given by Eq. (3.74), which we reproduce here:

$$\frac{d\langle\hat{n}\rangle}{dt} = \gamma_L(1 - \langle\hat{n}\rangle) - \gamma_R\langle\hat{n}\rangle. \quad (4.304)$$

This is because the Hamiltonian describing the interaction between the dot and the QPC commutes with the number operator \hat{n} – the measurement is a QND measurement of \hat{n} . However, if we ask for the *conditional* mean occupation of the dot *given* an observed current through the QPC, we do find a (stochastic) dependence on this current, as we will see later.

Exercise 4.33 Show that the stationary solution to Eq. (4.302) is

$$\rho_{ss} = \frac{\gamma_L}{\gamma_L + \gamma_R} |1\rangle\langle 1| + \frac{\gamma_R}{\gamma_L + \gamma_R} |0\rangle\langle 0|, \quad (4.305)$$

and that this is consistent with the stationary solution of Eq. (4.304).

Currents and correlations. It is important to distinguish the two classical stochastic currents through this system: the current $I(t)$ through the QPC and the current $J(t)$ through the quantum dot. Equation (4.302) describes the evolution of the reduced state matrix of the quantum dot when these classical stochastic processes are averaged over. To study the stochastic evolution of the quantum-dot state, conditioned on a particular measurement realization, we need the conditional master equation. We first define the relevant point processes that are the source of the classically observed stochastic currents.

For the tunnelling onto and off the dot, we define two point processes:

$$[dM_c^b(t)]^2 = dM_c^b(t), \quad (4.306)$$

$$E[dM_c^L(t)] = \gamma_L \langle (1 - \hat{n}) \rangle_c(t) dt = \gamma_L \text{Tr}[\mathcal{J}[\hat{c}^\dagger] \rho_c(t)] dt, \quad (4.307)$$

$$E[dM_c^R(t)] = \gamma_R \langle \hat{n} \rangle_c(t) dt = \gamma_R \text{Tr}[\mathcal{J}[\hat{c}] \rho_c(t)] dt. \quad (4.308)$$

Here b takes the symbolic value L or R and we use the subscript c to emphasize that the quantities are conditioned upon previous observations (detection records) of the occurrences of electrons tunnelling through the quantum dot and also tunnelling through the QPC barrier (see below). The current through the dot is given by the classical stochastic process

$$J(t)dt = [e_L dM_c^L(t) + e_R dM_c^R(t)], \quad (4.309)$$

where e_L and e_R are as defined in Section 3.5 and sum to e .

Next, we define the point process for tunnelling through the QPC:

$$[dN_c(t)]^2 = dN_c(t), \quad (4.310)$$

$$E[dN_c(t)] = \text{Tr}[\mathcal{J}[\tilde{\tau} + \hat{n}\tilde{\chi}] \rho_c] = [D + (D' - D)\langle \hat{n} \rangle_c(t)]dt. \quad (4.311)$$

This is related to the current through the QPC simply by

$$I(t)dt = e dN_c(t). \quad (4.312)$$

The expected current is thus eD when the dot is empty and eD' when the dot is occupied.

Exercise 4.34 Show that the steady-state currents through the quantum dot and QPC are, respectively,

$$J_{ss} = \frac{e\gamma_L\gamma_R}{\gamma_L + \gamma_R}, \quad (4.313)$$

$$I_{ss} = eD\left(\frac{\gamma_R}{\gamma_L + \gamma_R}\right) + eD'\left(\frac{\gamma_L}{\gamma_L + \gamma_R}\right). \quad (4.314)$$

(Note that the expression for J_{ss} agrees with Eq. (3.77) from Section 3.5.)

The SME describing the quantum-dot state conditioned on the above three point processes is easily derived using techniques similar to those described in Section 4.3. The result is

$$\begin{aligned} d\rho_c = & dM^L(t)\mathcal{G}[\sqrt{\gamma_L}\hat{c}^\dagger]\rho_c + dM^R(t)\mathcal{G}[\sqrt{\gamma_R}\hat{c}]\rho_c + dN(t)\mathcal{G}[\tilde{\tau} + \tilde{\chi}\hat{n}]\rho_c \\ & - dt \frac{1}{2}\mathcal{H}[\gamma_L\hat{c}\hat{c}^\dagger + \gamma_R\hat{c}^\dagger\hat{c} + (D' - D)\hat{n}]\rho_c. \end{aligned} \quad (4.315)$$

Equation (4.315) assumes that we can monitor the current through the quantum dot sufficiently quickly and accurately to distinguish the current pulses associated with the processes $dM^b(t)$. In this case, the dot occupation $\langle n \rangle_c(t)$ will jump between the values 0 and 1. It makes the transition $0 \rightarrow 1$ when an electron tunnels onto the dot, which occurs at rate γ_L . It makes the transition $1 \rightarrow 0$ when an electron leaves the quantum dot, which occurs at rate γ_R .

Exercise 4.35 Convince yourself of this from Eq. (4.315).

Next, we will also assume that D and D' are both much larger than γ_L or γ_R . This means that many electrons will tunnel through the QPC before the electron dot-occupation number changes. Thus the fluctuations in the QPC current $I_c(t)$ due to individual tunnelling events through the QPC (described by $dN(t)$) can be ignored, and it can be treated simply as a two-valued quantity:

$$\langle I \rangle_c(t) = eD + e(D' - D)\langle n \rangle_c(t). \quad (4.316)$$

The two values are eD and eD' , depending on the value of $\langle n \rangle_c(t)$, and transitions between them are governed by the transition rates γ_L and γ_R . A process such as this is called a *random telegraph process*.

Using known results for a random telegraph process [Gar85], we can calculate the stationary two-time correlation function for the QPC current,

$$\begin{aligned} R(t-s) &\equiv E[I(t), I(s)]_{ss} \\ &= e^2(D - D')^2 \frac{\gamma_L \gamma_R}{(\gamma_L + \gamma_R)^2} e^{-(\gamma_L + \gamma_R)|t-s|}. \end{aligned} \quad (4.317)$$

Here $E[A, B] \equiv E[AB] - E[A]E[B]$, and Eq. (4.317) is sometimes called the *reduced* correlation function because of the subtraction of the products of the means.

Exercise 4.36 Derive Eq. (4.317) from the master equation (4.302) by identifying $I(t)$ with the observable $eD + e(D' - D)\hat{n}(t)$, and using the quantum regression theorem (4.191).

As in the case of photocurrents, it is often convenient to characterize the dynamics by the *spectrum* of the current. We define it using the reduced correlation function:

$$S_{\text{QPC}}(\omega) = \int_{-\infty}^{\infty} d\tau e^{-i\omega\tau} R(\tau). \quad (4.318)$$

Exercise 4.37 Show that, for the situation considered above, the QPC spectrum is the Lorentzian

$$S_{\text{QPC}}(\omega) = e^2(D - D')^2 \frac{2\gamma_L \gamma_R}{(\gamma_L + \gamma_R)^2} \frac{\gamma_L + \gamma_R}{(\gamma_L + \gamma_R)^2 + \omega^2}. \quad (4.319)$$

Conditional dynamics. We now focus on the conditional dynamics of the quantum dot as the QPC current, $I(t)$, is monitored. That is, we average over the dot-tunnelling events described by $dM^b(t)$. Physically, this is reasonable because it would be very difficult to discern the charge pulses (less than one electron) associated with these jumps. It would be similarly difficult to discern the individual jumps $dN(t)$ which define the QPC current $I(t)$ according to Eq. (4.312). In the above, we avoided that issue by considering the limit in which the rate of tunnelling events through the QPC was so high that $I(t)$ could be treated as a random telegraph process, with randomness coming from the quantum-dot dynamics but no randomness associated with the QPC tunnelling itself. It is apparent from the results of the experiment (see Fig. 4.11) that this is a good, but not perfect, approximation. That

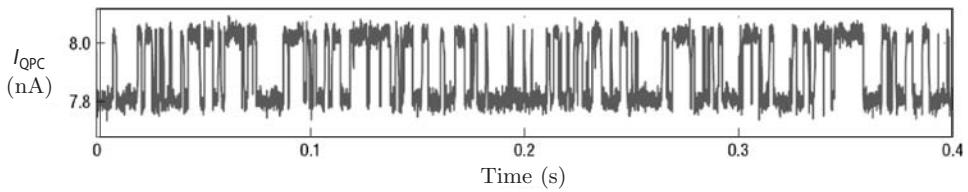


Fig. 4.11 A typical experimental record of the QPC tunnel current as it switches between two values depending on the occupation of the nearby quantum dot. Adapted by permission from Macmillan Publishers Ltd, *Nature Physics*, E. V. Sukhorukov *et al.*, **3**, 243, Fig. 1(c), copyright 2007.

is to say, it is evident that there is some noise on the current in addition to its switching between the values eD and eD' . This noise is due in part to the stochastic processes of electrons tunnelling through the QPC and in part to excess noise added in the amplification process. It is obvious that the individual jumps through the QPC are not resolved; rather, the noise appears to be that of a diffusion process.

We saw in Section 4.8.3 that, if the noise in an ideal current is a Wiener process and the excess noise is also a Wiener process, then the effect of the contaminating noise is simply to reduce the efficiency of the detection to $\zeta < 1$. Since this is the simplest model of imperfect detection, we will apply it in the present case. This requires finding a diffusive approximation to the quantum jump stochastic master equation for describing the conditional QPC current dynamics. As will be seen, this requires $|D' - D|/D \ll 1$. From Fig. 4.11 we see that in the experiment this ratio evaluated to approximately 0.03, so this approximation seems reasonable.

On averaging over the jump process dM^b , introducing an efficiency ζ as described above and assuming for simplicity that $\tilde{\tau}$ and $-\tilde{\chi}$ are real and positive (so that the relative phase $\theta = \pi$), Eq. (4.315) reduces to

$$\begin{aligned} d\rho_I = & dN(t)\mathcal{G}[\sqrt{\zeta}(\tilde{\tau} + \tilde{\chi}\hat{n})]\rho_I + \zeta\frac{1}{2}dt\mathcal{H}[2\tilde{\tau}\tilde{\chi}\hat{n} - (\tilde{\chi}\hat{n})^2]\rho_I \\ & + dt\{\gamma_L\mathcal{D}[\hat{c}^\dagger] + \gamma_R\mathcal{D}[\hat{c}] + (1 - \zeta)\mathcal{D}[\tilde{\tau} + \tilde{\chi}\hat{n}]\}\rho_I, \end{aligned} \quad (4.320)$$

where we have used a new subscript to denote conditioning on $I(t) = e dN/dt$, where

$$\mathbb{E}[dN(t)] = \text{Tr}\left[\mathcal{J}[\sqrt{\zeta}(\tilde{\tau} + \tilde{\chi}\hat{n})]\rho_c\right] = \zeta[D + (D' - D)\langle n \rangle_c(t)]. \quad (4.321)$$

This describes quantum jumps, in that every time there is a tunnelling event ($dN = 1$) the conditional state changes by a finite amount.

To derive a diffusive limit, we make the following identifications:

$$-\sqrt{\zeta}\tilde{\chi}\hat{n} \rightarrow \hat{c}; \quad \sqrt{\zeta}\tilde{\tau} \rightarrow \gamma. \quad (4.322)$$

Then, apart from the additional irreversible terms, Eq. (4.320) is identical to the conditional master equation for homodyne detection (4.66). Thus, if we assume that $\tilde{\tau} \gg -\tilde{\chi}$ (or, equivalently, $|D' - D|/D \ll 1$), we can follow the procedure of Section 4.4.2. We thus

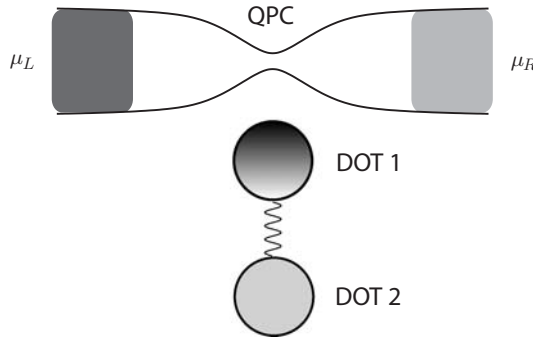


Fig. 4.12 A QPC is used to monitor the occupation of a quantum dot (1) coherently coupled by tunnelling to another quantum dot (2).

obtain the diffusive SME

$$d\rho_c(t) = dt(\gamma_L \mathcal{D}[\hat{c}^\dagger] + \gamma_R \mathcal{D}[\hat{c}] + \kappa \mathcal{D}[\hat{n}])\rho_c(t) + \sqrt{\kappa \zeta} dW(t) \mathcal{H}[\hat{n}]\rho_c(t), \quad (4.323)$$

where $\kappa = \tilde{\chi}^2$, and here $\kappa \ll D$. The current on which the state is conditioned is

$$I_c(t) = e\sqrt{\zeta D} \left[\sqrt{\zeta D} - \sqrt{\zeta \kappa} \langle \hat{n} \rangle_c(t) - \xi(t) \right], \quad (4.324)$$

where $\xi(t) = dW/dt$ as usual. Note the negative signs in Eq. (4.324), because of the sign of $\tilde{\chi}$, and also the constant term which dominates over the term containing the conditional mean, since $\kappa \ll D$.

We can now find the dynamics of the dot occupation, conditioned on the observed QPC current, as

$$\frac{d\langle \hat{n} \rangle_c}{dt} = \gamma_L(1 - \langle \hat{n} \rangle_c) - \gamma_R \langle \hat{n} \rangle_c + 2\sqrt{\zeta \kappa} \langle \hat{n} \rangle_c(1 - \langle \hat{n} \rangle_c) \xi(t). \quad (4.325)$$

Note that the noise ‘turns off’ when the dot is either occupied or empty ($\langle \hat{n} \rangle_c = 1$ or 0). This is necessary mathematically in order to prevent the occupation becoming less than 0 or greater than 1. Physically, if $\langle \hat{n} \rangle_c = 1$ (0), we are sure that there is (is not) an electron on the dot, so monitoring the dot cannot give us any more information about the state. Thus, there is no updating of the conditional mean occupation.

4.9.2 Monitoring a double quantum dot

In many ways the QPC coupled to a single quantum dot is not especially quantum; the state can be described by a single number, the occupation probability $\langle \hat{n} \rangle$, since quantum coherences are irrelevant. A modified model in which quantum coherence is important is the double quantum dot (DQD) depicted in Fig. 4.12. This was mentioned before briefly in Section 3.10.1. A system such as this can also be realized in a GaAs/AlGaAs structure [PJM⁺04, FWH07]. Here the DQD is not connected to leads (it always contains exactly

one electron), so the Hamiltonian for this system is

$$\hat{H} = \hat{H}_{\text{DQD}} + \hat{H}_{\text{QPC}} + \hat{H}_{\text{coup}}, \quad (4.326)$$

where

$$\hat{H}_{\text{DQD}} = \omega_1 \hat{c}_1^\dagger \hat{c}_1 + \omega_2 \hat{c}_2^\dagger \hat{c}_2 + \Omega(\hat{c}_1^\dagger \hat{c}_2 + \hat{c}_2^\dagger \hat{c}_1)/2, \quad (4.327)$$

$$\hat{H}_{\text{coup}} = \sum_{k,q} \hat{c}_1^\dagger \hat{c}_1 \left(\chi_{kq} \hat{a}_{Lk}^\dagger \hat{a}_{Rq} + \chi_{qk}^* \hat{a}_{Rq}^\dagger \hat{a}_{Lk} \right), \quad (4.328)$$

and \hat{H}_{QPC} is the same as in the previous model.

A detailed analysis of this model is given in Ref. [GM01]. Following the method used above, the conditional evolution of the DQD is described by the SME

$$\begin{aligned} d\rho_I = & dN(t) \mathcal{G}[\sqrt{\zeta}(\tilde{\tau} + \tilde{\chi} \hat{n}_1)] \rho_I + \zeta \frac{1}{2} dt \mathcal{H}[2\tilde{\tau} \tilde{\chi} \hat{n}_1 - (\tilde{\chi} \hat{n}_1)^2] \rho_I \\ & - i \left[(\omega_2 - \omega_1)(\hat{n}_1 - \hat{n}_2)/2 + \Omega(c_1^\dagger c_2 + c_2^\dagger c_1)/2, \rho_I \right] dt, \end{aligned} \quad (4.329)$$

where $\hat{n}_j = \hat{c}_j^\dagger \hat{c}_j$.

Averaging over the jump process gives the unconditional master equation

$$\dot{\rho} = \kappa \mathcal{D}[\hat{n}_1] \rho - i[\hat{V}, \rho]. \quad (4.330)$$

Here $\kappa = |\tilde{\chi}|^2$ as before, while $\hat{n}_j = \hat{c}_j^\dagger \hat{c}_j$ and the effective Hamiltonian is

$$\hat{V} = \frac{\Delta}{2} \hat{\sigma}_z + \frac{\Omega}{2} \hat{\sigma}_x \quad (4.331)$$

(cf. Eq. (3.31)). Here we have defined a Bloch representation by

$$\hat{\sigma}_x = \hat{c}_1^\dagger \hat{c}_2 + \hat{c}_2^\dagger \hat{c}_1, \quad (4.332)$$

$$\hat{\sigma}_y = i(\hat{c}_1^\dagger \hat{c}_2 - \hat{c}_2^\dagger \hat{c}_1), \quad (4.333)$$

$$\hat{\sigma}_z = \hat{c}_2^\dagger \hat{c}_2 - \hat{c}_1^\dagger \hat{c}_1, \quad (4.334)$$

so that $z(t) = 1$ and $z(t) = -1$ indicate that the electron is localized in dot 2 and dot 1, respectively.

Exercise 4.38 Verify that the above operators $\hat{\sigma}_k$ are Pauli operators.

The parameter Ω is the strength of the tunnelling from one dot to the other, while $\Delta = \omega_2 - \omega_1 + |\tilde{\tau}| |\tilde{\chi}| \sin \theta$ is the difference in energy levels between the two dots, which is influenced by the coupling to the QPC unless $\sin \theta = 0$. (Recall that θ is the relative phase of the $\tilde{\chi}$ and $\tilde{\tau}$.) The coupling to the QPC also destroys coherence between the dots at the decoherence rate κ .

Exercise 4.39 Derive the equations for the Bloch vector (x, y, z) from Eq. (4.330), and show that the steady state is $(0, 0, 0)$, a maximally mixed state.

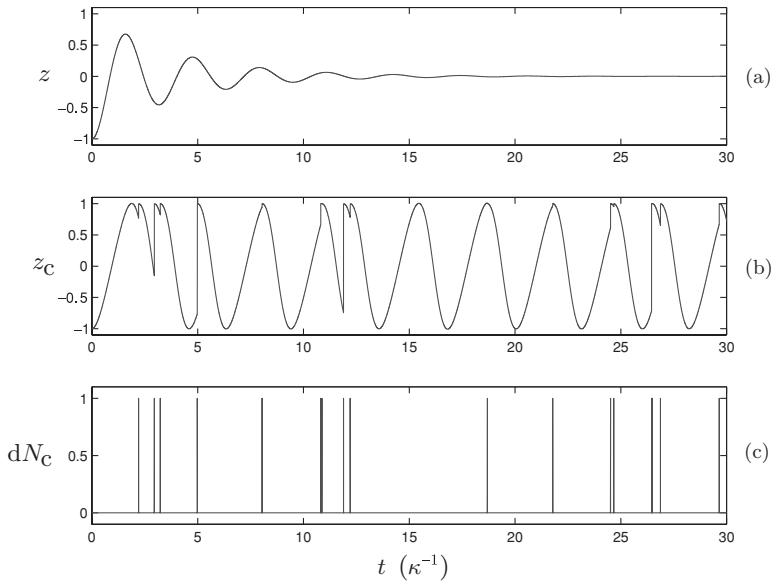


Fig. 4.13 Differences in behaviour between unconditional and conditional evolutions. The initial DQD state is $z = -1$ (dot 1). The parameters are $\zeta = 1$, $\Delta = 0$, $\theta = \pi$ and $D = \kappa = \Omega/2$, and time is in units of κ^{-1} . (Recall that $\kappa = |\tilde{\chi}|^2$ while $D = |\tilde{\tau}|^2$.) (a) Unconditional evolution of $z(t)$. (b) Conditional evolution of $z_c(t)$, interrupted by quantum jumps, corresponding to the stochastically generated QPC detection record shown in (c). Reprinted Figure 3 with permission from H-S. Goan and G. J. Milburn, *Phys. Rev. B* **64**, 235307, (2001). Copyright 2008 by the American Physical Society.

The unconditional evolution of $z(t)$ is shown in Fig. 4.13(a). It undergoes damped oscillations, tending towards zero, as expected for a maximally mixed steady state. The conditional time evolution is quite different. For simplicity we first consider the case, shown in Fig. 4.13(b), of $\theta = \pi$ and $D' = |\tilde{\tau} + \tilde{\chi}|^2 = 0$. That is, due to the electrostatic repulsion generated by the DQD electron, the QPC is blocked (no electron is transmitted) when dot 1 is occupied. As a consequence, whenever there is a detection of an electron tunnelling through the QPC barrier, the DQD state is collapsed into the state $z = 1$ (dot 2 occupied). Note that these jumps are more likely to happen when z is close to 1, so jumps tend to be small (contrast this with the conditioned evolution of a two-level atom under direct detection of its resonance fluorescence, Section 4.6.1). Between jumps, the evolution is smooth but non-unitary. Averaging over the many individual realizations shown in Fig. 4.13(b) leads to a closer and closer approximation of the ensemble average in Fig. 4.13(a).

The plot shown is for the case in which D is comparable to Ω . In the limit $D \gg \Omega$, the jumps become very frequent (with rate D) when the system is in (or close to) the state $z = 1$. Since each jump returns the system to state $z = 1$, as discussed above, the system tends to get stuck in state $z = 1$ (electron in dot 2). This is an example of the *quantum watched-pot*

effect, or *quantum Zeno effect*.⁴ In fact, the electron can still make a transition to dot 1 (the $z = -1$ state), but the rate of this is suppressed from $O(\Omega)$, in the no-measurement case, to $O(\Omega^2/D)$. In the limit $\Omega/D \rightarrow \infty$, the transition rate goes to zero.

The quantum diffusion limit. We saw in Section 4.9.1 that the quantum diffusion equations can be obtained from the quantum jump description under the assumption that $|\tilde{\tau}| \gg |\tilde{\chi}|$ (or equivalently $D \gg \kappa$).

Exercise 4.40 Derive the diffusive SME for the double-dot case, and hence the diffusive stochastic Bloch equations:

$$\begin{aligned} dx_c(t) = & -[\Delta dt + \sqrt{\zeta\kappa} \sin \theta dW(t)]y_c(t) - (\kappa/2)x_c(t)dt \\ & + \sqrt{\zeta\kappa} \cos \theta z_c(t)x_c(t)dW(t), \end{aligned} \quad (4.335)$$

$$\begin{aligned} dy_c(t) = & [\Delta dt + \sqrt{\zeta\kappa} \sin \theta dW(t)]x_c(t) - \Omega z_c(t)dt - (\kappa/2)y_c(t)dt \\ & + \sqrt{\zeta\kappa} \cos \theta z_c(t)y_c(t)dW, \end{aligned} \quad (4.336)$$

$$dz_c(t) = \Omega y_c(t)dt - \sqrt{\zeta\kappa} \cos \theta [1 - z_c^2(t)]dW. \quad (4.337)$$

The measured current gives information about which dot is occupied, as shown in the final term of Eq. (4.337), as expected. However, for $\sin \theta \neq 0$, it also gives information about the rotation around the z axis, as shown in the other two equations. That is, the effective detuning has a deterministic term Δ and a stochastic term proportional to the noise in the current.

In Figs. 4.14(a)–(d), we plot the conditional quantum-jump evolution of $z_c(t)$ and the corresponding detection record $dN_c(t)$, with various values of $(|\tilde{\tau}|/|\tilde{\chi}|)$. Each jump (discontinuity) in the $z_c(t)$ curves corresponds to the detection of an electron through the QPC barrier. One can clearly observe that, with increasing $(|\tilde{\tau}|/|\tilde{\chi}|)$, the rate of jumps increases, but the amplitude of the jumps decreases. When $D' = 0$ each jump collapses the DQD electron into dot 2 ($z = 1$), but as D' approaches D (from below) the jumps in z become smaller, although they are always positive. That is because, whenever there is a detection of an electron passing through QPC, dot 2 is more likely to be occupied than dot 1.

The case for quantum diffusion using Eqs. (4.335)–(4.337) is plotted in Fig. 4.14(e). In this case, infinitely small jumps occur infinitely frequently. We can see that the behaviour of $z_c(t)$ for $|\tilde{\tau}| = 5|\tilde{\chi}|$ in the quantum-jump case shown in Fig. 4.14(d) is already very close to that of quantum diffusion shown in Fig. 4.14(e). Note that for the case $\theta = \pi$ (which we have used in the simulations) the unconditional evolution does not depend on the parameter $|\tilde{\tau}|$. Thus all of these unravellings average to the same unconditioned evolution shown in Fig. 4.13(a).

The QPC current spectrum. We now calculate the stationary spectrum of the current fluctuations through the QPC measuring the coherently coupled DQD. This quantity is

⁴ The former name alludes to the saying ‘a watched pot never boils’; the latter alludes to the ‘proof’ by the Greek philosopher Zeno of Elea that motion is impossible. See Ref. [GWM93] for a review of this effect and an analysis using quantum trajectory theory.

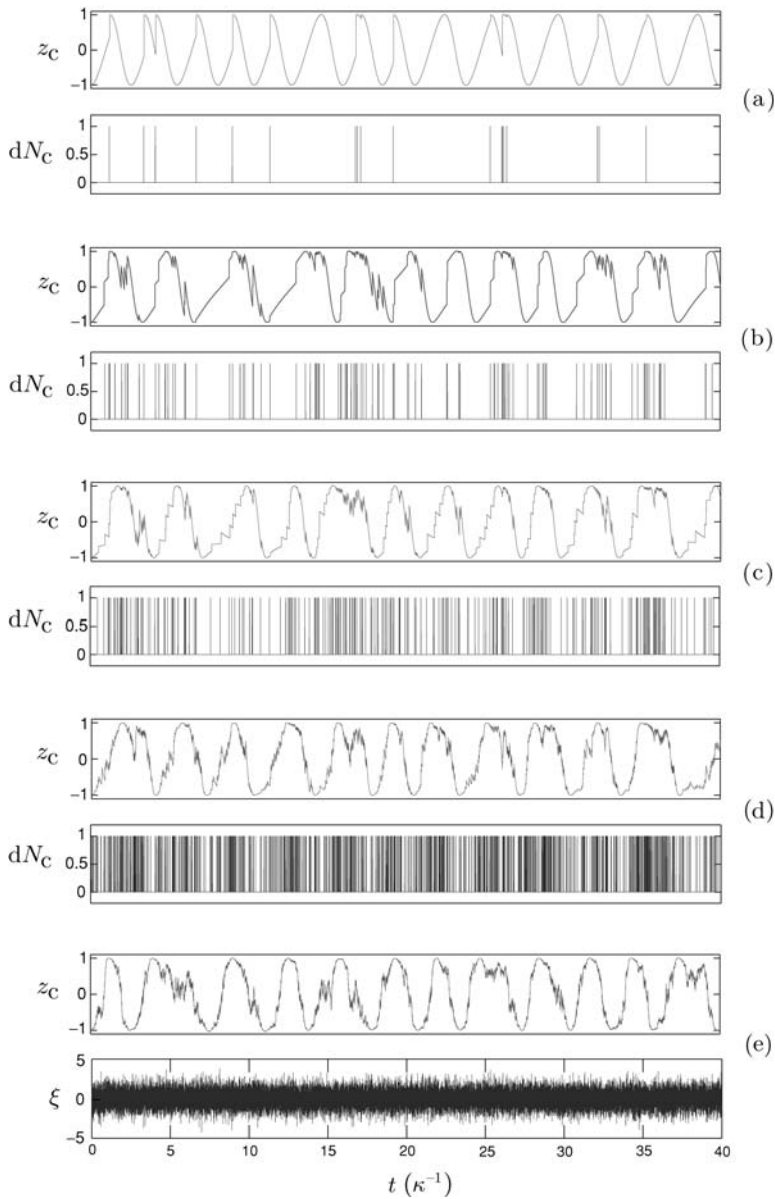


Fig. 4.14 Transition from quantum jumps to quantum diffusion. The parameters are $\zeta = 1$, $\Delta = 0$, $\theta = \pi$ and $\kappa = \Omega/2$, and time is in units of $\kappa^{-1} = |\tilde{\chi}|^{-2}$. In (a)–(d) are shown the quantum jump, conditional evolutions of $z_c(t)$ and corresponding detection moments with the following $|\tilde{\tau}|/|\tilde{\chi}|$ ratios: (a) 1, (b) 2, (c) 3 and (d) 5. In (e) the conditional evolutions of $z_c(t)$ in the quantum diffusive limit ($|\tilde{\tau}|/|\tilde{\chi}| \rightarrow \infty$) are shown. The variable $\xi(t) = dW/dt$, the noise in the QPC current in the quantum-diffusive limit, is scaled so as to have unit variance on the plot. Reprinted Figure 4 with permission from H-S. Goan and G. J. Milburn, *Phys. Rev. B* **64**, 235307, (2001). Copyright 2008 by the American Physical Society.

defined in Eq. (4.318), where

$$R(\tau) = E[I(t + \tau)I(t)] - E[I(t + \tau)]E[I(t)]. \quad (4.338)$$

This two-time correlation function for the current has been calculated for the case of quantum diffusion in Ref. [Kor01a]. Here we will present the quantum-jump case from Ref. [GM01], where $I(t) = e \, dN(t)/dt$.

Using the SME (4.329) and following the derivation in Section 4.3.2, we find that

$$E[I(t)] = eE[dN(t)]/dt = e\zeta \operatorname{Tr}[\{D + (D' - D)\hat{n}_1\}\rho(t)], \quad (4.339)$$

while, for $\tau \geq 0$,

$$\begin{aligned} E[I(t + \tau)I(t)] &= e^2 E[dN_c(t + \tau)dN(t)]/(dt)^2 \\ &= e^2 \zeta^2 \operatorname{Tr}[\{D + (D' - D)\hat{n}_1\}e^{\mathcal{L}\tau}\{\mathcal{J}[\tilde{\tau} + \tilde{\chi}\hat{n}_1]\rho(t)\}] \\ &\quad + e^2 \zeta \operatorname{Tr}[\{D + (D' - D)\hat{n}_1\}\rho(t)]\delta(\tau). \end{aligned} \quad (4.340)$$

In this form, we have related the ensemble averages of a classical random variable to the quantum averages with respect to the qubit state matrix. The case $\tau < 0$ is covered by the fact that the two-time autocorrelation function is symmetric by definition.

Now we are interested in the steady-state case in which $t \rightarrow \infty$, so that $\rho(t) \rightarrow I/2$ (see Exercise 4.39.) Thus we can simplify Eq. (4.340) using the following identities for an arbitrary operator B : $\operatorname{Tr}[e^{\mathcal{L}\tau}B] = \operatorname{Tr}[B]$ and $\operatorname{Tr}[Be^{\mathcal{L}\tau}\rho_\infty] = \operatorname{Tr}[B]/2$. Hence we obtain the steady-state $R(\tau)$ for $\tau \geq 0$ as

$$R(\tau) = eI_\infty\delta(\tau) + e^2\zeta^2(D' - D)^2\{\operatorname{Tr}[\hat{n}_1e^{\mathcal{L}\tau}(\hat{n}_1/2)] - \operatorname{Tr}[\hat{n}_1/2]^2\}, \quad (4.341)$$

where $I_\infty = e\zeta(D' + D)/2$ is the steady-state current.

Exercise 4.41 Verify Eq. (4.341).

The first term in Eq. (4.341) represents the shot-noise component. It is easy to evaluate the second term analytically for the $\Delta = 0$ case, yielding

$$R(\tau) = eI_\infty\delta(\tau) + \frac{(\delta I)^2}{4} \left(\frac{\mu_+ e^{\mu_- \tau} - \mu_- e^{\mu_+ \tau}}{\mu_+ - \mu_-} \right), \quad (4.342)$$

where $\mu_\pm = -(\kappa/4) \pm \sqrt{(\kappa/4)^2 - \Omega^2}$, and $\delta I = e\zeta(D - D')$ is the difference between the two average currents.

Exercise 4.42 Derive Eq. (4.342).

Hint: This can be done by solving the equations for the unconditioned Bloch vector – Eqs. (4.335)–(4.337) with $\Delta = \zeta = 0$ – with the appropriate initial conditions to represent the initial ‘state’ $\hat{n}_1/2$. This ‘state’ is not normalized, but the norm is unchanged by the evolution, so one can take out a factor of $1/2$ and use the normalized initial state \hat{n}_1 .

Fourier transforming this, as in Eq. (4.318), yields the spectrum of the current fluctuations as

$$S(\omega) = S_0 + \frac{\Omega^2(\delta I)^2\kappa/4}{(\omega^2 - \Omega^2)^2 + (\kappa/2)^2\omega^2}, \quad (4.343)$$

where $S_0 = eI_\infty$ represents the shot noise. Note that, from Eq. (4.343), the noise spectrum at $\omega = \Omega$ can be written as

$$\frac{S(\Omega) - S_0}{S_0} = \frac{(\delta I)^2}{(e\kappa)I_\infty}. \quad (4.344)$$

Exercise 4.43 Show that this ratio cannot exceed 4ζ .

For the case $\theta = \pi$ (real tunnelling amplitudes), this ratio can be written as

$$\frac{S(\Omega) - S_0}{S_0} = 2\zeta \frac{(\sqrt{D} + \sqrt{D'})^2}{(D + D')} \quad (4.345)$$

since $\kappa = (\sqrt{D} - \sqrt{D'})^2$ in this case. In the quantum-diffusive limit $(D + D') \gg (D - D')$, this ratio attains its upper bound, as was first shown in Ref. [Kor01a].

For $\kappa < 4\Omega$, the spectrum has a double-peak structure, indicating that coherent tunnelling is taking place between the two qubit states. This is illustrated in Figs. 4.15(a) and (b). Conditionally, the oscillations of $z_c(t)$ would be very nearly sinusoidal for $\kappa \ll 4\Omega$, but would become increasingly noisy and distorted as κ increases. When $\kappa \geq 4\Omega$, the measurement is strong enough substantially to destroy any coherence between the two dots, suppressing coherent oscillations. In this case, only a single peak, centred at $\omega = 0$, appears in the noise spectrum, as illustrated in Figure 4.15(c). In the limit $\kappa \gg 4\Omega$, the conditioned state of the DQD exhibits jump-like behaviour, with the electron being very likely to be in one well or the other at all times. That is, $z_c(t)$ can be modelled as a classical random telegraph process, with two states, $z_c = \pm 1$, just as in the single-dot case of Section 4.9.1.

4.9.3 Other theoretical approaches to monitoring in mesoscopic systems

In monitoring a solid-state quantum system, if one ignores or averages over the results, the only effect of the measurement is to decohere the system. The first step beyond this is to condition on a single property of the output (by which we mean the drain of the QPC, for example). The authors of Refs. [Gur97, SS98] considered conditioning on the number N of excess electrons that had tunnelled into the drain. This approach represents suboptimal conditioning of the system's state matrix because the information in the *times* of electron tunnelling events through the detector is unused. (In the case of a single-electron transistor (SET) as detector [SS98], further information is ignored – the times at which electrons tunnel onto the SET island from the source. See Ref. [Oxt07] for a discussion of this and other points in this section.)

A stochastic equation representing the conditional evolution of a solid-state system in real time was introduced into the phenomenological model by Korotkov [Kor99]. This was

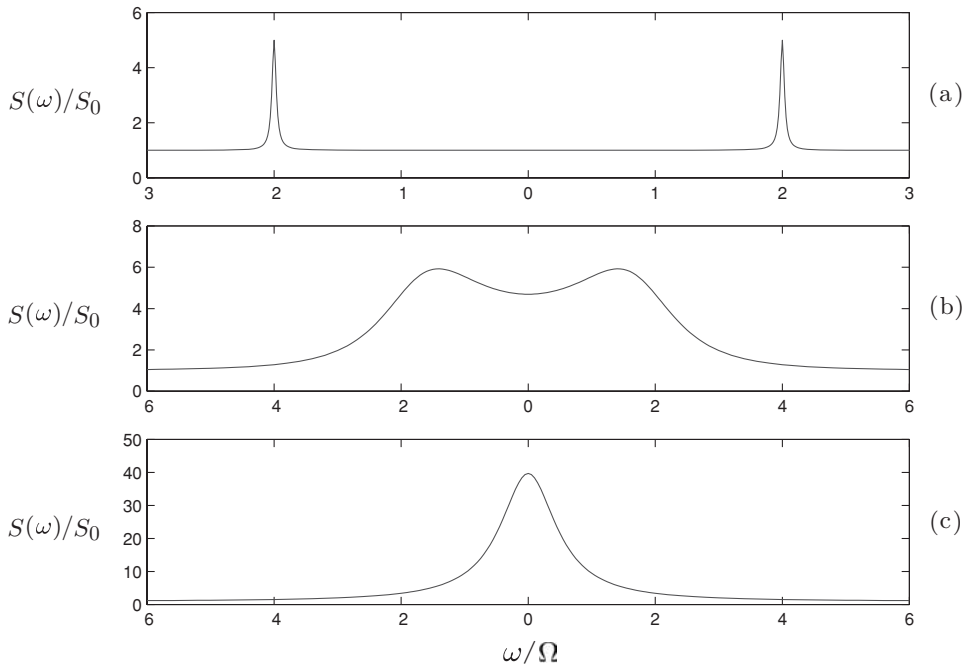


Fig. 4.15 A plot of the noise spectrum of the QPC current monitoring a double quantum dot. The spectrum is normalized by the shot-noise level, and is shown for various ratios of measurement strength κ to tunnelling strength Ω , with $\kappa/(4\Omega)$ equalling (a) 0.01, (b) 0.5 and (c) 2. For discussion, see the text. Reprinted Figure 5 with permission from H-S. Goan and G. J. Milburn, *Phys. Rev. B* **64**, 235307, (2001). Copyright 2008 by the American Physical Society.

later derived from a microscopic model in Ref. [Kor01b]. This model was restricted to a weakly responding detector (the diffusive limit discussed above), but has been extended to the case of a strongly responding detector (quantum jumps) [Kor03]. Korotkov's approach (which he called 'Bayesian') is completely equivalent to the quantum trajectory approach used above [GMWS01]. Quantum trajectories were first used in the solid-state context in Ref. [WUS⁺01], which included a derivation from a (rather simplistic) microscopic model.

From the beginning [Kor99, WUS⁺01], these theories of continuous monitoring in mesoscopic systems have allowed for non-ideal monitoring. That is, even if the initial state were pure, the conditional state would not in general remain pure; there is no description using a stochastic Schrödinger equation. The microscopic model in Ref. [WUS⁺01] is inherently non-ideal, while, in Ref. [Kor99], Korotkov introduced a phenomenological dephasing rate, which he later derived by introducing extra back-action noise from the detector [Kor01b]. Another sort of non-ideality was considered in Ref. [GM01], where the authors introduce 'inefficient' detection by a QPC, as used in Section 4.9.1 Here efficiency has the same sense as in quantum optics: some proportion $1 - \zeta$ of the detector output is 'lost'. This is of course equivalent to introducing extra decoherence as produced by an

unmonitored detector. As shown generally in Section 4.8.3, in the diffusive limit, the same conditioning equation results if extra white noise ('dark noise') is added to the detector output before it is recorded.

The theory of quantum trajectories for mesoscopic systems has recently been extended to allow for the noisy filtering characteristic of amplifiers used in such experiments [OWW⁺05, OGW08]. This was done using the same theory as that presented in Section 4.8.4, but taking into account correlations between noise that disturbs the system and noise in the recorded current. Such 'realistic' quantum trajectories are essential for optimal feedback control, because the optimal algorithms are based upon the state conditioned on the measurement record, as will be discussed in Section 6.3.3. Note that the authors of Ref. [RK03] do consider the effect of a finite-bandwidth filter on a feedback algorithm, but that is a quite distinct idea. There, the feedback algorithm is not based on the state of the system conditioned on the filtered current, and indeed no such conditional state is calculated.

4.10 Further reading

There are several books that discuss continuous quantum measurement theory in the context of open quantum systems. *An Open Systems Approach to Quantum Optics* by Carmichael [Car93] was a very influential book in the quantum-optics community, and introduced many of the terms used here, such as 'quantum trajectory' and 'unravelling'. Much of this material is contained in volume 2 of Carmichael's recently published *Statistical Methods in Quantum Optics* [Car99, Car07]. *Quantum Noise* by Gardiner and Zoller [GZ04] is not confined to quantum optics. It has material on quantum trajectories and quantum stochastic differential equations, but also covers quantum noise in a more general sense. *The Theory of Open Quantum Systems* by Breuer and Pettrucione [BP02] emphasizes the application of stochastic Schrödinger equations for numerical simulations of open quantum systems, both Markovian and non-Markovian.

In this chapter we restricted our attention to systems obeying a Markovian master equation, and indeed a master equation of the Lindblad form. The reason is that it is only in this case that a measurement of the bath to which the system is coupled can be performed without altering the average evolution of the system [GW03, WG08]. In particular, the non-Markovian stochastic Schrödinger equations developed by Diósi, Strunz and Gisin [SDG99, Dió08] cannot be interpreted as evolution equations for a system conditioned upon a measurement record. This is despite the fact that in the Markovian limit they can reproduce the quantum trajectories for homodyne and heterodyne detection [GW02] and even for direct detection [GAW04]. In fact, the only physical interpretation for these equations is in terms of hidden-variable theories [GW03].